COMBINING A MULTISPECTRAL SATELLITE IMAGE AND ANCILLARY DATA FOR VEGETATION CLASSIFICATION IN BIG BEND NATIONAL PARK

THESIS

Presented to the Graduate Council of
Southwest Texas State University
in Partial Fulfillment of
the Requirements

For the Degree

Master of APPLIED GEOGRAPHY

By

Terence Patton Booth, B.S.

San Marcos, Texas
May 2000

To Madison and all those who
will experience and enjoy Big Bend National Park

ACKNOWLEDGEMENTS

Many individuals have helped and supported me through my graduate career and especially during the research and writing of this thesis. I would like to express my sincere appreciation to:

- My thesis advisor, Dr. Pamela Showalter, for her support and guidance throughout this project.
- Dr. David Butler and Dr. Ron Eyton, for sharing their knowledge and expertise in the fields of biogeography and remote sensing, respectively.
- Betty and Tom Alex, of the Science and Resource Management Division at Big Bend National Park, for the invaluable assistance they provided during my field trips to the park.
- My daughter, Julie, who has been my camping buddy and enthusiastic observer of nature on our many trips to Big Bend National Park since our first trip in 1981.
- My father, Jean Booth, who showed me by example that graduate education after age forty can be rewarding, challenging, and lead to a whole new direction in life.
- My manager, David Ritter, and my co-workers, especially Doris Morris, who have graciously accommodated my reduced work load during this thesis project.
- Above all, my wife, Dawn, who has richly supported me physically, mentally, and spiritually throughout my graduate career.

April 2000

TABLE OF CONTENTS

LIST OF TABLES

LIST OF FIGURES

CHAPTER I

INTRODUCTION

The United States National Park System is the repository of some of this country's most valued treasures. The stated mission of the Nation Park Service is "to conserve the scenery and the natural and historic objects and the wildlife therein and to provide for the enjoyment of the same in such manner and by such means as will leave them unimpaired for the enjoyment of future generations.[1]". The National Park Service, therefore, protects the 34 million hectares of the 378 components of the national park system from direct human activities such as agriculture, mining, and grazing by domestic livestock (National Park Service 1999a). The protected status of national parks allows them to serve as excellent natural laboratories. Because national parks, many of them covering millions of contiguous acres, are shielded from the direct effects of human activities, they are ideal places to study regional and global effects of climate, pollution, changes to animal population, and successional changes in vegetation communities all of which affect the ecosystems in any given park.

For scientists and resource managers responsible for preservation and restoration of national parks, documenting and managing change is crucial to ensuring the sustainability of the park system. One key element of documenting and managing change is the development of accurate and consistent vegetation maps. A. W. Küchler, in the preface to the book Vegetation Mapping (Küchler and Zonneveld 1988) articulates four primary uses for vegetation maps as follows:

> 1. vegetation maps present an inventory of existing plant communities, their location, extent, and geographical distribution in the landscape at the time of their mapping;
> 2. vegetation maps are scientific tools for analyzing the environment and the relationships between vegetation and the site on which it occurs. This helps to explain the distribution of plant communities on the basis of the physical and chemical features of the landscape. On the other hand, plant communities allow conclusions on the nature of the environment;
> 3. vegetation maps are valuable standards of reference for observing and measuring changes in the vegetation, their direction and their speed, i.e. the rate of change. This is important because the character of vegetation is dynamic and is increasingly affected by man;
> 4. vegetation maps can serve as a scientific basis for planning future land-use, especially with regard to forestry, range management, and agriculture in all its forms and variations. Such ecologically based planning permits an optimal land-use, managing for highest yields on a sustained basis without damaging the environment. (p. 1)

Considering these four uses, the purpose of this thesis is to develop accurate and consistent vegetation maps of a portion of one major component of the national park system, Big Bend National Park.

Big Bend National Park in West Texas (Figure 1) is a natural preserve covering 324,154 hectares (801,000 acres) of the northern Chihuahuan Desert (National Park Service 1999b, Powell 1998). Given the size, remoteness, and difficult terrain of the park, ground survey methods are inadequate for producing such maps. However, with the

[1] National Park Service Organic Act, 16 U.S.C. 1, August 25, 1916

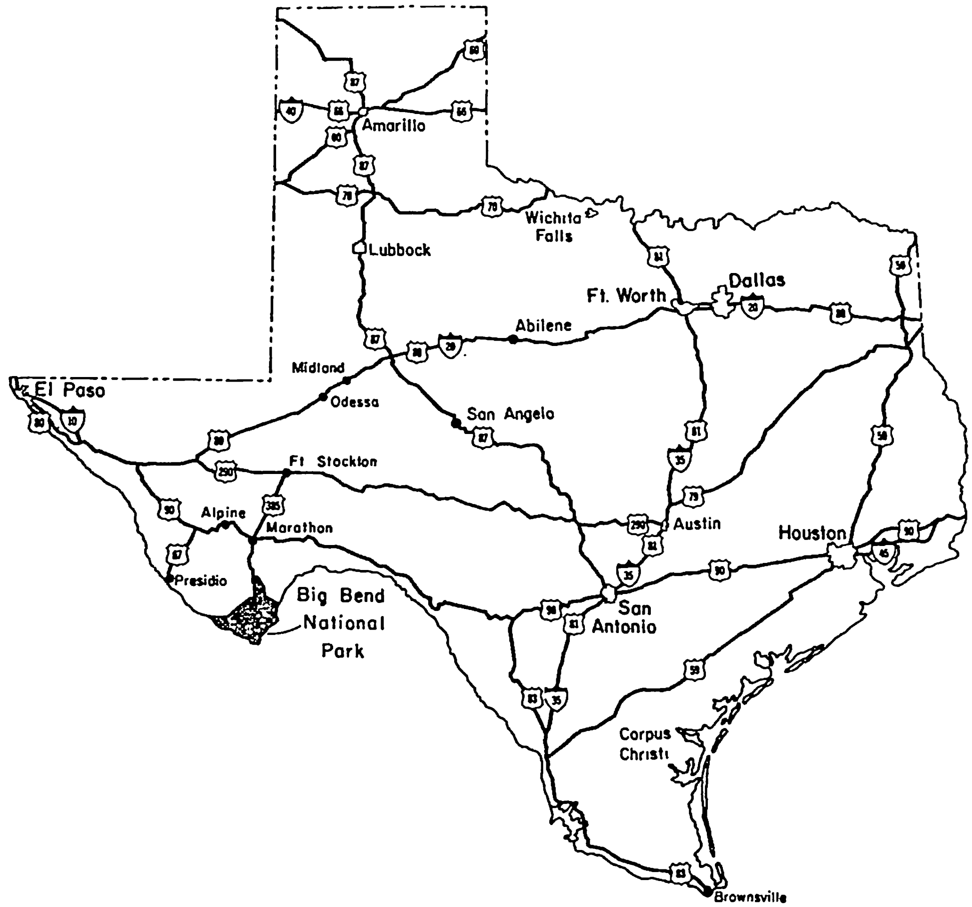

Figure 1. Map Showing Location of Big Bend National Park. Adapted from Maxwell et al. (1967).

increasing availability of remotely sensed data including satellite imagery, aerial photography, and airborne radar images it is a practical undertaking to develop reliable maps covering an extensive area, in this case a national park approximately the size of the state of Rhode Island. Moreover, the accuracy and utility of vegetation maps can be enhanced by incorporating remotely sensed data with other data in digital form such as digital elevation models (DEMs), soil maps, and digital line graphs (DLGs) into a geographical information system (GIS). The efficacy of combining remote sensed data with DEM data, soil maps, and derived data such as slope and runoff maps into a GIS for use as a resource management tool has been demonstrated by Walsh (1985). Potential uses of vegetation maps of Big Bend National Park are:

- Analyzing response of vegetation to climatic change
- Assessing the dynamics of successional change, for example, between grasses and woody shrubs like mesquite
- Monitoring the transition of rangeland recently grazed by cattle as it is restored to a more natural state
- Monitoring the long-range effects of air pollution on the park's ecosystems
- Comparing protected vegetation communities within the park to vegetation communities in adjacent lands in both the United States and Mexico

The most recent vegetation maps for Big Bend National Park were created by Gregory A. Plumb, then at the University of Kansas, as part of his dissertation in 1988 (Plumb 1988). Plumb developed new vegetation classification system (described below) as part of his dissertation research. Plumb then designed and implemented a knowledge-based system. This knowledge-based system combined Landsat Thematic Mapper (TM) images in conjunction with Digital Elevation Model (DEM) data and soils data to produce vegetation maps of a substantial portion of the park.

In the years since Plumb's research, Big Bend National Park has increased in area through the acquisition of 36,421 additional hectares (90,000) acres at the north end of the park (Figure 2). No vegetation maps exist for some parts of this new area. Whitson (1970) mapped vegetation in the North Rosillos ranch at the northern end of the new area. However, Whitson's classification system was not consistent with Plumb's classification system.

This research project is intended to remedy the problem of missing and mismatched vegetation maps of the recently acquired areas of Big Bend National Park. Remotely sensed satellite data will be combined with ancillary data to produce vegetation maps of the new areas of the park according to Plumb's classification system. These vegetation maps will document the type and extent of vegetation communities that exist now, establishing a baseline that can be used for future research.

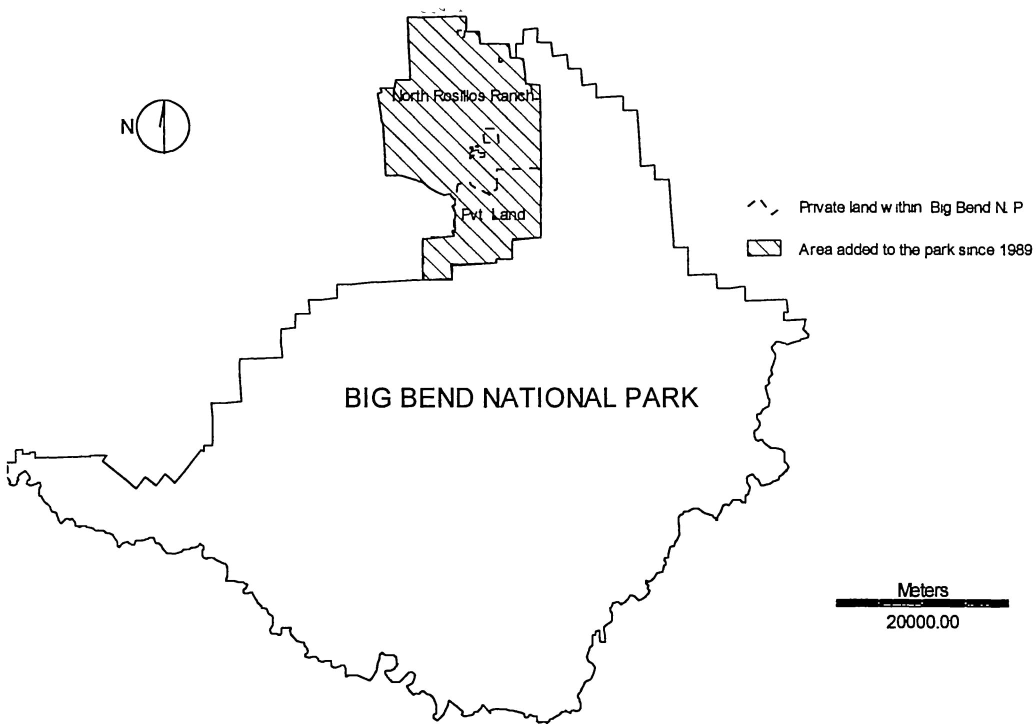

Figure 2. Map of Big Bend National Park Including Areas Added since 1989

Consistency of classification is a critical factor in maximizing the utility of the proposed vegetation mapping. Jensen (1996) stated the issue clearly:

> This brings us to another important consideration. If a reputable classification system already exists, it is foolish to develop an entirely new system that will probably only be used by ourselves. It is better to adopt or modify existing nationally recognized classification systems. This allows us to interpret the significance of our classification results in light of other studies and makes it easier to share data. (p. 205)

While Plumb's classification system may or may not be nationally recognized, it is the only system to date that has been used for park wide vegetation mapping that is based on thoroughly researched, rigorous, quantitative sampling, and analysis.

CHAPTER II

PHYSICAL SETTING

Big Bend National Park and Surrounding Areas

Big Bend National Park, the largest national park in Texas, is located in the southernmost part of Brewster County, Texas. The Rio Grande River forms the southern boundary of the park and separates the park from Mexico. Elevation varies from 530 m (1740 ft) on the Rio Grande at the extreme east side of the park to 2385 m (7825 ft) at Emory Peak in the Chisos Mountains. The terrain is diverse ranging from riparian areas, desert plains, badlands, Chisos Mountains and foothills, limestone mountains and foothills, alluvial outwash plains, floodplains along the Rio Grande and major drainages (Maxwell et al. 1967). Figure 3 shows the general physiography of Big Bend.

Riparian areas are limited to the Rio Grande River and a few of the major arroyos. The Rio Grande is the only permanently flowing stream in the region. Major drainages such as Tornillo Creek and Terlingua Creek do not normally have flowing water except after rain. The Rio Grande floodplain supports groves of trees, tall reed grasses, and, in some places, dense thickets of mesquite, tamarisk, and other woody vegetation. The major drainages support sporadic clusters of riparian vegetation such as Desertwillow and Seepwillow on their lowest terraces and channel bars.

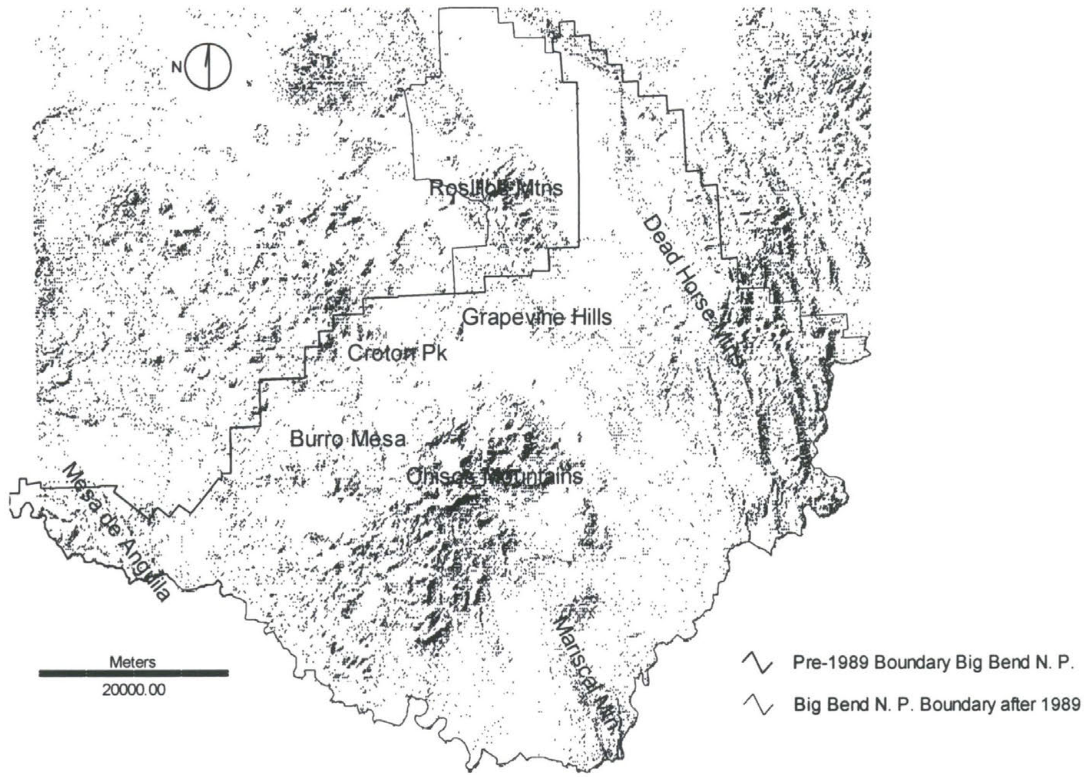

Figure 3. Physiography of Big Bend National Park

The desert plains and badlands are the lowest and driest parts of the park. This area is also the most extensive and the plant cover is the sparsest (Wauer 1971, Plumb 1988). Visually the desert plains and badlands correspond to most people's image of what constitutes a "desert."

The foothills, smaller desert mountains, and mesas are also dry, but the variable relief of terrain, somewhat higher elevations, and better moisture holding characteristics of soil result in denser and more diverse vegetation cover. Areas representative of this environment include the Dead Horse Mountains, Sierra Del Carmen Mountains, Burro Mesa, and Mesa de Anguila.

The Chisos Mountains have enough mass, extent, and elevation to accommodate forest type vegetation. Vegetation density in the Chisos Mountains ranges from moderately-high to high except for rock outcrops, steep cliffs, and talus (Plumb 1988). Although the Rosillos Mountains are less extensive and the elevations are not as high (reaching 1660 m) as the Chisos Mountains, they still harbor some forest vegetation. Other small mountain ranges to the north, the Christmas Mountains and Santiago Peak also have forest vegetation near their peaks.

The average annual temperature for the region is about 19°C (66°F) and generally ranges from an average daily temperature of around 7°C (44°F) in December and January to an average daily temperature of 28°C (82°F) in July. Rainfall varies from an average of less than 10mm (0.4 in) per month in March, April and May to an average of about 40mm (1.6 in) in July and August (Schmidt 1983).

The earliest human occupation of the region dates to about 9000 B.C.E. (Wauer 1973). The archeological evidence shows more or less continuous habitation by successive native tribes though the 1860s when European settlement in the area became firmly established. The Spanish explorers whose expeditions criss-crossed the region from the 1600s to the 1790s used the term *despoblado*, meaning "uninhabited land" to describe the area in recognition of the difficult terrain, the lack of water, and the scorching heat (Tyler 1975). Ranching began in the1880s with the establishment of the G4 Ranch (Wauer1973). By the time World War I ended, ranches had completely encircled the Chisos Mountains and livestock had begun moving up into the more remote parts of the mountains. Despite the dry climate, when the first ranches were established the area was covered in abundant grass (Langford 1952). Unfortunately, most of the settlers who came to the region overestimated the carrying capacity the land for livestock, and as a result, much of the area was already becoming overgrazed by 1900 (National Park Service 1998). J. O. Langford who, from 1909 to 1913, homesteaded a section of land on the Rio Grande near Boquillas Canyon on the east side of the park eloquently described the changes that had taken place by the time he returned to the area in 1927:

> During the war, cattle prices and the prices of goats and sheep had soared. And to take advantage of these prices, ranchers had poured livestock into that vast region of grassland as fast as they could buy the animals. And now, where once I'd thought there was more grass than could ever be eaten off, I found no grass at all. Just the bare, rain-eroded ground. And where once beautiful pools of clear, cold water had stood in Tornillo Creek, now I found only great bars of sun-baked sand and gravel. (Langford 1952, p. 153)

In 1942, the State of Texas purchased most of the privately held ranches in what would become Big Bend National Park in 1944. The ranchers were then given free grazing privileges until the actual creation of the park. For those two years, livestock herds were dramatically increased to take advantage of the situation. By the time the livestock removal was completed in 1945, the overgrazing had severely impacted native plant and animal species (Wauer 1973).

The Rosillos Mountains Area

The primary region of interest in this study is the area surrounding the Rosillos Mountains, which was acquired by the park after Plumb's dissertation was published in 1988. The landscape is dominated by the Rosillos Mountains that rise above the surrounding flatlands. The highest elevations in the mountains reach 1660 m (5445 ft.) while the surrounding flatlands generally range from 850-950 m above sea level. The Rosillos Mountains were formed by a laccolith, an igneous intrusion, in the late Cretaceous-early Tertiary, which domed up the overlying rock. After the intruding magma cooled, the overlying rock eroded exposing the underlying granite. The name Rosillos is derived from the Spanish word for "roan," a fitting reference to the reddish color of the rocks (Maxwell et al. 1967).

The earliest record of land ownership of the area dates from 1899 when the Lou F. Buttrill family began ranching operations (Wulfkuhle 1986). The land changed hands several times over the next several decades, usually as a result of failure of owners to make even a marginal profit from ranching in the semi-arid rangeland (National Park Service Division of Science and Resource Management Big Bend National Park, 1998). Edward and Houston Harte, brothers in a family prominent in the publishing business, purchased about 17,800 hectares (44,000 acres) north of the Rosillos Mountains in 1958 and another 8,500 hectares (21,000 acres) covering the north side of the Rosillos Mountains in the 1960s. The Harte ranch was not a major part of the Harte brothers' real estate holdings. Rather than subdividing the ranch like the Terlingua Ranch to the north, they preferred to donate the land to the National Park to avoid perpetuating the cycle of overuse and overgrazing that characterized land use practices in and around the park in the late nineteenth and twentieth centuries. Approximately 23,100 hectares (57,000 acres) were donated to the park in January 1989 and an additional 4,000 hectares (10,000 acres) of adjoining property were acquired in 1994. The Rosillos Ranch, which encompasses the south half of the Rosillos Mountains, as well as some very small tracts within the park proper are still privately held, but still considered part of the national park. According to Tom Alex, National Park Service archeologist (personal communication 1999), this status results from the National Park Service having the authorization, but not the appropriated money, to acquire the land.

CHAPTER III

LITERATURE REVIEW

Vegetation Classification and Plant Community Structure

A number of vegetation classifications have been developed for Big Bend National Park over the last fifty years. Plumb (1988; 1992) reviewed eight different classifications comparing the purposes, the areal coverage, and the strengths of each classification. Plumb found that while each of the earlier classifications may have served the authors' needs quite well, none of them were fully sufficient for creating a cover map at the 1:24,000 to 1:100,000 scale he desired. For example, Wauer (1971; 1973a) designed his classification based on the distribution of breeding birds and thus needed only six categories of vegetation to meet his needs. On the other hand, Denyes (1956) was interested in mammalian distribution in the park and found that a single category called Riverbank was sufficient to characterize all types of riparian vegetation for his purposes.

A classification by Henrickson and Johnston (1983) was used to characterize the entire Chihuahuan desert region. The classification describes several communities such as Tobosa Grassland and Sand Dune Scrub, which, while abundant in the southern regions of the Chihuahuan desert, do not occur in Big Bend National Park. Other researchers (Cochran and Rives 1985; Maxwell et al. 1967) have described the relationship between vegetation and geological formations and soils, which were incorporated into Plumb's classification algorithms.

While each vegetation classification developed for the park has useful attributes, the one best suited to the purposes of this thesis is the classification system of Plumb, primarily because it was designed for the medium scale (1:24,000 to 1:100,000) mapping that is the focus of this project. The choice of the 1:24,000 scale for the vegetation maps developed in this project is driven by two major factors. First, the potential uses of vegetation maps stated in the introduction have a temporal dimension ranging from a year to perhaps a decade or more and a spatial dimension ranging from less than a hundred meters to several kilometers. A map scale is required which allows the user to visualize changes of these dimensions (Forman 1995). At the same time, the scale should not show more detail than the resolution of data being used to produce the map. A scale in the range from 1:10,000 to 1:100,000 meets these criteria. Second, the most accurate base maps of Big Bend National Park are the 7.5 minute USGS topographic maps (1:24,000 scale). In addition, most of the ancillary data that will be used in this project (digital elevation models, soil maps, digital raster graphs) are based on USGS topographic maps.

It is possible that Plumb's classification will need to be extended or modified to account for potentially different vegetation communities in the newly acquired areas of the park because they were so recently used for grazing domestic livestock. Plumb acknowledges the possibility for extending or revising his classification, stating, "New classifications still need to be developed for research themes with purposes that have been inadequately addressed for the region. For instance, more work needs to be accomplished within Big Bend regarding the formidable task of examining vegetation associations and their synecologies" (1992, p. 386).

Several papers (McAuliffe 1994; Montaña 1992; Montaña, et. al. 1990; Peters et. al.1997; Silvertown and Wilson 1994; Turner 1990; Warren et al. 1996) report relevant research conducted in other parts of the Chihuahuan desert and other arid and semi-arid regions. Silvertown and Wilson (1994) argue that desert vegetation communities have significant structure where focal shrubs like creosote bush or large cacti accumulate an associated flora of other perennials around them in a non-random sequence. Montaña (1992) shows that vegetation patches in the Chihuahuan region are often arc-shaped, aligned along elevation contours, and tend over time to migrate up-slope. Some researchers have shown that it is possible to detect growth patterns by using a time series of satellite imagery (Peters et. al. 1997). These studies depended on monitoring change in vegetation over time, and they substantiate the need for establishing baseline vegetation maps of Big Bend for use in multitemporal analysis.

Issues with Use of Satellite Imagery in Arid and Semi-arid Regions

Using remote sensed data such as satellite imagery or aerial photographs to classify vegetation in arid environments presents several problems. First, the vegetation generally does not form a complete cover. Second, in multispectral satellite images the soil matrix may dominate the reflectance in many pixels (Abeyta and Franklin 1998; Eastman 1999b). Third, except during and immediately after rain events, plants (especially grasses) may be senescent and not give separable reflectance signatures (Huete and Jackson 1987). Fourth, many plants adapted to arid conditions, including cacti and other succulents, may show a high degree of variability in spectral response depending on local soil and meteorological conditions (Tueller 1987). Finally, slope, aspect, and elevation as well as local soil conditions have a strong, even controlling, influence on the distribution of vegetation. Remote sensed data alone cannot account for all these variables (Henrickson and Johnston 1983; Tueller 1987).

To overcome difficulties in classifying vegetation in arid regions using satellite imagery and aerial photography, techniques have been developed in three major areas. First, vegetation indices have been developed to mitigate or separate the effect of soil background (Eastman 1999a; Todd and Hoffer 1998). Second, ground sampling methods have been developed to quantify training sites to improve accuracy of classification based on reflectance signatures (Treitz et al. 1992). Third, multitemporal studies that compare vegetation cover over time and under varying climatic conditions can improve both the utility and the accuracy of maps derived from remotely sensed data (Foran 1987; Peters et. al. 1997; Turner 1990).

Methods for Classifying the Remotely Sensed Data

There are two general methods of classifying remotely sensed data such as satellite images or aerial photographs: unsupervised and supervised. In unsupervised classification, computer analysis of the image creates groups of similar spectral signatures, and then the user identifies the cover types the signatures represent. With supervised classification, the user develops spectral signatures according to a predetermined classification scheme and then the computer analysis assigns each unit of image (a picture element or pixel) to the most similar cover type based on the spectral signature of the unit (Eastman 1999a).

Supervised classification is justified when sufficient knowledge of the possible ground cover types can be determined before the classification is performed (Jensen 1996). Representative examples of each cover type (a training site) must be located on the ground and the ground location must be transferred to the image to be analyzed. The transfer of ground location to image implies that the image must be georeferenced to a known coordinate system.

In general, some level of quantitative assessment of the training site must be performed to verify that the site actually represents the cover type it is supposed to represent. There are a number of methods for sampling vegetation cover including the line intercept method used by the Texas Parks and Wildlife Department (Simpson et al. 1996). Etchberger and Krausman (1997) evaluated five different methods for quantifying desert vegetation. The most accurate of the five methods was found to be a variant of the line intercept method.

Since Plumb performed very rigorous sampling of 131 sites with known locations, it is not necessary to perform additional sampling at those sites. However, each of Plumb's sites used in this project will be visually inspected to insure Plumb's classification is still valid. Short-term weather patterns or human disturbance may have changed the vegetation cover since the original ground sampling was performed. Alternatively, in some cases the precise location of the training site may be in question since Plumb did not leave permanent markings to identify the sites. The line intercept method will be employed, where necessary, in the previously unmapped areas of the park. The specific procedures employed in this study will be based on guidelines published by the Texas Parks and Wildlife Department (Simpson et al. 1996).

CHAPTER IV

DATA SOURCES

Sources of Digital Data Used in This Study

Satellite Imagery

A multispectral image covering a substantial portion of the park and surrounding areas taken by the French SPOT[2] satellite was obtained from the Division of Science and Resource Management, Big Bend National Park, Texas. Figure 4 shows the coverage of the satellite image in relation to the park boundary. SPOT multispectral images provide three bands of data in the following wavelengths; green (0.50-0.59 μm), red (0.61-0.68 μm), and near infrared (0.79-0.89 μm). The pixel size for SPOT multispectral images is 20 m x 20 m. The image is in SPOTView™[3] format, that is, the image was georeferenced to Universal Transverse Mercator (UTM) zone 13, North American Datum 1927. In addition, parallax errors caused by relief had been removed from the image. Figure 5 is a color composite view of the satellite image. Image specifications regarding time, date, location, cartographic parameters and data format are shown in Table 1.

---

[2] Satellite Pour l'Observation de la Terre. The image was obtained from the SPOT Image Corp., Reston, VA.

[3] SPOT IMAGE, SPOTView are Registered Trade Marks of SPOT IMAGE and SPOT IMAGE CORP. (USA).

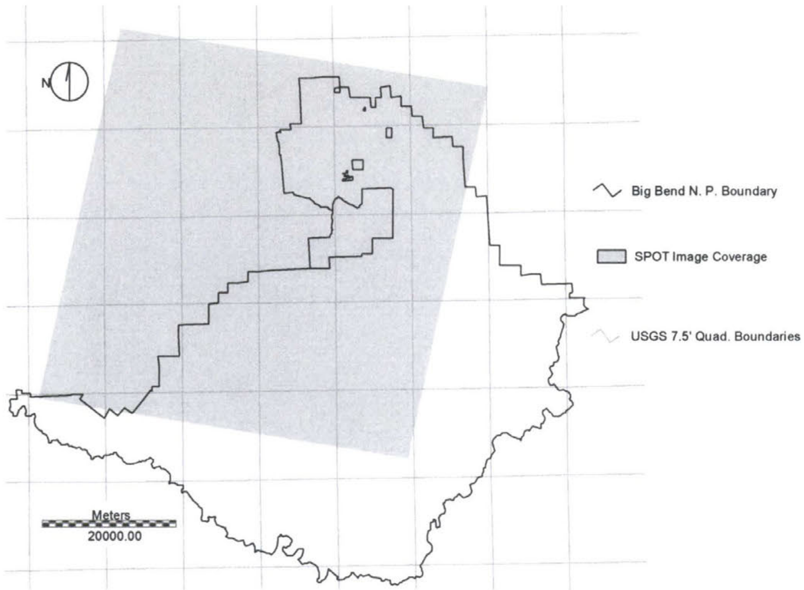

Figure 4. SPOT Image Coverage in Relation to Big Bend N. P.

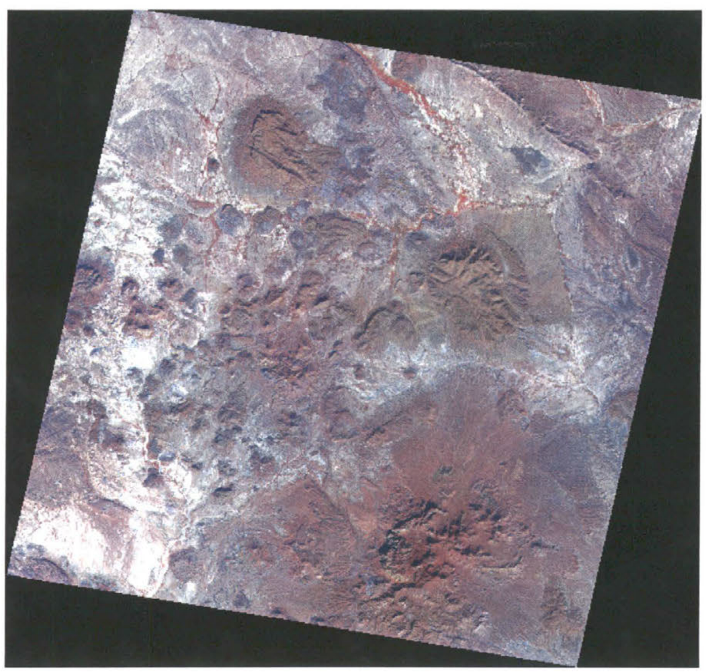

Figure 5. Color Composite of the SPOT image

Table 1. Parameters of Satellite Image Used in This Study

Image Date	December 3, 1990
Imaging Time	17:41:17 UTC
Sun Azimuth	162.10°
Sun Elevation	36.60°
Projection	Universal Transverse Mercator
Zone	13
Horizontal Datum	1927 North American datum
Spheroid	Clarke 1866
Upper Left Latitude	29.77111°
Upper Left Longitude	-103.598611°
Upper Right Latitude	29.679167°
Upper Right Longitude	-102.987500°
Lower Left Latitude	29.242778°
Lower Left Longitude	-103.737778°
Lower Right Latitude	29.151111°
Lower Right Longitude	-103.130000°
X (Easting) Origin	622230.00 m
Y (Northing) Origin	3294130.00 m
X Extent	72160.0 m
Y Extent	68060.0 m
Rows	3403
Columns	3608
Bands	3
Cell Value (reflectance value)	0-255
Cell Dimension	20 m x 20 m

Digital Elevation Models

The primary ancillary data used in this study were digital elevation models (DEMs) obtained from the United States Geological Survey (USGS) web site[4]. The USGS DEM data is available in Spatial Data Transfer Standard (SDTS) format at no cost (except for the indirect cost of the Internet connection). The DEM data was derived from 1:24,000 scale USGS topographic maps having a vertical resolution of one meter and a horizontal resolution of 30 m. The data is derived from and is packaged to correspond to USGS 7.5-minute Quadrangle maps. Forty-one DEMs representing a like number of quadrangles were obtained to ensure complete coverage of Big Bend National Park and the entire area covered by the SPOT satellite image. The DEMs are georeferenced to the same coordinate system and the same horizontal datum as the SPOT image.

Soil Data

Soil data in digital form was obtained from the U.S. Department of Agriculture, Soil Conservation Service State Soil Geographic (STATSGO) database for Texas. The information in the STATSGO database pertaining to the Big Bend National Park area was derived from the soil survey by Cochran and Rives (1985). Their original survey defines eight general soil map units and twenty-six detailed soil map units. Common plants found in each soil map unit are mentioned. In general, soil type by itself does not control the plants (at least those plants which form the dominant vegetation in the classification system). Vegetation types are found across many or most soil map units and soil map units contain more than one example of each major vegetation type. Two soil map units,

---

[4] http://edcwww.cr.usgs.gov/doc/edchome/ndcdb/ndcdb.html

Brewster-Rock Outcrop-Hurds and the Puerta-Madrone, have fairly limited vegetation types. These two units are found only in the higher elevations of the Chisos Mountains so it is reasonable to assume that elevation may control the vegetation to an equal or greater extent than soil type. Plumb (1988) had a digital form of the detailed mapping units which he was able to use in his vegetation classifications. However, the STATSGO database only had a generalization of the general soil map units. Furthermore, the source from which the soil units were digitized was 1:250,000 maps. The soil data proved to be too generalized and mapped at too small a scale for use in this project.

According to the United States Department of Agriculture, National Resource Conservation Service web site[5], the Soil Survey Geographic Database (SSURGO) will soon include a more detailed digital soil map of Brewster County, Texas including Big Bend National Park. The SSURGO database is intended to duplicate the most detailed soil survey existing for a region in digital form. When this data becomes available for Big Bend National Park, it may be a valuable addition for future research.

Digital Raster Graphs

A Digital Raster Graph (DRG) is a scanned version of a USGS 7.5-minute topographic map. DRGs are available on CD or on-line from the USGS[6]. DRGs representing the same forty-one DEM quadrangles described above were downloaded from the Texas Natural Resources Information System (TNRIS)[7]. At the time of this research TNRIS provided the DRGs on-line at no cost, but this service is no longer

---

[5] http://www.ftw.nrcs.usda.gov/soils_data.html
[6] http://mapping.usgs.gov/
[7] http://www.tnris.state.tx.us/index.html

available. Instead, TNRIS uses GeoCommunity's GIS Data Depot[8]. DRG data was not used directly in the vegetation classification, but the information proved very valuable in locating and establishing UTM coordinates for training and validation sites. DRGs are georeferenced to the same coordinate system as DEM data.

Digital Line Graphs

Digital Line Graphs (DLGs) were also used in this study. DLGs are vector representations of features digitized from USGS topographic maps. Features such as roads, hydrography, and boundaries are separated into layers. These layers can then be imported into a GIS. The source maps for the DLG data available for this study were USGS 15-minute quadrangles. As in the case of DRGs, DLG information was not used directly in vegetation classification, but was employed in the creation of overlays for superimposing boundaries and roads on the vegetation maps. Hydrographic data (stream and river vectors) were converted to raster representations and subsequently used in the creation of probability maps correlating riparian vegetation classes to distance to water. Even though the 1:100,000 scale of the source data for the DLG hydrographic data has a lower resolution than the 1:24,000 scale data of the DEM and DRG data, the use of this data is justified because the process of converting vector data to a usable raster format generalizes the information to a degree that negates the scale difference. For example, the vector to raster conversion process converts a line segment to a 20 m x 20 m pixel. In addition, the minimum resolution required to determine if a pixel in satellite imagery was near water was 120 m. This level of generalization is required because the source

[8] http://data.geocomm.com/catalog/US/61085/sublist.html

topographic maps, whether 1:24,000 or 1:100,000 scale, only show one stream channel (presumably the main channel at the time the map was created). Many of the streams in this region, particularly on the flats, have braided channels, which form intricate, complex, and constantly changing bars and little islands which are potential sites of vegetation growth (Leopold et al. 1964).

Digital Orthophoto Quarter Quadrangles

Digital Orthophoto Quarter Quadrangles (DOQQs) covering a majority of the new area of the park and surrounding areas inside and outside the park were obtained from the USGS. DOQQs are derived from aerial photographs taken in the Nation Aerial Photography Program (NAPP) and are rectified and georeferenced using DEM data and photogrammetric techniques. Each DOQQ covers a 3.75 minute by 3.75 minute section of a USGS topographic map plus an overlap with adjoining DOQQs of approximately 200 m. The DOQQs obtained for this study were 3-band color infrared images with 1 m resolution. Theoretically it would be possible to perform vegetation classification directly on these images, however each image is quite large. A single DOQQ image contains more than 50 million pixels in each of the three bands. By contrast, the entire SPOT image used in this classification contained 8 million pixels. The time and computing capacity to classify DOQQs is beyond the scope of this project. The images were very useful as an aid in accurately digitizing training sites and in the accuracy assessment of the classification.

Cover Type Classifications Used in This Study

This study employed a subset of the cover classification developed by Plumb (1988). There is strong justification for using Plumb's classification system. First, the classification system was built on cover definitions from many previous researchers. Second, Plumb used a rigorous and extensive sampling methodology to develop and define his own system of cover classification. Third, because Plumb documented the location of many of his training sites it was possible to use the same locations as training sites in this study, helping insure continuity between the two research projects. Fourth, Plumb developed his maps of vegetation communities based on supervised classification of remotely sensed satellite data as was done in this study. Finally, one of the major aims of this study is to map vegetation using a consistent classification of cover types. The vegetation maps Plumb developed cover nearly all of the park's area as it existed at the time of his research. Therefore, it is highly desirable to use the same classification system to the extent possible in mapping extensions to the park's area.

Plumb established 26 cover classifications in his research. He defined five riparian cover classes, five classes found in the desert plains, eight classes found primarily in desert foothills, mountains and mesas, and eight cover classes found almost exclusively in the higher altitudes of the Chisos Mountains. In this study three of the five riparian categories, all five of the desert plains classes, five of eight classes for desert plains foothills and mesas, and all eight Chisos Mountains classes were used as cover classifications. In addition, a classification for bare soil was also used. Table 2 summarizes the floristic and structural characteristics of each classification.

Table 2. Structural and Floral Characteristics for Cover Types within Big Bend National Park. Adapted from Plumb (1988)

Vegetation Cover Type	Dominant Structural Components and Dominant Floral Components
Riparian	
Mesquite Thicket	Trees, large shrubs *Prosopis, Larrea, Opuntia*
Reed Grass (Not used in this project)	Tall grasses *Phragmites, Arundo*
Cottonwood Grove (Not used in this project)	Trees *Populus, Tamarix,* and other large tree species
Desertwillow	Shrub-trees, small shrubs *Chilopsis, Hymenoclea*
Mixed Riparian	Mixture of the cover types listed above
Desert Mountains, Foothills, and Mesas	
Lechuguilla-Grass-Prickly Pear (Not used in this project)	Small succulents, large shrubs, grasses *Agave, Larrea, Erioneuron, Aristida, Opuntia*
Lechuguilla-Grass-Candelilla (Not used in this project)	Small succulents, grasses *Bouteloua, Agave, Euphorbia, Larrea*
Lechuguilla-Grass-Hechtia (Not used in this project)	Small succulents, grasses *Agave, Hechtia, Bouteloua*
Lechuguilla-Grass	Small succulents, grasses *Agave, Bouteloua*
Lechuguilla -Grass-Viguiera	Grasses, small succulents, large shrubs *Agave, Bouteloua, Aristida, Viguiera, Dalea*
Sotol-Lechuguilla-Grass	Grasses, small succulents *Agave, Dasylirion, Aristida, Bouteloua, Heteropogon*
Sotol-Nolina-Grass	Grasses, large succulents, forbs, large shrubs *Dasylirion, Nolina, Juniperus, Bouteloua, Aristida, Eriogonum*
Yucca-Sotol	Large succulents, grasses *Dasylirion, Yucca, Bouteloua*

Table 2. Continued	
Desert Plains	
Creosote Flats	Large shrubs *Larrea*
Creosote-Grass	Grasses, large shrubs *Cathestecum, Larrea, Bouteloua, Erioneuron*
Creosote-Lechuguilla	Large shrubs, small succulents, grasses *Larrea, Agave, Erioneuron, Opuntia, Parthenium*
Creosote-Tarbush	Large shrubs, small shrubs, grasses, small succulents *Parthenium, Larrea, Flourensia, Agave, Tridens*
Creosote-Yucca-Grass	Large shrubs, grasses, small shrubs, large succulents, forbs *Bouteloua, Parthenium, Larrea, Yucca, Opuntia*
Chisos Mountains	
Mixed Scrub	Large shrubs, grasses, small shrubs *Bouteloua, Acacia, Rhus, Xanthocephalum, Parthenium, Fallugia, Aloysia*
Oak Scrub	Large shrubs, small shrubs *Quercus, Cercocarpus, Rhus, Garrya*
Mixed Oak	Trees, large shrubs *Quercus, Rhus*
Oak-Ponderosa-Cypress	Trees *Quercus, Cupressus, Arbutus, Pinus*
Pinyon-Juniper-Grass	Grasses, trees, large shrubs, forbs *Stipa, Pinus, Rhus, Juniperus, Eragrastis, Muhlenbergia, Bouteloua*
Pinyon-Oak-Juniper	Trees, grasses, forbs *Quercus, Piptochaetium, Juniperus, Pinus*
Forest Meadow	Grasses *Stipa, Muhlenbergia, Eragrostis, Bouteloua*
Pinyon-Talus	Trees, shrubs *Pinus, Populus, Prunus, Rhus*

The descriptions of the cover classes used in this study are based on information described by Plumb and other researchers as well as direct observation in the field. It should be noted that in several cases the taxonomy used by Plumb has undergone several revisions (Powell 1998). The nomenclature used here follows Powell (1998) for trees and shrubs. For grasses, this paper uses nomenclature by Gould (1978). Plumb follows the same author, but cites an earlier publication (Gould 1975).

Riparian

Mesquite Thicket (Figure 6) is one of the more common vegetation cover types occurring in and along arroyos, streambeds, and runoff areas. It is also frequently found near springs, stock tanks and some steep-walled canyons in foothills and lower elevations of mountains. The vegetation cover ranges from moderately thick to dense and in some cases is almost impenetrable. The dominant vegetation typically consists of small mesquite trees *(Prosopis glandulosa)*. Other tree-shrubs found in this assemblage may include javelinabush (*Condalia ericoides*), and lotebush (*Ziziphus obtusifolia*). Creosote (*Larrea tridentata*) may also be present.

The Desertwillow (Figure 7) vegetation cover type is found on the channel bars and margins of the arroyos and larger washes of the park. The vegetation is usually sparse, consisting of the tree-shrubs Desertwillow (*Chilopsis linearis*) and Seepwillow (*Baccharis* spp.). Other species commonly found in this cover type are sparse and generally consist of annual grasses such as Sixweeks Grama (*Bouteloua barbata*). Riparian cover types often occur in relatively long, thin patches separated by exposed rock and dirt in and along streambeds and arroyos.

Figure 6. Mesquite Thicket

Figure 7. Desertwillow

In some cases, the resolution (20 m) of the satellite imagery used in this study is insufficient to fully distinguish one riparian type cover from another. The cover type Mixed Riparian is used to describe a cover type which includes the Mesquite Thicket and Desertwillow cover types as well as the other two riparian classes, Cottonwood Grove and Reed Grass, defined by Plumb but not used in this study.

The Cottonwood Grove cover type refers to closed or nearly closed canopy formed by large Cottonwood (*Populus augustifolia*) and tamarisk (*Tamarix chinensis*) trees found in the Rio Grande flood plain. The two major stands of this cover type in Big Bend National Park are located in the Cottonwood and Rio Grande Village campgrounds. Neither of these two sites is located in the area mapped in this study. To the extent that one or a few individuals of the large arboreals in this cover type occur within the areas being mapped, they will be considered part of the Mixed Riparian cover type.

The Reed Grass cover type is also found almost exclusively along the banks of the Rio Grande River, and consists primarily of very dense growths of the tall grasses Giant Reed (*Arundo donax*) and Common Reed (*Phragmites australis*). While common along the Rio Grande, the Reed Grass cover type is not known to occur in the area mapped in this study.

Desert Plains

The Creosote Flats cover type (Figure 8) is the sparsest of the vegetation classifications defined in this study and consists primarily of Creosotebush (*Larrea tridentata*). Individual plants ranging from a 0.5-1.5 m tall are widely scattered across otherwise bare soil.

Figure 8. Creosote Flats

Other plants, notably Tasajillo (*Opuntia leptocaulis*), sometimes share the cover provided by the Creosotebush, but these contribute little to the overall ground cover. This cover type is found on the lower elevations and low relief areas of the desert plains, and usually occurs on hardpan, alkaline soils, and desert pavement.

The Creosote-Lechuguilla cover type is similar to the Creosote Flats cover type except that Lechuguilla (*Agave lechuguilla*) is found in roughly equal numbers as Creosotebush. Lechuguilla is one of the most widely distributed plants in the Big Bend region and is considered an indicator plant for the Chihuahuan Desert (Powell 1998). Other plants typically occurring in this assemblage include Tasajillo, a few scattered forbs, and small patches of grasses such as Fluffgrass (*Erionueron pulchellum*). Ocotillo (*Fouquiera splendens*) may be present in some locales, but does not contribute significantly to the overall vegetation mass. Where the Creosote-Lechuguilla cover type intergrades with the Creosote Flats cover type, the Creosote-Lechuguilla type generally occupies the higher elevation.

The Creosote-Grass cover type (Figure 9) in the desert plains occurs most commonly in areas with gentle relief. Density of cover is usually greater than Creosote Flats and Creosote-Lechuguilla. Creosote is still a conspicuous shrub, but grasses, including False Grama (*Cathestecum erectum*) and Fluffgrass, dominate the vegetation cover. Succulents and semi-succulents, e.g., Cane Cholla (*Opuntia imbricata*), Ocotillo, and Leatherstem (*Jatropha dioica*) are often present. This cover type occurs on many low desert hills.

Figure 9. Creosote-Grass

Creosote-Tarbush is a cover type indicating a high degree of disturbance (Warnock 1970). Tarbush (*Flourensia cernua*) and Creosote are often found in moderately dense covers along with a number of woody shrubs, e.g. Mariola (*Parthenium incarnum*), and other scrub vegetation on moderate slopes on the lower flanks of hills and mountains. The presence of this plant assemblage often results from overuse by grazing (Warnock 1970).

The Creosote-Yucca-Grass (Figure 10) cover type is another plant assemblage that is indicative of severe disturbance from overgrazing. While the Creosote-Yucca-Grass cover type is similar to Creosote-Tarbush, it contains large semi-succulent Yucca species, most conspicuously the Giant Dagger (*Yucca faxoniana*). The Creosote-Yucca-Grass assemblage forms a somewhat denser cover than the Creosote-Tarbush cover. This cover type is only found in the extreme northeast part of the park in Dagger Flats and may possibly exist in the northern extensions of the Dead Horse Mountains.

Figure 10. Creosote-Yucca-Grass

Desert Mountains, Foothills, and Mesas

Plumb (1988) defined five cover types consisting of Lechuguilla, Grass, and another significant component. Plumb's training sites for three of these cover types, Lechuguilla-Grass-Prickly Pear, Lechuguilla-Grass-Candelilla, and Lechuguilla-Grass-Hechtia are located outside the extent of the satellite imagery used in this study. Candelilla (*Euphorbia antisyphilitica*) and Hechtia, or False Agave, (*Hechtia texensis*) do not occur in significant amounts in the area of interest in this study. While Prickly Pear cactus (*Opuntia* spp.) occurs throughout the park and sometimes is found as the locally dominant plant, it has not been located in the specific assemblage defined by Plumb in the region of interest in this study. For these reasons, these three cover types are not used as separate classifications in this study.

The cover type Lechuguilla-Grass (Figure 11) commonly occurs on the igneous derived soils of the desert mountains in Big Bend National Park and the surrounding areas. The vegetation coverage of this assemblage ranges from moderately dense to dense. Grasses, predominately grama grasses (*Bouteloua* spp.), contribute slightly more than Lechuguilla and other *Agave* species.

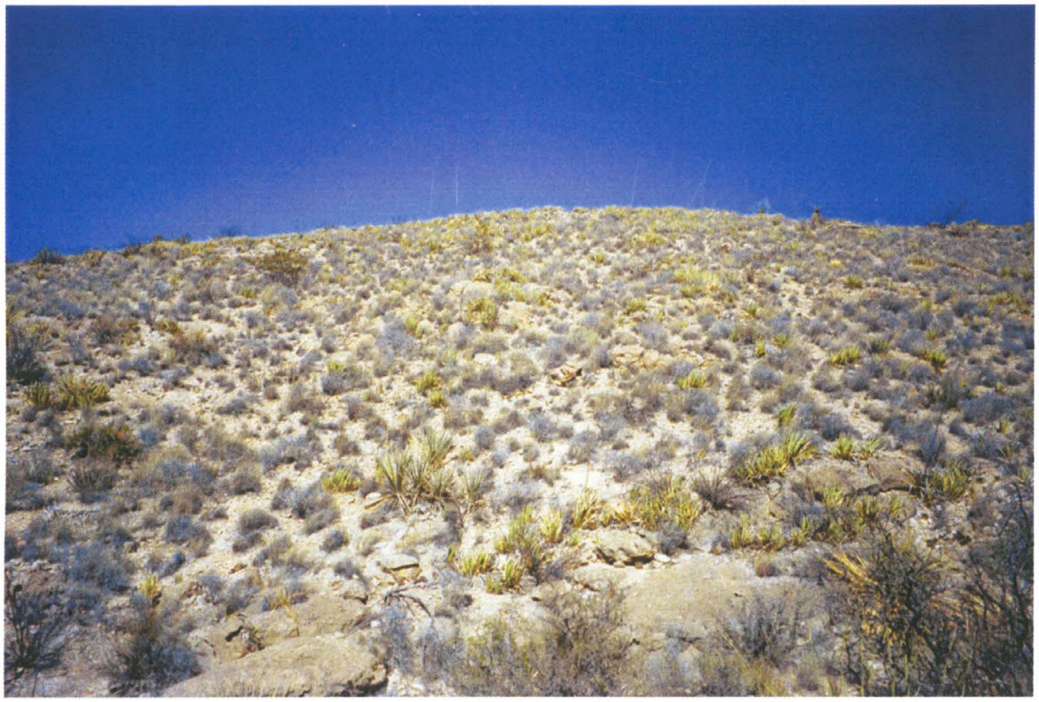

Figure 11. Lechuguilla-Grass

The Lechuguilla-Grass-Viguiera cover type occurs over the gentler slopes of foothills and the higher elevations of desert plains. This cover type may have approximately the same range of densities as the Lechuguilla-Grass cover type, but the species diversity is higher. In addition to Skeleton Leaf Goldeneye (*Viguiera stenoloba*), the shrubs Ceniza (*Leucophyllum frutescens*), Catclaw Mimosa (*Mimosa aculeaticarpa* var. *biuncifera*) and others are often found in this assemblage. Varieties of threeawn (*Aristida* spp.) and Fluffgrass are found along the dominant grama grasses. To the extent components of the Lechuguilla-Grass classes; Prickly Pear cactus (*Opuntia* spp.), Candelilla (*Euphorbia antisyphyilitica*) and Hechtia (*Hectia texensis*) occur in the area of interest they are included in this cover type.

The Sotol-Lechuguilla-Grass (Figure 12) cover type is found on the steeper slopes of the foothills to the Chisos, Rosillos, and other mountains in the Big Bend National Park area. Sotol (*Dasylirion leiophyllum*) is a conspicuous component on this community and contributes significantly to the density of vegetation cover even though Lechuguilla and grasses may constitute a majority of the cover. The species diversity is greater for this cover than the Lechuguilla-Grass cover type. Grasses typically found in this cover type include threeawn (*Aristida* spp.) and grama (*Bouteloua* spp.) species. Powell (1998) notes that Sotol is found at elevations from 670-1980 m (2200-6500 ft). Forbs are commonly found in this community but do not contribute significantly to the overall cover. Shrubs are infrequent.

Figure 12. Sotol-Lechuguilla-Grass

The Sotol-Nolina-Grass cover type is closely related to the Sotol-Lechuguilla-Grass cover type. This assemblage occurs on the higher slopes of foothills of the desert mountains forming a moderate to dense cover on moderately sloping ground. At the elevations where this cover type is found Lechuguilla is absent and is replaced by the large semi-succulent Nolina, or Beargrass (*Nolina erumpens*).

The Yucca-Sotol (Figure 13) cover occurs most frequently on the higher elevations of the limestone mountains and mesas of the park. Any of the species of yucca (*Yucca faxoniana*, *Yucca thompsoniana*, and *Yucca torreyi* are the most common) may be found in this cover along with Sotol. Lechuguilla may also be present at lower elevations. Grasses contribute significantly to the density of ground cover. Forbs are a minor component if present.

Figure 13. Yucca-Sotol

Chisos Mountains

Mixed Scrub (Figure 14) is a cover type Plumb (1988, 1992) includes in the Chisos Mountains cover types, but notes that it is also found in small and medium-sized washes of both plains and foothills. In mountainous areas it is found in culturally disturbed areas of relatively gentle slopes such as in the vicinity of roadways and campgrounds. The composition of this cover type is varied and diverse, and the cover density is moderately high to very high. The dominant vegetation is large shrubs and tree-like shrubs, including Catclaw Acacia (*Acacia roemeriana*), Whitethorn Acacia (*Acacia constricta*), Catclaw (*Mimosa borealis*), Common Beebrush (*Aloysia gratissima*), Sumac (*Rhus* spp.), Javelinabush (*Condalia ericoides*), and Lotebush (*Ziziphus obtusifolia*). Various species of grasses including grama grasses, threeawns, and Bush Muhly (Muhlenbergia porteri) may contribute to the cover density. Where mixed scrub occurs along arroyos and washes it is likely to contain components of the mixed riparian classes as well as species of adjacent upland cover types.

Figure 14. Mixed Scrub

Oak Scrub is another medium to medium-high density cover type found in desert mountains. Oak Scrub is often found where deep-cut canyons and drainages open up and slopes become gentler. Shrubs are the dominant component and include Coahuila Scrub Oak (*Quercus intricata*), Sumac, Snakeweed (*Guiterrezia* spp.), and Silktassel (*Garrya* spp.). Grasses contribute significantly to the density of vegetation cover. Forbs and large succulents and semi-succulents may also be present.

The Mixed Oak cover type is found at the base of massive escarpments and in narrow canyons and drainages in the Chisos Mountains and to a lesser extent in the higher elevations of the Rosillos and Christmas Mountains. Various species of oak trees dominate the nearly closed canopies of this cover type. The commonly found varieties of oaks in this assemblage are Chisos Oak (*Quercus graciliformis*), Emory Oak (*Quercus emoryi)*, and Gray Oak (*Quercus grisea*). Ground cover is usually sparse consisting of grasses (*Muhlenbergia* and *Bouteloua* spp.) and infrequent shrubs (e.g., sumac).

The Oak-Ponderosa Pine-Cypress cover type is found in the upper canyons of the Chisos and other mountains. This cover type is similar to Mixed Oak but large trees such as Ponderosa Pine[9], Arizona Cypress (*Cupressus arizonica*), and Douglas-Fir (*Pseudotsuga menziesii*) grow taller than the oak trees which are also likely to be present. The understory of this cover type is usually sparse because of the presence of large boulders or the effects of human disturbance.

---

[9] The tree generally called Ponderosa Pine in the Chisos Mountains is actually *Pinus arizonica* var. *stormiae*. True Ponderosa Pines occur in Texas only in the Davis and Guadalupe Mountains (Powell 1998).

The relatively open canopy of the Pinyon-Juniper-Grass cover type (Figure 15) contrasts with the closed or nearly closed canopies of the Mixed Oak and Oak-Ponderosa Pine-Cypress cover types. Grasses and trees contribute roughly equally to the moderately high densities of vegetation cover. The trees in this cover type include scatter Oak, Pinyon (*Pinus cembroides*), at least two varieties of Junipers - Alligator Juniper (*Juniperus deppeana* var. *deppeana*), and Weeping Juniper (*Juniperus flaccida*), along with tree-like shrubs such as Littleleaf Sumac and Snakeweed. Grama grasses, Bush Muhly, and Lovegrasses (*Eragrostis* spp.) contribute to the grass cover.

The distinguishing characteristic of the Pinyon-Oak-Juniper cover type is the closed or nearly closed canopy. In addition to the trees, this assemblage includes shrubs, succulents like Century Plant (*Agave havardiana*) and semi-succulents such as Nolina and Sotol. Grama grasses form the dominant ground cover. Forbs contribute a minor part of the ground cover.

The Forest Meadow cover type occurs in open, grassy areas of the higher elevations. A variety of grasses including species of *Stipa*, *Bouteloua*, *Eragrostis*, and *Muhlenbergia* compose most of the cover. Small shrubs and forbs are minor components.

Pinyon-Talus is a cover type referring to large trees growing on rocky surfaces in the higher elevation of the Chisos and other mountains.

Figure 15. Pinyon-Juniper-Grass

CHAPTER V

METHOD FOR IMAGE CLASSIFICATION

Selection of Training Sites

A training site is a representative example of each of the cover types to be identified. The spectral response patterns of the training site are extracted from the image to create a signature for the cover type. Subsequent computer analysis then assigns each pixel in the image to the most similar cover type based on the spectral signature of the pixel compared to signatures of the cover types. Training sites for each of the vegetation classes described above were located during field trips to Big Bend National Park on November 15-17, 1998, April 4-8, 1999, and May 2-7, 1999. The approach was to use Plumb's training sites wherever possible and augment them with additional training sites in the new areas of the park. Plumb identified 130 training sites covering each of the 26 vegetation classes plus water (Rio Grande) and bare soil classes. Since there are very few roads and trails relative to the size of the park, Plumb was not able to use a stratified-random approach for site selection. To maximize the number of training sites, Plumb selected his sites close to roads and trails. However all sites were at least 50 meters away from the nearest road or trail to minimize the problem of cultural structures altering the true character of the vegetation (Plumb 1988). The same methodology was followed in identifying additional training sites in the new areas of the park.

Plumb recorded the approximate location of his training sites by a description based on road or trail, for example "0.8 mi S of park boundary, 150 m W of highway" (1988, p. 402). He also marked the location of each training site on a 1:100,000 map of Big Bend National Park enclosed in his dissertation. From this information, it was possible to determine approximate UTM coordinates for each site accurate to within approximately 100 m. The estimated locations of 86 of Plumb's sites were visited on the ground to ascertain the suitability of the location as a training site in this study. A site was considered acceptable if the vegetation on the ground agreed with Plumb's classification, the approximate elevation and slope determined from topographic maps conformed to Plumb's recorded data, and the areal extent of the cover was considered broad enough for digitization during the classification process. In cases where the estimated coordinates of the site was off by more than a hundred meters, revised coordinates were established using a handheld Global Positioning System (GPS) receiver. Additional training sites were located using Plumb's methodology.

The locations of the selected training sites were digitized on the satellite image as vector polygons and then converted to raster format. The prospective training sites to be used in the classification were then used to extract a signature, a statistical characterization of each cover type, from the three bands of the SPOT image. The statistical characterization of signatures includes the minimum, maximum, and mean values of the pixels in each band. A histogram of each training site for each band was examined to determine uniformity, i.e., to insure each signature approximated a normal distribution and was unimodal. Histograms with more than one mode generally indicate the presence of multiple cover type within the training site and should be avoided (Jensen 1996). By an iterative process, training sites were refined or discarded until a satisfactory signature was obtained for each cover type. The aim was to have at least 10 times the number of pixels in each signature for each cover type as the number of bands in the image (i.e. 30 pixels) (Eastman 1999b). This goal was achieved for all training sites except Pinyon-Talus (16 pixels) and Sotol-Nolina-Grass (27 pixels). Any conclusions regarding the accuracy of these two classifications have to be tempered with the understanding that their occurrence is based on very limited training site data. Except for very isolated locations, the Pinyon-Talus cover type occurs only in the Chisos Mountains and should not affect the vegetation mapping of the new areas of the park. Likewise, the Sotol-Nolina-Grass assemblage was not observed to occur anywhere in the new areas of the park. The Sotol-Nolina-Grass cover type's absence in vegetation maps of the Rosillos Mountains area can be considered a valid finding. Appendix A is a table of the statistical data for the training sites used in this project.

Preliminary Image Analysis

Scatter diagrams (Figure 16-18) comparing each of the three bands of the input image to each other show a high degree of correlation between the bands. The lack of variability between bands is common in imagery of arid and semi-arid environments because the sparsity of vegetation and dryness results in most pixels containing a reflectance value based on a mixture of both vegetation and bare soil. Overall, high correlation between bands makes classification more difficult (Eastman 1999a).

Inspection of the mean values of selected signatures across the three bands (Figure 19 and Figure 20) illustrates another challenge in classifying the image. Many of the plots lie very close together and are nearly parallel. Signatures with nearly coincident mean plots are difficult to separate (Eastman 1999a).

Two techniques are employed to improve the ability to separate cover types. One technique is to use vegetation indices to produce an image representing the amount of vegetation present or to indicate vegetative vigor. The second technique uses ancillary data to incorporate a body of prior knowledge about probability of vegetation occurring in varying environments.

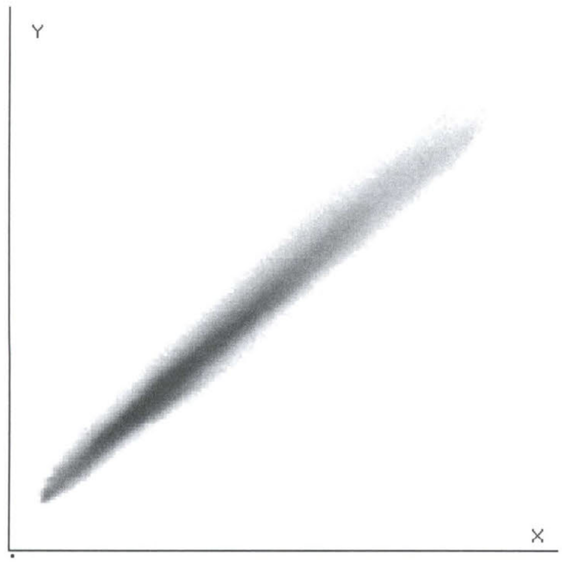

Figure 16. Scatterplot of the Green Band (Y axis) and the Red Band (X axis)

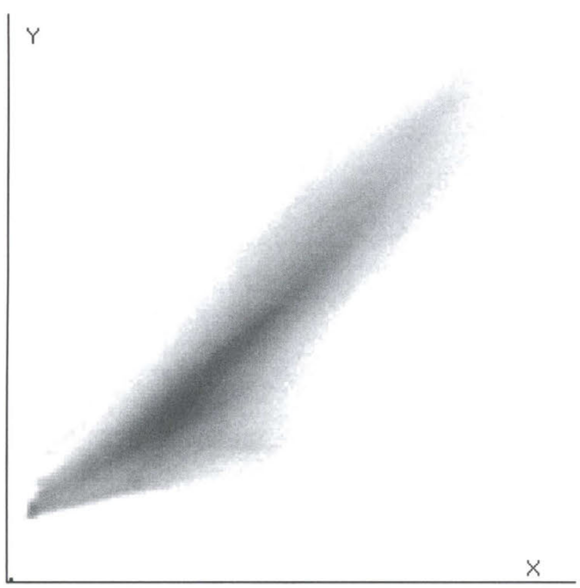

Figure 17. Scatterplot of the Green Band (Y axis) and the Infrared Band (X axis)

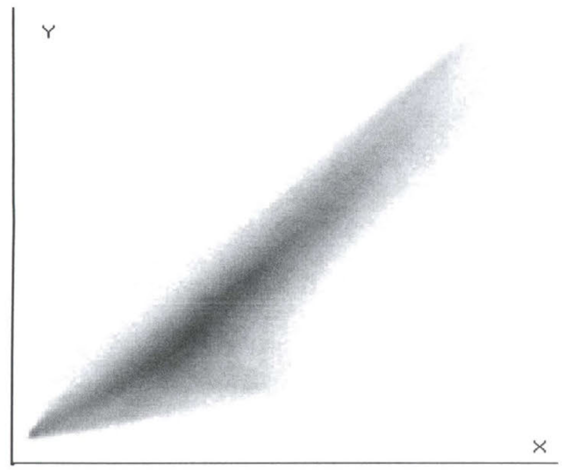

Figure 18. Scatterplot of the Red Band (Y axis) and the Infrared Band (X axis)

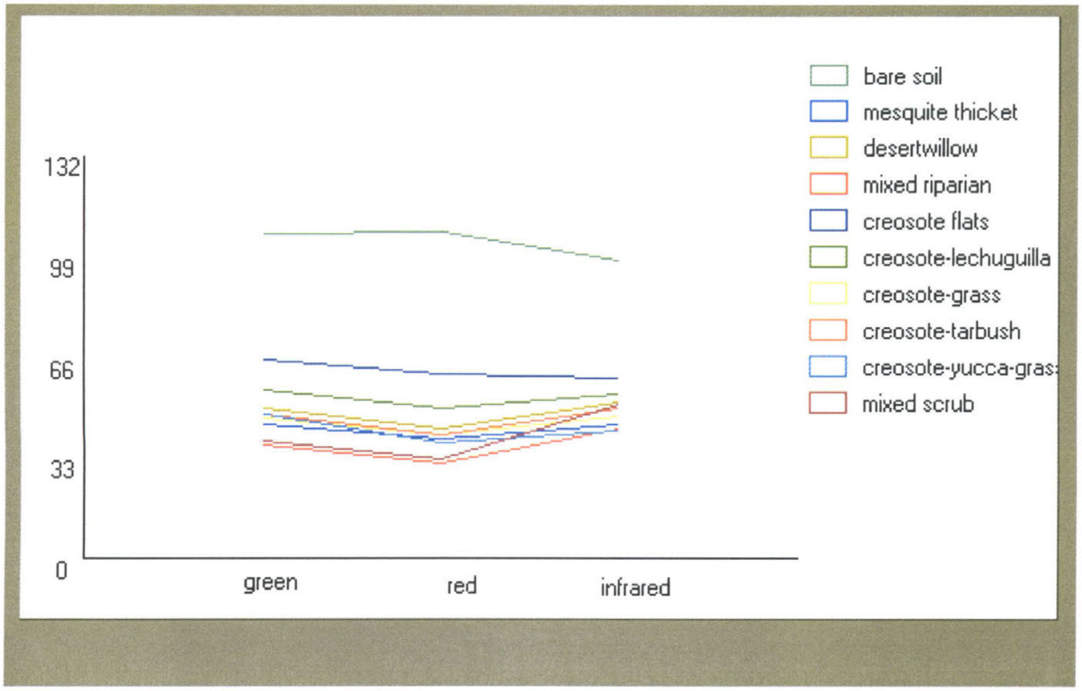

Figure 19. Signature Mean Comparison Chart 1

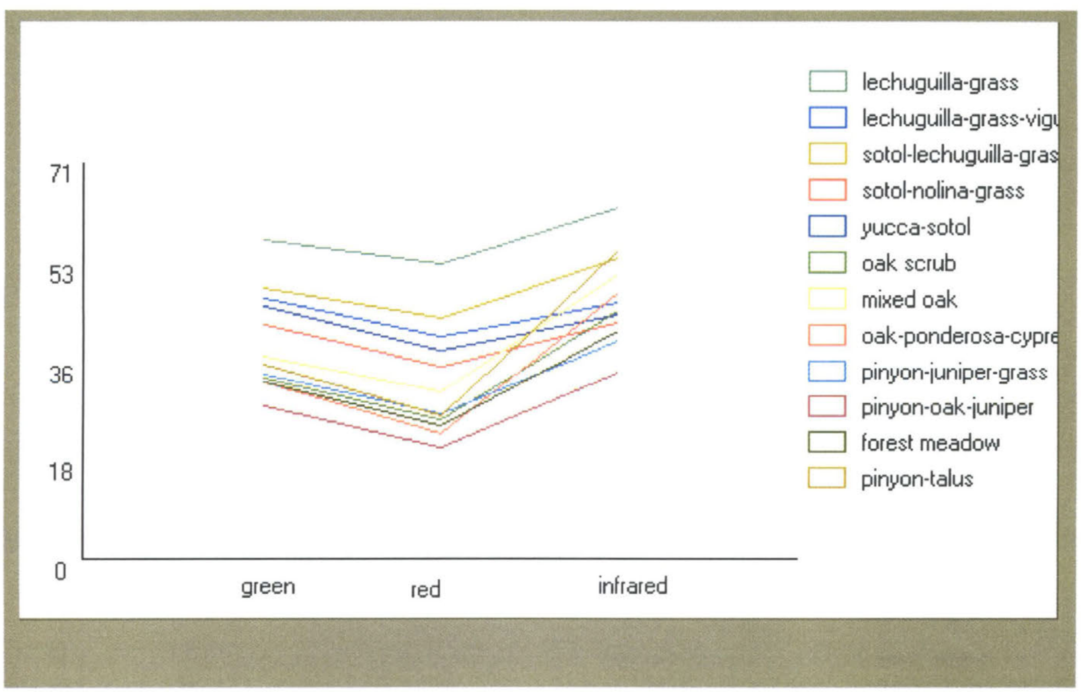

Figure 20. Signature Mean Comparison Chart 2

Application of Vegetation Indices to the Classification

A vegetation index is created by mathematically manipulating two bands on a pixel-by-pixel basis to create a new image with pixel values that can be analyzed to reveal the character of the vegetation present. A considerable body of literature exists discussing the wide variety of vegetation indices that have been created. The information presented here is from texts by Eastman (1999a) and Jensen (1996).

Vegetation indexes fall into three major families: slope-based, orthogonal transformation, and distance-based. The slope-based vegetation indices are simple linear combinations that use only the reflectance information from two bands (usually red and infrared). Band ratioing, created by dividing the reflectance values of one band by another and the Normalized Difference Vegetation Index (NDVI) are widely used examples of slope-based vegetation indices. The slope-based indices are so named because the values in the index form a spectrum of lines that pass through the origin and differ in their slope value. The slope value is indicative of the abundance of vegetation and vigor of the biomass.

In arid and semi-arid lands where the vegetation cover is rarely closed, the most effective indices are the ones that effectively model the relative density of vegetation and minimize the effect of reflectance due to soil brightness. The distance-based vegetation indices are based on the concept that the reflectance values of bare soil of varying degrees of moisture content will form a line (known as the soil line). Pixels with little vegetation are assumed to lie close to the soil line, as measured by the perpendicular distance, and pixels with higher vegetation content will lie farther away from the soil line. The soil line is developed through a linear regression of the infrared band against the red band for a sample of bare soil pixels. Some distance-based vegetation indexes require the red band to be the independent variable and others require the infrared band to be the independent variable. The specific application of a slope-based vegetation index is discussed below.

A third family of vegetation indices, the orthogonal transformation indices, transform the available spectral bands into a new set of uncorrelated bands within which a green vegetation index band can be identified. The Tasseled Cap transformation and Principal Component Analysis are examples of this family of vegetation indices. Such indices are very useful when many bands of data are available, from hyperspectral imagery or Landsat Thematic Mapper, for example. Since the SPOT image used in this project has only three bands of data, vegetation indices of this family were not used.

To make use of distance-based vegetation indices, a soil line was developed from a sample of 76 bare soil pixels selected from all areas of the image. Bare soil areas in the SPOT image are easy to detect by inspection of the satellite image because of their brightness (high reflectance values). For most pixels in the sample, it was possible to confirm the pixels represented bare soil from field notes or by inspection of 1.0 m DOQQs. In all other cases, the determination of bare soil was obvious as in the case of graded dirt roads or dry streambeds. Twelve different vegetation indices were derived from the red and infrared bands of the satellite image. By visual inspection, comparison to DOQQs, and comparison to training sites, the Weighted Difference Vegetation Index (WDVI) was determined to provide the best contrast, and to show the most variation in both high vegetation and low vegetation areas. The formula for the WDVI (Eastman 1999a) is:

$$WDVI = \rho n \cdot \gamma \rho r$$

Where

ρn = reflectance of near infrared band

ρr = reflectance of visible red band

γ = slope of the soil line

From Eastman (1999a, p.118), "The effect of weighting the red band with the slope of the soil line is the maximization of the vegetation signal in the near-infrared band and the minimization of the effect of soil brightness." The soil line for the WDVI is computed with the infrared band as the independent variable. The soil line equation determined from the sample is:

$$Y = -20.639343 + 1.290923X$$

Application of Prior Knowledge to the Classification

The main software package used in this project is IDRISI32©[10], a raster-based GIS and image processing system designed to operate on personal computers equipped with Microsoft Windows 32 bit operating systems. IDRISI32© has the capability of incorporating prior knowledge about the cover categories to be classified as probability images. A probability image for a given cover type has a value from 0 to 1 for each pixel

[10] ©1999, Clark Labs, Clark University, Worcester, MA

indicating the prior probability for the particular cover type to occur in that location. Multiple sources of information can be incorporated into a single probability map. For example, if it is known that a plant community only occurs at elevations above 1500 meters, one can create a probability image from a DEM that has a value of 1.0 for all locations above 1500 meters and 0.0 for all locations below 1500 meters. If one also has information indicating the plant community favors north-facing slopes a probability map can be created from an aspect model that has high values for north-facing slopes (i.e., having an aspect azimuth ranging from 315° to 45°, for example) and lower probabilities for all other locations. In addition, IDRISI32© has built-in functions to create fuzzy set membership functions in which the transition between locations definitely included in the set and those definitely excluded is gradual. A fuzzy set is characterized by a fuzzy membership grade, or possibility, that ranges from 0.0 to 1.0, which indicates a continuous increase from nonmembership to complete membership (Eastman 1999a). In the aspect example above, if aspect azimuths from 330° to 30° are assigned a probability of 1.0, and azimuth values from 45° to 315° are given value of 0.0, then values in the ranges from 315° to 330° increase gradually from 0.0 to 1.0, and values in the range from 30° to 45° decrease gradually from 1.0 to 0.0. Several possible functions are available to mathematically describe the gradual transition in the fuzzy membership grade from probability 0.0 to probability 1.0. Three functions are provided with IDRISI32©. These functions are linear, J-shaped, and sigmoid (s-shaped). In this project, the sigmoid function was used for the creation of all fuzzy sets because its characteristic s-shape is representative of many natural phenomena in that it resembles the cumulative probability density function for a normal distribution (Kreyszig 1968). Once probability functions are constructed for each of the relevant bodies of knowledge (variables) for a cover type the probability functions can be combined into a single probability image using a "min" function. The min function, defined as the intersection operator for fuzzy sets (Eastman 1999a), assigns the minimum value among all the pixel values considered at a particular location. The resulting image represents at each location the lowest probability that the cover type will occur. Using the min operator on fuzzy sets is analogous to performing a logical "and" operation on discrete sets. The process of creating probability images is repeated for each classification cover type. The probability maps are then used as an input to the classifier.

Probability images are a powerful tool in resolving ambiguities in classification if the prior knowledge about the cover types to be classified can be properly characterized in fuzzy sets. As noted in the literature review, many researchers including Warnock (1970, 1977), Powell (1998), Wauer (1973a, 1973b), and Henrickson and Johnston (1983) have studied vegetation in the Big Bend region and developed a considerable body of knowledge concerning the vegetation communities found in the region. Plumb's research built on this body of knowledge by rigorously quantifying the data he collected. Creating probability images that incorporate this prior knowledge is one of the most valuable steps in developing more accurate vegetation maps. Probability images are especially important in creating vegetation maps for semi-arid terrain given the inherent difficulties classifying vegetation cover. Plumb, in his dissertation research (1988), incorporated a priori knowledge from the researchers before him in the development of his classification system. He then formalized the knowledge acquired in his own research into rules-based algorithms embodied in computer programs. Probability images effectively accomplish the same end as rules based algorithms, but they have the advantage of being easier to develop and easier to modify for non-programmers. Probability images do not depend on a programming language to make use of the encapsulated knowledge. Instead, probability images depend only on the ability to perform basic mathematical functions on large arrays of data. Of course, the IDRISI32© software used in this project had these mathematical functions packaged in powerful, relative easy-to-use modules, but most other commonly available GIS packages such as ArcView®[11] and ERDAS IMAGINE®[12] have the ability to perform the same underlying mathematical functions. The key point is that carrying forward the body of knowledge captured in probability maps for future research is dependent primarily on the existence of GIS software with the ability to perform basic mathematical functions and not on a particular software package.

The most effective knowledge about the distribution of vegetation communities in Big Bend National Park was related to elevation. Most researchers of vegetation in Big Bend National Park delineate vegetation communities by elevations in which the various communities are found (Plumb 1988, Powell 1998, Warnock 1977, Wauer 1973b). Since rainfall and temperature are both correlated to elevation (Plumb 1988, Schmidt 1983), elevation is, in effect, an indirect surrogate for those variables as well. Elevation is quantified in readily usable form in a DEM. If one has knowledge of the elevations where

[11] ® Environmental Systems Research Institute, Inc., Redlands, CA

vegetation communities grow, then it is straightforward to process this information into a probability image for each vegetation cover type. The following example illustrates the process. Elevation data for the training sites is extracted from the DEM. From this information basic statistics including mean, standard deviation, maximum, minimum, and range are calculated. This data from the training sample is compared with Plumb's data to confirm concordance between the Plumb's training sample and the training data gathered in this project. The mean value of the training sample with the higher number of pixels is then used as the center of the range of values given the highest probability. In the case of Sotol-Lechuguilla-Grass, the mean value for elevation from Plumb's training data is 1227 m and the standard deviation is 127 m. All elevations within 2.00 standard deviations (973-1481 m) of the mean are assigned a probability of 1.0. All elevations between 2.00 and 2.32 standard deviations (973-934 m, 1481-1519 m) are assigned monotonically decreasing probabilities from 1.0 at 2.00 standard deviations to 2.32 standard deviations. The idea is that given a valid sample 95.44% of all occurrences of Sotol-Lechuguilla-Grass should be found between 973 m and 1481 m and virtually no occurrences of Sotol-Lechuguilla-Grass should be found outside of the range of 934-1519 m. Similar reasoning was used in developing probability images for each set of training data and for each factor.

Slope is the next most important factor considered. Most researchers indicate by qualitative description whether particular vegetation assemblages are found on flat ground or rolling hills or steep canyon walls. Both Cochran and Rives (1985) and Plumb

---

[12] ® ERDAS, Inc., Atlanta, GA.

(1988) quantified this knowledge. Cochran and Rives also relate slope to runoff and soil type in their soil survey of Big Bend National Park. Thus, slope data can be considered to represent those factors. Slope data is derived directly from DEM data, and therefore, can be transformed into a probability image.

Aspect, the direction of slope, is another factor related to the occurrence of vegetation communities. Most researchers note the difference in vegetation growing on west and south-facing slopes compared to vegetation on north and east-facing slopes. For example Powell (1998) states, "Ponderosa Pine and *P. arizonica* are not restricted to the highest elevations but may also occur on north and east slopes and in protected canyons at intermediate locations" (p. 10). However, Plumb recorded aspect information for all of his training sites but could not substantiate a definite aspect preference for any vegetation type. Qualitative field observations suggests that it is common to find differences in both vegetation density and vegetation cover type based on aspect, but preference is very localized. In some locations, notably in the foothills on the western side of the Chisos Mountains, the Sotol-Lechuguilla-Grass assemblage was found only on north facing slopes while Lechuguilla-Grass grew only on south facing slopes. Plumb's data, on the other hand, indicated that Sotol-Lechuguilla-Grass appears to favor south facing slopes and is one of only two classes that showed even a weak preference toward a particular aspect (1988). Aspect data was only incorporated into probability maps for Sotol-Lechuguilla-Grass and Lechuguilla-Grass cover types. Training sites for these two cover types were digitized as additional interim categories in the location west of the Chisos where the aspect preference was obvious. Probability maps based on aspect preference for these interim classes were then created with probabilities assigned accordingly. After classification was complete, the interim classes were combined with their respective original classes.

Distance to water is another factor strongly related to vegetation type. The riparian vegetation classes grow only where water flows at least some of time in ephemeral streams, springs, and stock tanks. DLGs of hydrology features are one source for determining the location of water sources. As noted earlier, only main channels of streams are digitized; many smaller drainages, which are clearly visible in both satellite imagery and DOQQs, are not digitized. To augment the DLG data a RUNOFF function, which calculates the accumulation of rainfall units per pixel as if one unit of rainfall was dropped on every location, was used to derive a drainage network from the satellite image. The computed drainage network was combined with the rasterized DLG data to produce a single image showing the consolidated drainage network for an area corresponding to the satellite image. From this image, a probability map was created with the highest probabilities assigned to locations within 100 m of the drainage network and decreasing to zero probability for distances greater that 200 m from water.

Prior knowledge of the spatial distribution of one vegetation cover type, Creosote-Yucca-Grass, was incorporated in a probability map. Plumb (1988) identified this vegetation cover as occurring on the extreme northeast sections of the park. Henrickson and Johnston (1983) using the term Yucca Woodland only note locations in the Mexican part of the Chihuahuan Desert. The only occurrence of Faxon Yucca or Giant Dagger (*Yucca faxoniana*), one of the key yucca species in this assemblage, Powell (1998) identifies within Big Bend National Park is the same Dagger Flat location of Plumb's two training sites. Powell also indicates that another key species in the cover type, Thompson Yucca (*Yucca thompsoniana*), is abundant only in the Black Gap Refuge east of Big Bend National Park. Preliminary classification results showed that both the minimum-distance-to-mean and maximum likelihood classifier overestimated the occurrence of Creosote-Yucca-Grass. A probability image was created to indicate a high probability for Creosote-Yucca-Grass to within 1,000 meters of the training sites then decreasing to a probability of 0.0 at distance of 3.000 meters. It should be noted that Yucca species other than Faxon Yucca occur throughout the park and the Yucca-Sotol assemblage is not limited to the Dagger Flat area.

The Weighted Difference Vegetation Index (WDVI) image was also used to create probability images for each cover type. The pixel values from the WDVI image corresponding to the location for each training site were extracted from the image. From this information, basic statistics such as mean and standard deviation were used to determine the characteristic values of each training site relative to the vegetation index. These values were then used to create a probability image for each cover type.

The specific values used in the creation of probability maps for all cover types are given in Table 3. Except where noted, values in the table are the inflection points of a sigmoid (s-shaped) curve. If four values are given, the set has both an upper and lower range of membership values (e.g. elevations above 900-1000 m and below 2000-2100 m) If only 2 values are given the membership set has only one transition range (e.g. slopes greater than 45-50%). Monotonically decreasing means the probability is decreasing from

1.0 to 0.0 through the range. Monotonically increasing means the probability increasing from 0.0 to 1.0.

Table 3. Specific Values Used to Create Probability Images for Each Vegetation Cover Type

Vegetation Cover Type	Factor	Fuzzy Membership Function
Bare Soil	Elevation	None
	Slope	None
	Aspect	None
	Distance to Water	None
	WDVI	-1.728588 -1.284754 monotonically decreasing
Mesquite Thicket	Elevation	1100, 1300 m monotonically decreasing
	Slope	3, 4 % monotonically decreasing
	Aspect	None
	Distance to Water	120, 360 m monotonically decreasing
	WDVI	-1.32509, -0.837753, 2.086269, 2.573606
Desertwillow	Elevation	1100, 1300 m monotonically decreasing
	Slope	3, 4 % monotonically decreasing
	Aspect	None
	Distance to Water	120, 360 m monotonically decreasing
	WDVI	-0.816589, -0.389873, 2.170423 2.597139
Mixed Riparian	Elevation	1500, 1300 monotonically increasing
	Slope	3, 4 % monotonically decreasing
	Aspect	None
	Distance to Water	None (to allow for unmarked springs & tanks)
	WDVI	0.5904, 0.7821362, 2.0904538, 2.28219
Lechuguilla-Grass	Elevation	789, 816,1180,1207
	Slope	0%, 3% monotonically increasing
	Aspect	None
	Distance to Water	60 m, 120 m monotonically increasing
	WDVI	-0.2240, -0.0003, 1.5262, 1.7499
Lechuguilla-Grass-south facing	Elevation	789, 816,1180,1207
	Slope	0%, 3% monotonically increasing
	Aspect	90, 135, 270, 315 monotonically increasing
	Distance to Water	60 m, 120 m monotonically increasing
	WDVI	-0.2240, -0.0003, 1.5262, 1.7499
Lechuguilla-Grass-Viguiera	Elevation	810 m, 840 m, 1240 m, 1277 m
	Slope	0%, 3% monotonically increasing
	Aspect	None
	Distance to Water	60 m, 120 m monotonically increasing
	WDVI	.0958 .3410 2.0137 2.2258
Sotol-Lechuguilla-Grass	Elevation	934 m, 73 m, 1481 m, 1519 m
	Slope	0%, 3% monotonically increasing
	Aspect	None
	Distance to Water	None
	WDVI	-0.4036, -0.0465, 2.3906, 2.477

Table 3. Continued

Vegetation Cover Type	Factor	Fuzzy Membership Function
Sotol-Lechuguilla-Grass-north facing	Elevation	934 m, 73 m, 1481 m, 1519 m
	Slope	0%, 3% monotonically increasing
	Aspect	1-prob[south and east facing]
	Distance to Water	None
	WDVI	0.1441, 0.3286, 1.5871, 1.7716
Sotol-Nolina-Grass	Elevation	1296 m, 1334 m, 1790 m, 1828 m
	Slope	3.0%, 3.8%, 14.5%, 15.3%
	Aspect	None
	Distance to Water	None
	WDVI	1.40474, 1.446152, 1.910104, 1.941887
Yucca-Sotol	Elevation	1296 m, 1334 m, 1790 m, 1828 m
	Slope	None
	Aspect	None
	Distance to Water	None
	WDVI	0, 0.08, 0.92,1.0
Creosote Flats	Elevation	1100 m, 1300 m monotonically decreasing
	Slope	7.24%, 7.84% monotonically decreasing
	Aspect	None
	Distance to Water	20 m, 40 m monotonically increasing
	WDVI	-1.2, -1.268677, -0.066750, -0.0001
Creosote-Grass	Elevation	1040 m, 1120 m monotonically decreasing
	Slope	42.53%, 51.30% monotonically decreasing
	Aspect	None
	Distance to Water	None
	WDVI	0.1414, .2933, 1.3406, 1.4924
Creosote-Lechuguilla	Elevation	1100 m, 1300 m monotonically decreasing
	Slope	7%, 11% monotonically increasing
	Aspect	None
	Distance to Water	None
	WDVI	0.50962, -0.3840, 1.1442, 1.2667
Creosote-Tarbush	Elevation	828 m, 893 m, 1213 m, 1268 m
	Slope	6%, 10% monotonically increasing
	Aspect	None
	Distance to Water	None
	WDVI	0.4813, 0.6126, 1.5081, 1.6393
Creosote-Yucca-Grass	Elevation	905 m, 938 m, 1158 m, 1191 m
	Slope	None
	Aspect	None
	Range from Training Site	2000 m, 3000 m monotonically decreasing
	WDVI	None

Table 3. Continued

Vegetation Cover Type	Factor	Fuzzy Membership Function
Mixed Scrub	Elevation	1782 m, 1844 m monotonically decreasing
	Slope	None
	Aspect	None
	Distance to Water	None
	WDVI	0.763769, 1.14921, 3.417833, 3.796985
Oak Scrub	Elevation	1340 m, 1440 m monotonically increasing
	Slope	None
	Aspect	None
	Distance to Water	None
	WDVI	0.476841, 1.045771, 4.459351, 5.02281
Mixed Oak	Elevation	1340 m, 1440 m monotonically increasing
	Slope	None
	Aspect	None
	Distance to Water	None
	WDVI	0.603003, 1.130167, 4.293151, 4.820315
Oak-Ponderosa-Cypress	Elevation	1340 m, 1670 m monotonically increasing
	Slope	3%, 6*%, 94*%, 97%
	Aspect	None
	Distance to Water	None
	WDVI	1.208388, 1.763646, 1.763646, 1.763646
Pinyon-Juniper-Grass	Elevation	1340 m, 1670 m monotonically increasing
	Slope	None
	Aspect	None
	Distance to Water	None
	WDVI	
Pinyon-Oak-Juniper	Elevation	1340 m, 1670 m monotonically increasing
	Slope	None
	Aspect	None
	Distance to Water	None
	WDVI	1.599827, 1.758928, 2.713534, 2.872635
Forest Meadow	Elevation	1340 m, 1670 m monotonically increasing
	Slope	36%, 45% monotonically decreasing
	Aspect	None
	Distance to Water	None
	WDVI	1.260307, 1.563951, 3.385815, 3.689459
Pinyon-Talus	Elevation	1340 m, 1670 m monotonically increasing
	Slope	30%, 36.6% monotonically increasing
	Aspect	None
	Distance to Water	None
	WDVI	2.389029, 2.743384, 4.869514, 5.223869

Image Classification

Once training sites and probability images are completed, the three bands of satellite image are ready for classification. IDRISI32© has three hard classifiers available, so called because they make a definitive decision about the membership category of each pixel. The three hard classifiers implemented in IDRISI32© are parallelepiped, minimum distance to means, and maximum likelihood. They are all based on logic that assigns the expected position of a class (determined from training site signatures) in band space, and then judges the class to which each pixel belongs by some measure of the location of the pixel relative to the class positions.

The parallelepiped classifier assigns a pixel to a class based on whether the pixel's location lies in a rectangle drawn around the location of the training site pixels. Figure x is a two-dimensional example of training site signatures drawn as rectangles and overlaid on the scatter diagram for band 1 (green) and band 2 (red) of the satellite image used in this project. A clear drawback of the parallelepiped classifier can be seen in the figure. The signatures show considerable overlapping. For pixels lying in areas of overlap, the assignment to a class is arbitrary. In addition, pixels lying outside the rectangles are unassigned.

The minimum distance to means classifier calculates the mean location of each of the training sites and assigns pixels based on which class mean is nearest. Although the minimum distance to means classifier accounts for class mean, it does not take into

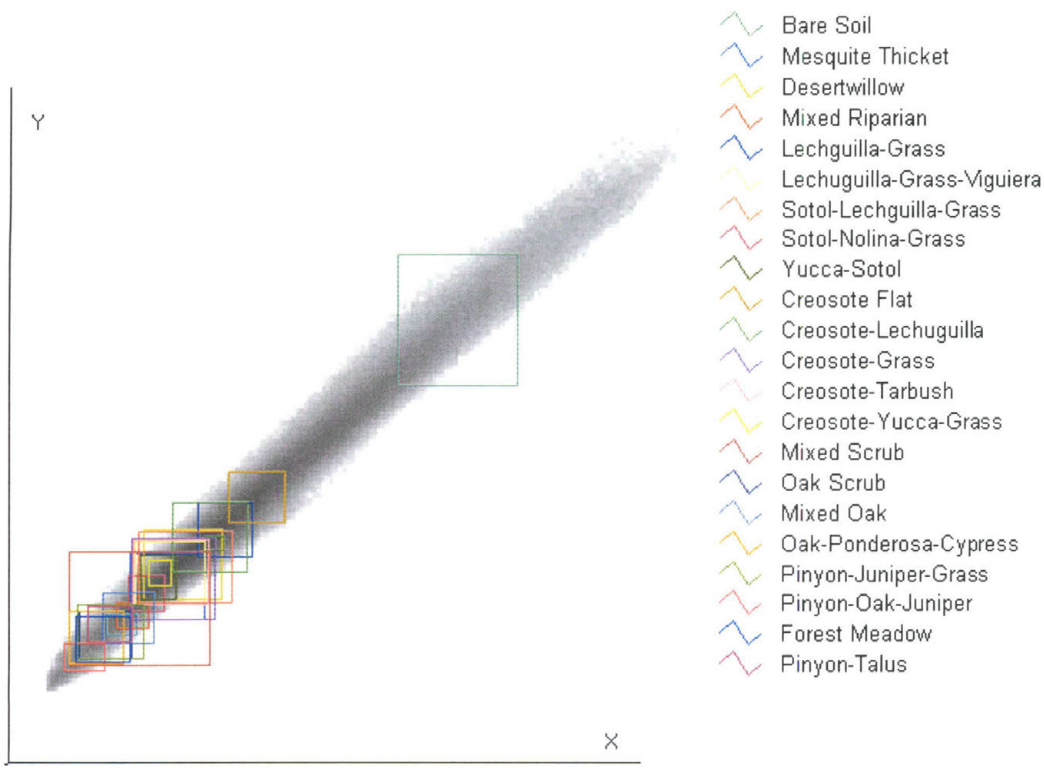

Figure 21. Parallelepiped Signatures Overlaid on Scatterplot of the Green Band (Y-axis) and the Red Band (X-axis).

account the differing variability between signatures. It performs poorly when the means of signatures are close to each other or when training sites have high variability.

The maximum likelihood classifier use both mean and variance of the training signature to estimate the probability that a pixel belongs to a certain class. Because the maximum likelihood classifier uses the most refined statistical characterization of the training sites, it tends to produce the most accurate results. The drawback of the maximum likelihood classifier is that it is computationally intensive and runs slower than the other two hard classifiers. All three hard classifiers were used to classify the satellite image. As expected, the parallelepiped classifier performed poorly. Although it runs very quickly due to the simple underlying methodology, it performs poorly when signatures overlap as they do in this image. The minimum distance to means classifier performed better than the parallelepiped classifier, but cursory inspection showed it to be unacceptable. For example, all of the Riparian classes were shown to be widely and thinly distributed uniformly across the image, Chisos Mountain classes were shown in desert plains regions, and Desert Plains classes were detected in the high Chisos region. These same problems still occurred, but to a considerably lesser extent, when the maximum likelihood classifier was used without the probability images, i.e., when an equal probability of occurrence is assigned to every cover type at every location. The most satisfactory results were obtained with the combination of the maximum likelihood classifier and probability maps.

Images of the vegetation maps resulting from the classifications are shown in the following figures:

Figure 22. Vegetation Map of the SPOT Image Area.

Figure 23. Vegetation Map of Areas of Big Bend N. P. Added since 1989.

Figure 24. Vegetation Map of the Bone Spring Quadrangle.

Figure 25. Vegetation Map of the Butterbowl Quadrangle.

Figure 26. Vegetation Map of the Grapevine Hills Quadrangle.

Figure 27. Vegetation Map of the Persimmon Gap Quadrangle.

Figure 28. Vegetation Map of the Sombrero Peak Quadrangle.

Figure 29. Vegetation Map of the Twin Peaks Quadrangle.

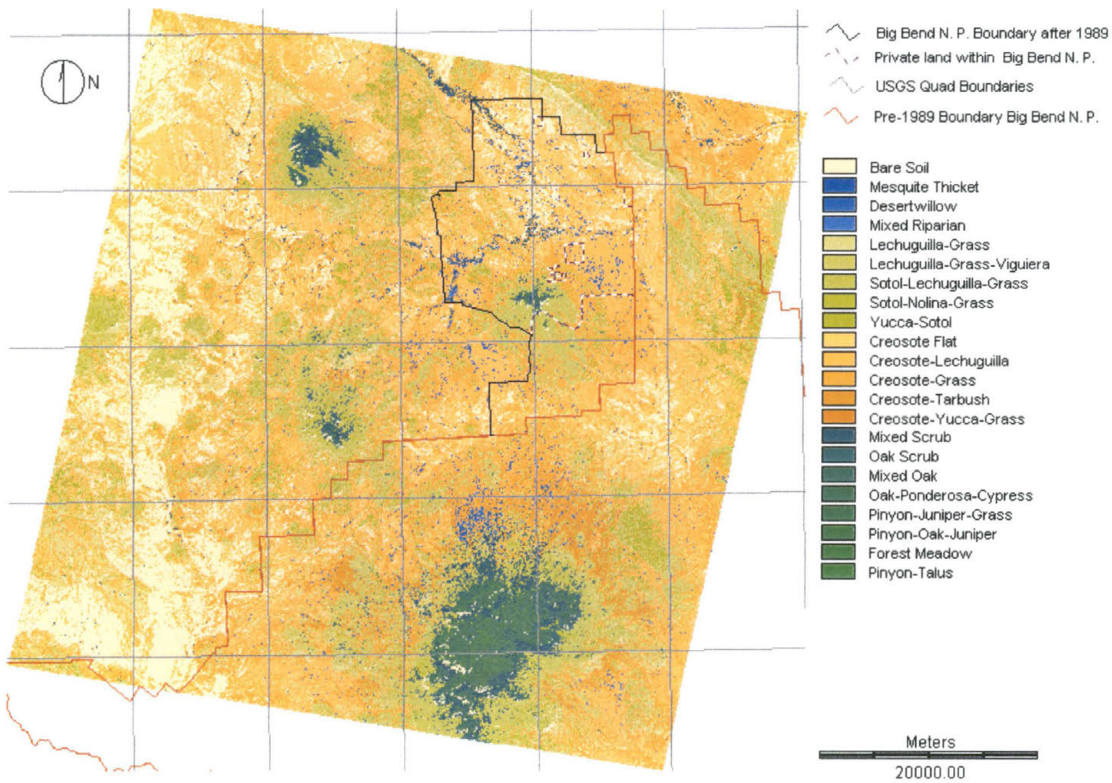

Figure 22. Vegetation Map of the SPOT Image Area.

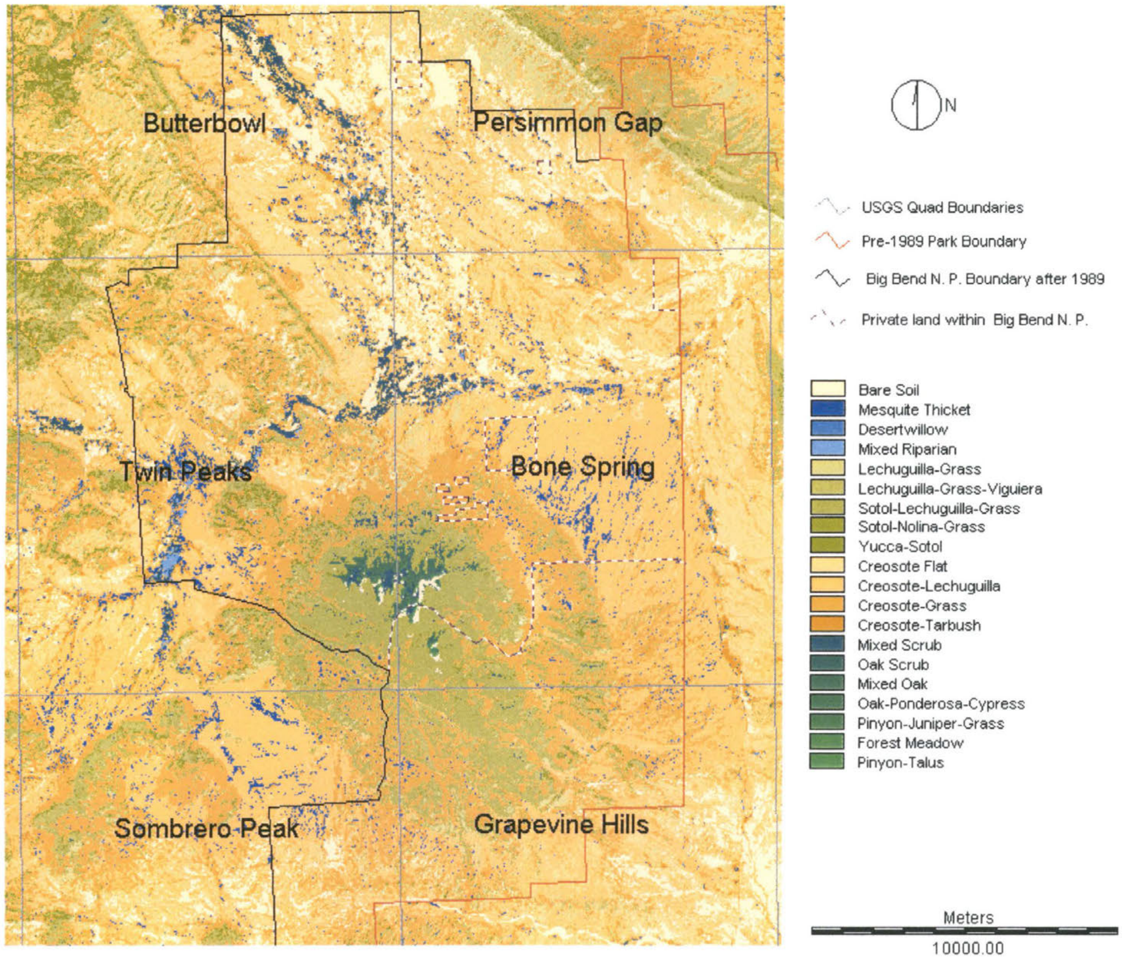

Figure 23. Vegetation Map of Areas of Big Bend N. P. Added since 1989.

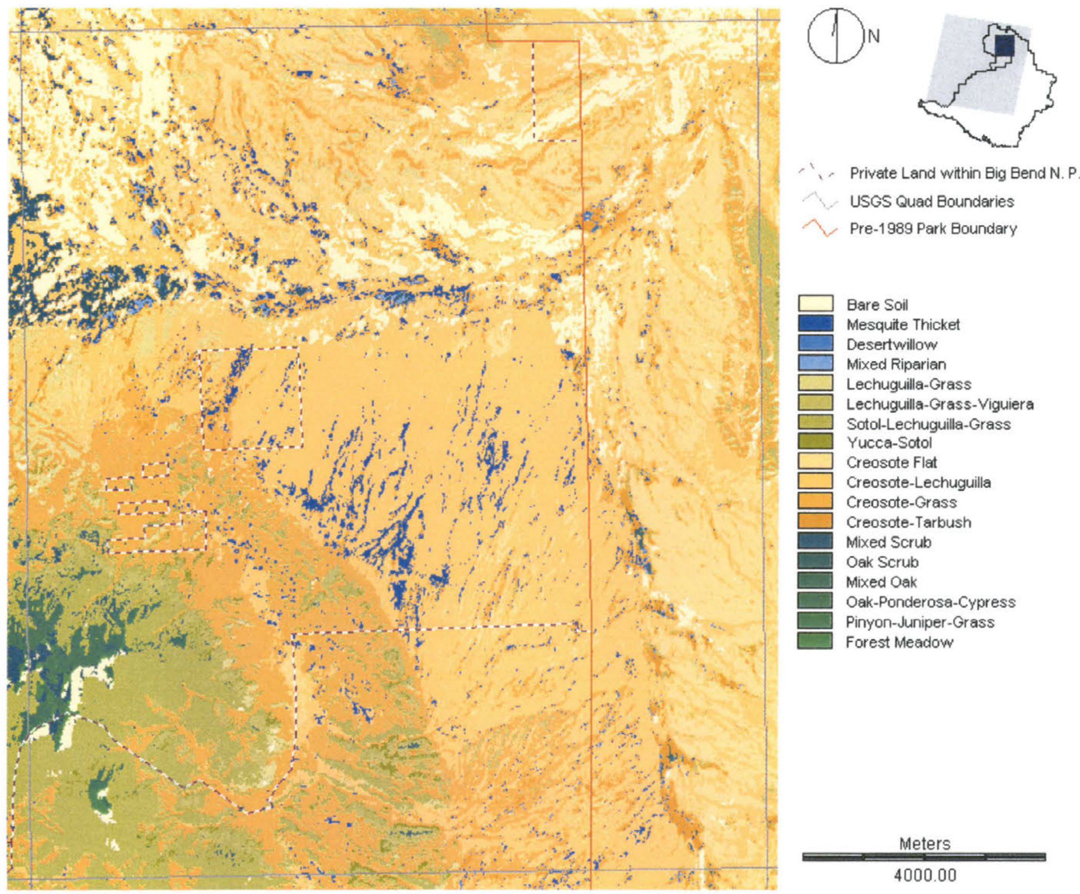

Figure 24. Vegetation Map of the Bone Spring Quadrangle.

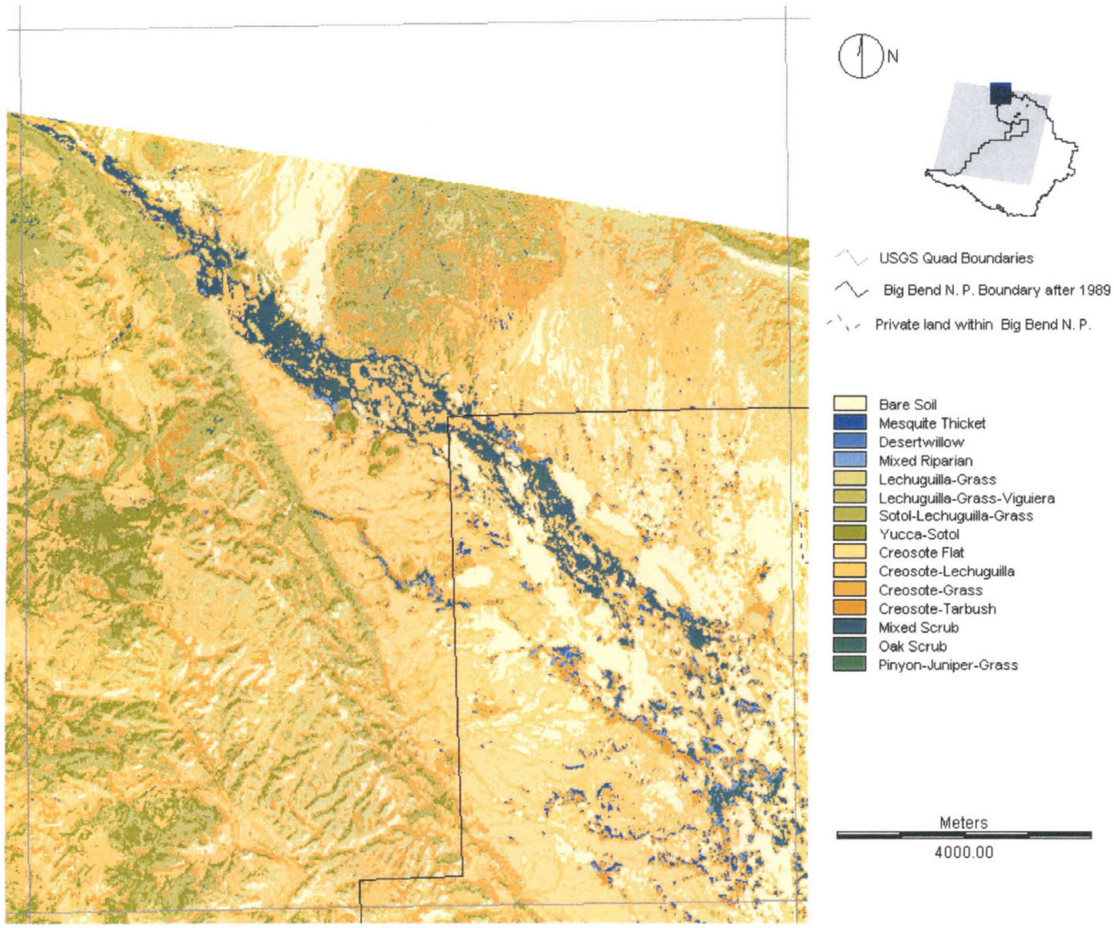

Figure 25. Vegetation Map of the Butterbowl Quadrangle.

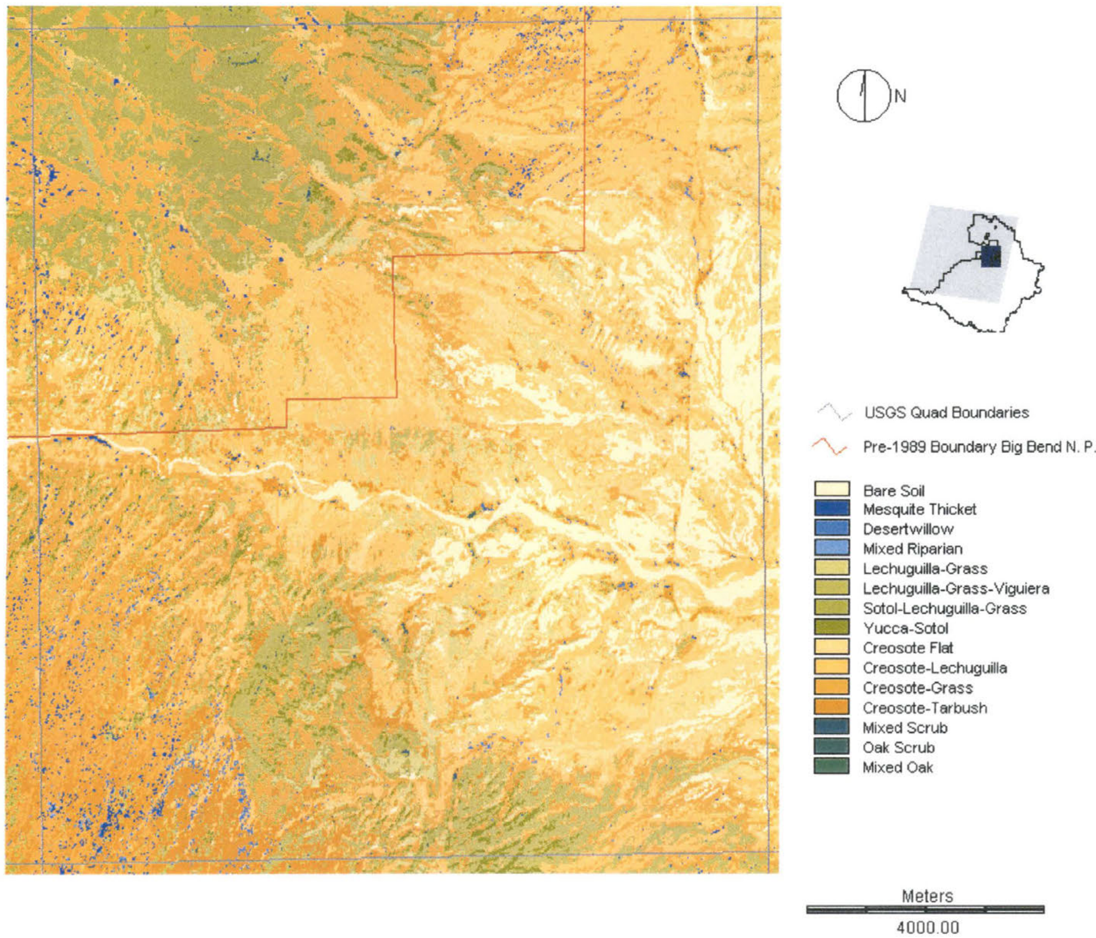

Figure 26. Vegetation Map of the Grapevine Hills Quadrangle.

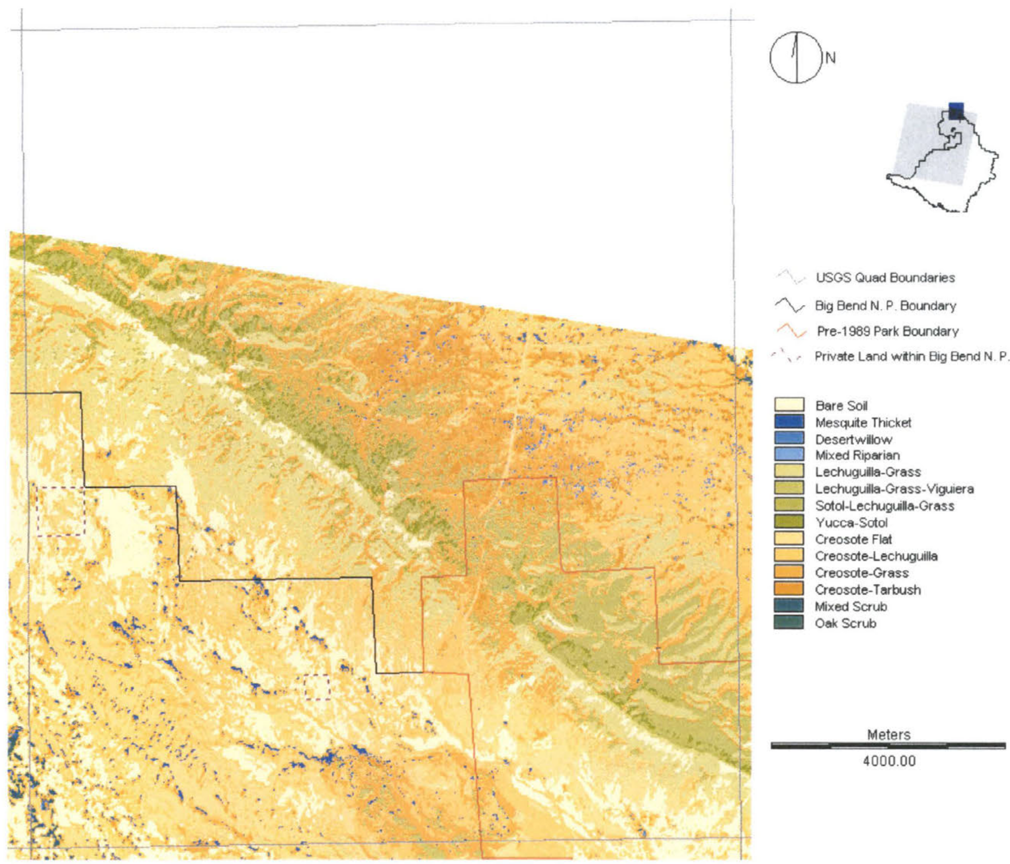

Figure 27. Vegetation Map of the Persimmon Gap Quadrangle.

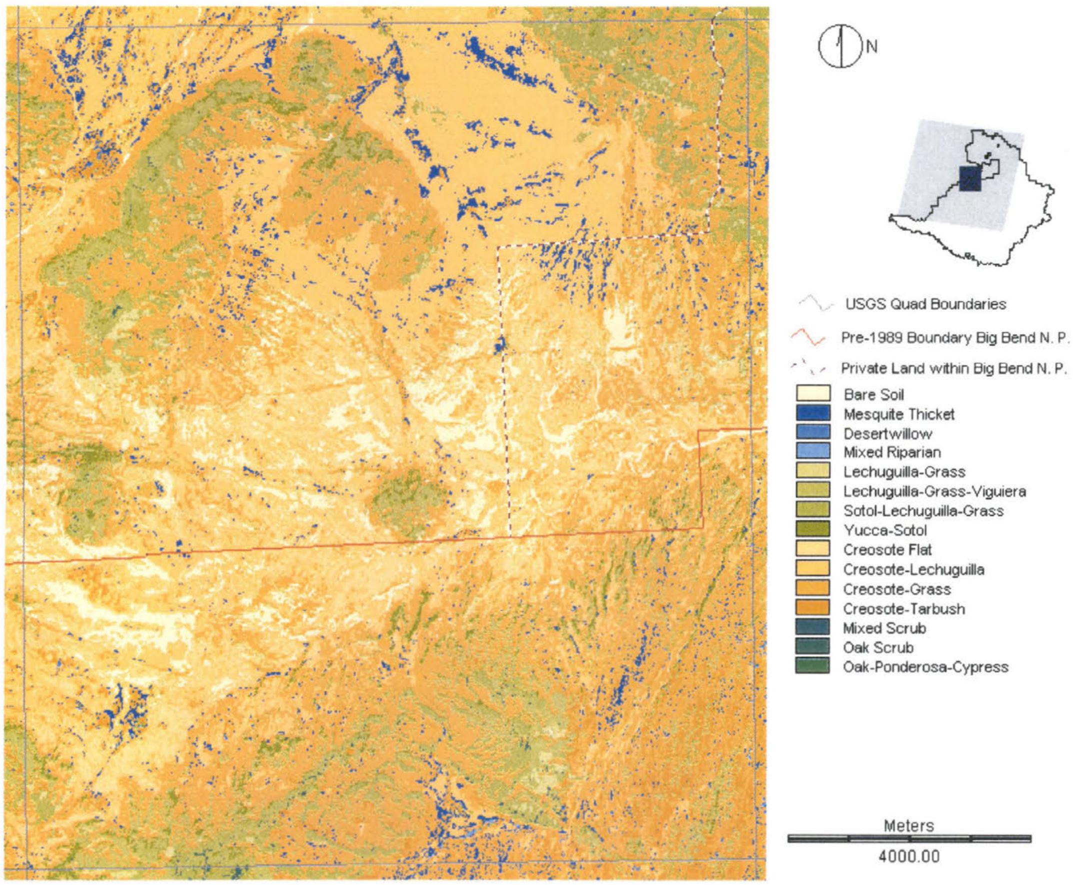

Figure 28. Vegetation Map of the Sombrero Peak Quadrangle.

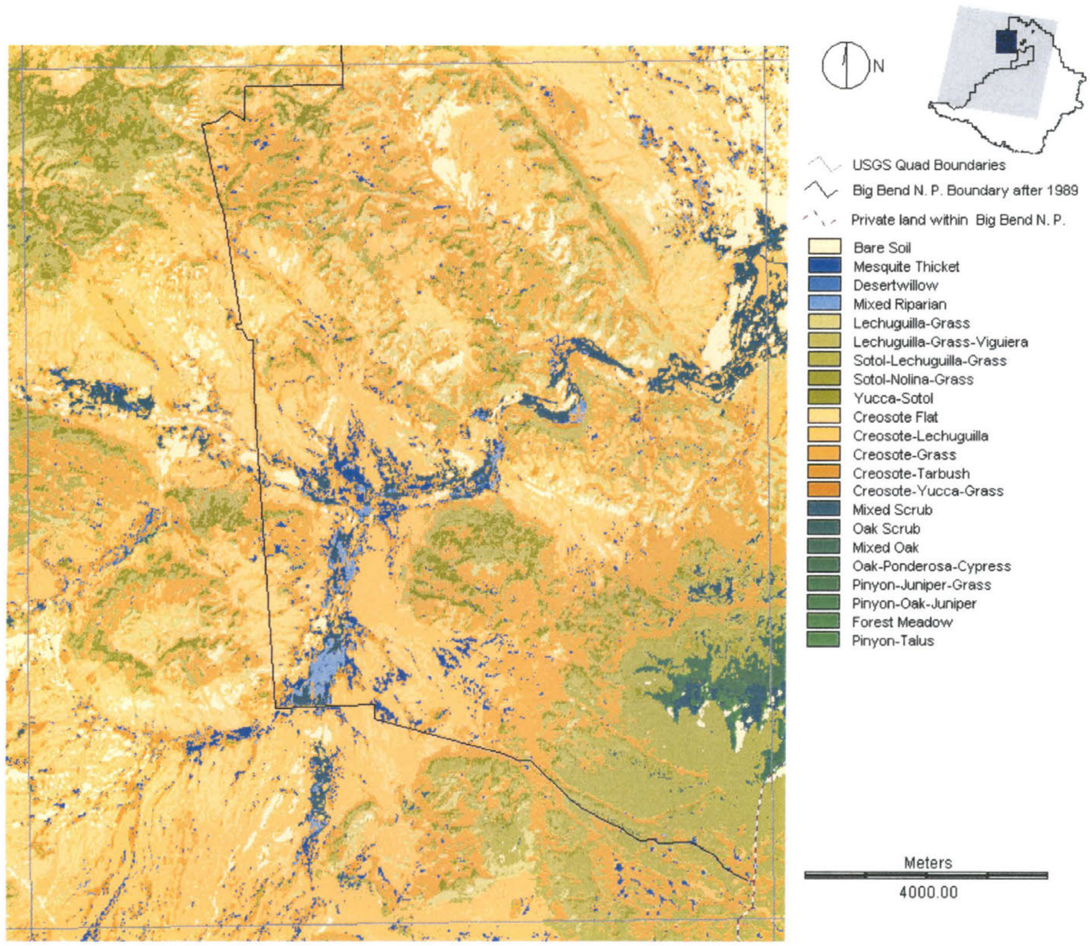

Figure 29. Vegetation Map of the Twin Peaks Quadrangle.

Soft classifiers are also available in IDRISI32©. These classifiers evaluate the degree to which each pixel belongs to a set of land cover classes. The output of a soft classifier is a set of real-number images for each class that expresses set membership on a 0-1 scale. Soft classifiers have a strong theoretical base that have the potential to be very powerful tools in classifying ground cover. However, in the context of this project the use of a soft classifier would have required a different approach to establishing training sites. To get the best results from the maximum likelihood classifier, training sites should represent the "ideal" sample for the class. Where possible in this project, training sites were selected on the basis of homogeneity of cover and compactness to avoid mixed pixels (pixels with multiple cover types). The prime motivation for using a soft classifier is sub-pixel classification (Eastman 1999a). Training sites for soft classifiers are based, not on homogeneity of cover type, but on the ability to accurately estimate the proportion of different cover types contained in the training site. Soft classifiers have some other practical disadvantages: they take a long time to run, and they consume an enormous amount of disk space.

Assessing Accuracy of Maps

Once vegetation maps have been produced, it is important to assess their accuracy. There are many sources of errors in classification of remotely sensed data including spectral overlap, scale reduction, and approximating vegetation continuums with discrete classification (Steele et al. 1998). Congalton (1991) published a summary of assessment techniques, all of which involve sampling sites on the ground (or sometimes aerial photographs) to characterize how many pixels are correctly categorized and how many are not. Validation sites were identified during the three field trips to the park. Where possible, validation sites were selected by locating multiple examples of the each of the cover types. The criteria for selecting a validation site were essentially the same used for finding training sites: the presence of homogenous cover, and broad enough extent to digitize a large (50 or more pixels) sample that would not be affected by neighboring cover types. The validation sites are converted to a raster image in the same manner as training sites. Using this method, adequate samples were found for 21 of 22 cover classes. The validation sample for Desertwillow contained only 47 pixels. This situation is not surprising because Desertwillow is associated with channel bars and narrow margins of dry streambeds. The conclusion one can draw is that imagery with 20 m spatial resolution is insufficient for the cover type. Future research in mapping the Desertwillow cover types and probably all riparian types would probably be more satisfactory using higher resolution imagery, such as 1 m DOQQs.

The Forest Meadow cover type had only 53 pixels in its validation sample and the validation sites were in close proximity to the training sites. This is not necessarily due to the lack of abundance, but to the lack of accessibility of suitable validation sites. This cover type only occurs in high elevations in the Chisos Mountains, and a few other mountains. Time restraints coupled with the difficulty of reaching suitable sample sites mean that more definitive statements about the accuracy of the classification will have to be withheld until more research is done.

In most discussions about thematic map accuracy, two types of errors are identified. Errors of omission (or Producer's Error) indicate the cover type is absent when it actually exists on the ground. Errors of commission (or User's Error) occur when the map indicates a cover type is present when, in fact, it is not. Using the validation sites to determine which pixels are correctly identified and which are misidentified, one can create an error matrix (also called a confusion matrix) to quantify the accuracy achieved by the classification. The error matrix contains a tabulation of the number of sample pixels found in each possible combination of correct true versus mapped cover types. Tabulations along the diagonal of the matrix show the number of pixels where the mapped category matched the true category. Off-diagonal tabulations represent errors in classification and are shown as totals in the margins. The rightmost column of the matrix gives the proportion of errors of commission for each cover type. The bottom row gives the proportion of errors of omission for each cover type. The lower right corner is the total proportional error for the sample. The error matrix for this classification is shown in Table 4.

Table 4. Error Matrix Analysis of Validation Site (columns: truth) against Vegetation Classification (rows : mapped)

	BS	MT	DW	MR	L-G	L-G-V	S-L-G	S-N-G	Y-S	CF	C-L	Total	Errors of Commission
Bare Soil (BS)	749	0	0	0	8	0	0	0	0	15	0	772	0.0298
Mesquite Thicket (MT)	0	43	11	16	0	0	0	0	0	0	0	71	0.3944
Desertwillow (DW)	0	0	4	2	0	0	0	0	0	0	1	7	0.4286
Mixed Riparian (MR)	0	2	0	21	0	0	0	0	0	0	0	23	0.0870
Lechuguilla-Grass (L-G)	0	1	0	2	384	0	0	0	0	10	0	398	0.0352
Lechuguilla-Grass-Viguiera (L-G-V)	0	0	0	0	57	145	3	0	8	0	0	239	0.3933
Sotol-Lechuguilla-Grass (S-L-G)	0	0	0	0	0	36	91	0	0	0	0	145	0.3724
Sotol-Nolina-Grass (S-N-G)	0	0	0	0	0	0	0	51	0	0	0	56	0.0893
Yucca-Sotol (Y-S)	0	0	0	0	5	0	16	0	57	0	0	101	0.4356
Creosote Flat (CF)	0	0	1	0	4	0	0	0	0	71	0	76	0.0658
Creosote-Lechuguilla (C-L)	2	1	13	22	24	6	0	0	0	42	144	321	0.5514
Creosote-Grass (C-G)	0	5	11	7	37	5	7	0	0	6	8	565	0.1611
Creosote-Tarbush (C-T)	0	1	0	8	0	0	0	0	0	0	5	164	0.1098
Creosote-Yucca-Grass (C-Y-G)	0	0	0	0	0	0	0	0	1	0	0	106	0.0094
Mixed Scrub (MS)	0	0	0	30	0	4	0	0	0	0	0	251	0.1554
Oak Scrub (OS)	0	0	0	1	0	1	0	0	0	0	0	85	0.1059
Mixed Oak (MO)	0	0	0	0	0	0	0	0	0	0	0	101	0.3564
Oak-Ponderosa-Cypress (O-P-C)	0	0	0	0	0	0	0	0	0	0	0	159	0.3019
Pinyon-Juniper-Grass (P-J-G)	0	0	0	0	0	0	0	8	0	0	0	96	0.1563
Pinyon-Oak-Juniper (P-O-J)	0	0	0	0	0	0	0	0	0	0	0	61	0.0820
Forest Meadow (FM)	0	0	0	0	0	0	0	0	0	0	0	26	0.1154
Pinyon Talus (PT)	0	0	0	0	0	0	0	0	0	0	0	69	0.0145
Total	751	53	40	109	519	197	117	59	66	144	158	3892	
Errors of Omission	0.0027	0.1887	0.9000	0.8073	0.2601	0.2640	0.2222	0.1356	0.1364	0.5069	0.0886		

Table 4. Continued

	C-G	C-T	C-Y-G	MS	OS	MO	O-P-C	P-J-G	P-O-J	FM	PT	Total	Errors of Commission
Bare Soil (BS)	0	0	0	0	0	0	0	0	0	0	0	772	0.0298
Mesquite Thicket (MT)	1	0	0	0	0	0	0	0	0	0	0	71	0.3944
Desertwillow (DW)	0	0	0	0	0	0	0	0	0	0	0	7	0.4286
Mixed Riparian (MR)	0	0	0	0	0	0	0	0	0	0	0	23	0.0870
Lechuguilla-Grass (L-G)	1	0	0	0	0	0	0	0	0	0	0	398	0.0352
Lechuguilla-Grass-Viguiera (L-G-V)	11	9	6	0	0	0	0	0	0	0	0	239	0.3933
Sotol-Lechuguilla-Grass (S-L-G)	2	0	0	2	14	0	0	0	0	0	0	145	0.3724
Sotol-Nolina-Grass (S-N-G)	0	0	0	4	0	0	0	1	0	0	0	56	0.0893
Yucca-Sotol (Y-S)	0	0	23	0	0	0	0	0	0	0	0	101	0.4356
Creosote Flat (CF)	0	0	0	0	0	0	0	0	0	0	0	76	0.0658
Creosote-Lechuguilla (C-L)	60	7	0	0	0	0	0	0	0	0	0	321	0.5514
Creosote-Grass (C-G)	474	5	0	0	0	0	0	0	0	0	0	565	0.1611
Creosote-Tarbush (C-T)	4	146	0	0	0	0	0	0	0	0	0	164	0.1098
Creosote-Yucca-Grass (C-Y-G)	0	0	105	0	0	0	0	0	0	0	0	106	0.0094
Mixed Scrub (MS)	0	0	0	212	0	0	3	2	0	0	0	251	0.1554
Oak Scrub (OS)	0	0	0	3	76	0	1	0	0	3	0	85	0.1059
Mixed Oak (MO)	0	0	0	23	0	65	1	2	0	0	10	101	0.3564
Oak-Ponderosa-Cypress (O-P-C)	0	0	0	0	0	0	111	0	0	0	48	159	0.3019
Pinyon-Juniper-Grass (P-J-G)	0	0	0	5	0	0	1	81	0	1	0	96	0.1563
Pinyon-Oak-Juniper (P-O-J)	0	0	0	0	0	5	0	0	56	0	0	61	0.0820
Forest Meadow (FM)	0	0	0	0	0	0	0	2	1	23	0	26	0.1154
Pinyon Talus (PT)	0	0	0	0	0	1	0	0	0	0	68	69	0.0145
Total	553	167	134	249	90	71	117	88	57	27	126	3892	
Errors of Omission	0.1429	0.1257	0.2164	0.1486	.01556	0.0845	0.0513	0.0795	0.0175	0.1481	0.4603		0.1837

Referring to Table 4, the lower right cell of the error matrix shows that the maximum likelihood classifier combined with probability images had a proportional error of 0.1837. This means that 18.37% of the total number of pixels in the validation sample were identified incorrectly. To state a positive result, 81.63% of the validation sample pixels were identified correctly. Ten cover types were correctly identified to a consistently high degree, having errors of commission and omission of 20% or less. Of these categories Forest Meadow was based on a small validation sample, which means the accuracy assessment may be overly optimistic when applied region-wide. The Bare Soil cover type was correctly identified in 98% of the pixels, which is understandable given its easily distinguishable spectral signature. This is an important result because in assessing vegetation changes over time the change in coverage of bare soil will be a key indicator of the status of many types of vegetation. In general, the classifier performed well for all the Chisos Mountain cover types. This result is even more encouraging considering where misidentification occurs it is almost always among the other Chisos Mountain cover types. The classifier also gave good results with the Desert Plains cover types. The weakest performance in this group was the result of Creosote Flats pixels being classified as Creosote Lechuguilla. Creosote Flats cover was also misidentified as Bare Soil. This is a reasonable result considering that the bare soil, creosote flats, and creosote-lechuguilla are often found intergrading into each other and are the least dense cover types. The classifier worked reasonably well with the Desert Mountain, Foothills, and Mesas cover types. Most of the confusion is understandable since all cover share common vegetation types.

The classifier performed poorly in the Riparian classes. As discussed earlier, much of this result can be attributed to the nature of the spatial distribution of the cover type and the inherent mismatch with 20 m pixels.

Although the error matrix shows the vegetation maps produced in this project have a high degree of accuracy it is important to recognize that the validation sites were not randomly selected and they were chosen on the basis on homogenous cover types. In addition, as much as any careful researcher wants to avoid it, the possibility of researcher bias cannot be completely discounted. A random sample of validation sites observed by an independent researcher could find somewhat less optimistic results.

CHAPTER VI

CONCLUSIONS

Big Bend National Park in West Texas is a large natural preserve covering an area larger than the state of Rhode Island. One key element to the preservation and restoration of this park is availability of accurate and consistent vegetation maps. Gregory Plumb (Plumb 1988) first developed a vegetation classification system that was suitable for mapping vegetation occurring in Big Bend National Park at medium scale (1:24000). Based on this vegetation classification system, Plumb combined Landsat Thematic Mapper satellite images and ancillary data into a rules-based system to create vegetation maps of most of the park. In the years since Plumb's research, Big Bend National Park has acquired more than 36,000 additional hectares of land. Some parts of the newly acquired area have not been mapped. Other parts have been mapped, but with classification systems that are not consistent with the rest of the park

The primary purpose of this thesis was to develop consistent and accurate vegetation maps of the recently acquired portion of Big Bend National Park by combining a multispectral satellite image and ancillary data. For the purpose of consistency, Plumb's classification system was used and many of his training sites were located and verified.

To achieve the goal of accuracy, the problems associated with satellite images of arid and semi-arid regions had to be overcome. One major problem is the interference between the reflectance of vegetation and background soil. Another major problem is the lack of variability between spectral bands. The concept of vegetation indexes was applied to mitigate the problem of soil reflectance mixing with vegetation reflectance. In this study, the Weighted Difference Vegetation Index (WDVI) proved to be effective at helping separate soil and vegetation reflectance. The WDVI was also effective in enhancing the separability of vegetation cover types. A key method for improving the ability to distinguish between vegetation cover types was the development of probability images. Probability images allow prior knowledge about the distribution of different cover types to transform ancillary data into a probability statement about the occurrence of a given cover type occurring at a particular location.

Digital elevation models were the primary source of ancillary data used in this study. Digital line graphs and digital raster graphs were secondary sources. Slope, aspect, water runoff, and elevation information were derived from this data. The concept of fuzzy set membership also proved valuable in the creation of probability images. Fuzzy set membership allowed the overlap and ambiguity between vegetation cover types to be quantified and incorporated into the probability images.

This project demonstrated that accurate vegetation maps could be created by combining multispectral satellite imagery and ancillary data. An existing well-researched vegetation classification system was successfully adapted to the methods and data used in this project resulting in consistent vegetation maps being available for nearly all of Big Bend National Park. The use of probability images has been demonstrated to be a powerful method of incorporating prior knowledge into the classification process. The concepts of fuzzy set membership and vegetation indices, which were successfully applied to the construction of probability images, were also valuable in overcoming the inherent difficulty in classifying remotely sensed data in arid and semi-arid regions. It is reasonable to believe that the methods used in this project can be successfully used to create vegetation maps in many regions and certainly in other arid and semi-arid regions. Once consistent and accurate vegetation maps are produced, a baseline for monitoring changes in vegetation has been established.

A few of the original objectives of the project remain undone. The vegetation maps produced in this study overlapped Plumb's maps. More work could be done to assess the differences between this project's results and Plumb's results to determine how much of the difference is due to real changes in vegetation and how much represents differences in underlying methodologies. Another unrealized goal is the analysis of vegetation differences among areas adjacent to Big Bend National Park still being ranched, the areas recently acquired, and the original areas of the park that have been protected from overgrazing for 50 years. The vegetation maps produced in this study could be used as a baseline in such an endeavor. A body of knowledge about the relationship between soil and vegetation was not incorporated into this study because the scale of the digital soil data available from the STATSGO database was too small. When more large scale data is available in digital form from the SSURGO database, a fruitful area of research will open up. Another area that needs exploration is mapping vegetation, particularly the riparian vegetation, at much larger scales. One-meter imagery is available now, and undoubtedly more will be available in the future. This data could be used in detailed change-over-time studies of the distribution and movement of exotic species, such as Tamarisk, that are expanding in arid land waterways.

There are plenty of unanswered questions for the aspiring researcher to tackle. However, whether conducting research or not, the Big Bend region is beautiful, serene, mysterious, challenging, and even a little dangerous. That is reason enough to go back.

APPENDIX A

STATUS OF TRAINING AND VALIDATION SITES

Table A1. Status of Plumb's Training Sites

Plumb Site #	Easting	Northing	Cover Type	Elev	Slope (%)	Aspect (deg)	Verified Site?	Loc Valid?	Cover Valid?	Note
1	681795	3268849	Creosote Flats	878	0	N/A	Yes	Yes	Yes	
2	691302	3262012	Creosote Flats	631	0	N/A	No			
3	674100	3254435	Lechuguilla-Grass	993	45	275	Yes	Yes	Yes	
4	652442	3215377	Creosote-Grass	646	14	235	No			
5	653283	3231164	Creosote-Grass	960	5	235	Yes	No	Yes	Location coordinates adjusted
6	665471	3250539	Creosote-Tarbush	1085	2	10	Yes	Yes	Yes	
7	674381	3245350	Sotol-Lech-Grass	1121	5	60	Yes	Yes	Yes	
8	658833	3239722	Creosote-Tarbush	1121	3	290	Yes	Yes	Yes	
9	675136	3248251	Creosote-Tarbush	1024	3	100	Yes	Yes	Yes	
10	672440	3250115	Creosote-Tarbush	1048	3	45	Yes	Yes	Yes	
11	677009	3243191	Sotol-Lech-Grass	1060	18	230	Yes	Yes	Yes	
12	652110	3228039	Creosote-Grass	856	11	295	Yes	Yes	Yes	
13	677398	3250061	Creosote-Lechuguilla	963	2	240	Yes	Yes	No	Not enough lech to consider C-L
14	679815	3251749	Creosote-Lechuguilla	908	2	35	Yes	Yes	Yes	
15	652632	3228866	Creosote-Lechuguilla	865	3	320	Yes	Yes	Yes	
16	678959	3239356	Lech-Grass-Viguiera	937	7	90	Yes	No	Yes	Location coordinates adjusted
17	653402	3234058	Creosote-Lechuguilla	957	2	250	Yes	Yes	Yes	
18	675722	3254592	Creosote-Grass	935	11	345	Yes	No	Yes	Unable to verify location
19	677423	3283751	Lechuguilla-Grass	899	29	5	Yes	Yes	Yes	
20	676968	3283398	Ecotonal	911	3	40	Yes	Yes	Yes	
21	681501	3239623	Creosote-Lechuguilla	908	0	N/A	Yes	Yes	Yes	
22	679984	3239012	Lech-Grass-Viguiera	939	4	135	Yes	Yes	Yes	
23	678874	3240510	Creosote-Grass	1054	65	270	Yes	Yes	Yes	
24	676649	3282163	Ecotonal	859	2	0	Yes	No	Yes	Location coordinates adjusted
25	702066	3231872	Lech-Grass-Candelilla	567	23	45	No			
26	679953	3277501	Ecotonal	795	7	275	Yes	Yes	Yes	
27	680720	3258551	Creosote-Lechuguilla	853	0	N/A	Yes	Yes	Yes	
28	688210	3264240	Lech-Grass-Candelilla	1030	0	N/A	Yes	Yes	Yes	
29	677231	3280734	Ecotonal	832	2	225	Yes	Yes	Yes	
30	680773	3255545	Creosote-Lechuguilla	850	3	325	Yes	Yes	No	Found Creosote-Flat

Table A1. – Continued.

Plumb Site #	684294	3214267	Creosote-Grass	603	2	170	No			
32	697200	3231810	Lech-Grass-Hectia	652	19	175	No			
33	694830	3233005	Ecotonal	621	6	200	No			
34	678066	3233020	Lech-Grass-Candelilla	963	17	270	No			
35	680438	3255618	Desertwillow	847	0	N/A	Yes	Yes	Yes	
36	673574	3243720	Ecotonal	1243	19	20	No			
37	677228	3237443	Lechuguilla-Grass	1121	32	170	Yes	Yes	Yes	
38	652358	3227999	Lech-Grass-Viguiera	902	25	270	Yes	Yes	Yes	
39	661875	3246362	Lechuguilla-Grass	1097	27	120	Yes	Yes	Yes	
40	681788	3262809	Creosote-Lechuguilla	899	3	100	Yes	Yes	Yes	
41	680902	3272056	Lechuguilla-Grass	841	3	250	Yes	Yes	Yes	
42	680690	3254308	Creosote-Grass	887	0	N/A	Yes	Yes	Yes	
43	688747	3267533	Lech-Grass-Candelilla	1097	12	345	Yes	Yes	Yes	
44	688562	3264043	Lech-Grass-Candelilla	1042	8	240	Yes	Yes	Yes	
45	685741	3263564	Lech-Grass-Candelilla	975	9	205	Yes	No	Yes	Location coordinates adjusted
46	687096	3263683	Lechuguilla-Grass	1036	6	225	Yes	Yes	Yes	
47	676551	3243283	Creosote-Tarbush	1067	3	50	Yes	Yes	Yes	
48	664953	3235765	Pinyon-Oak-Juniper	2194	60	175	No			
49	676474	3241633	Lech-Grass-Viguiera	1103	7	80	Yes	No	Yes	Location coordinates adjusted
50	670194	3247571	Lech-Grass-Viguiera	1158	3	40	Yes	No	Yes	Location coordinates adjusted
51	657730	3232612	Sotol-Lech-Grass	1292	12	220	Yes	Yes	Yes	
52	668879	3244312	Sotol-Lech-Grass	1341	40	110	Yes	Yes	Yes	
53	687158	3263925	Lech-Grass-Viguiera	1021	11	60	Yes	Yes	No	Site dominated by forbs
54	675247	3237186	Sotol-Lech-Grass	1231	19	120	Yes	Yes	Yes	
55	655922	3233538	Sotol-Lech-Grass	1109	25	200	Yes	Yes	Yes	
56	667716	3241310	Sotol-Lech-Grass	1524	12	10	Yes	Yes	Yes	
57	689015	3266116	Creosote-Yucca-Grass	1060	3	190	Yes	Yes	Yes	
58	689197	3267838	Creosote-Yucca-Grass	1070	9	315	Yes	Yes	Yes	
59	689432	3267193	Yucca-Sotol	1097	8	280	Yes	Yes	Yes	
60	667492	3241889	Mixed Scrub	1554	58	165	Yes	Yes	Yes	

Table A1. – Continued.

Plumb Site #	Easting	Northing	Cover Type	Elev	Slope (%)	Aspect (deg)	Verified Site?	Loc Valid?	Cover Valid?	Note
61	666894	3239711	Pinyon-Juniper-Grass	1737	62	285	Yes	Yes	Yes	
62	668633	3242492	Mixed Scrub	1426	4	30	Yes	Yes	Yes	
63	663433	3239406	Oak Scrub	1439	67	345	Yes	Yes	Yes	
64	662474	3240028	Sotol-Lechuguilla-Grass	1432	49	215	Yes	Yes	Yes	
67	664569	3240002	Mixed Scrub	1506	3	280	Yes	Yes	Yes	
68	665727	3239505	Mixed Scrub	1634	16	325	Yes	Yes	Yes	
69	670638	3238745	Sotol-Nolina-Grass	1600	7	75	Yes	Yes	Yes	
70	688914	3233963	Lech-Grass-Prickly Pear	676	2	120	No			
71	666190	3239092	Oak Scrub	1859	40	305	Yes	Yes	Yes	
72	693782	3230554	Desertwillow	582	0	N/A	No			
73	694299	2321048	Lech-Grass-Candelilla	609	14	180	No			
74	664130	3236338	Oak Scrub	2042	39	340	Yes	Yes	Yes	
75	695646	3232005	Lech-Grass-Hectia	655	3	225	No			
76	664961	3239858	Mixed Oak	1512	7	270	Yes	Yes	Yes	
77	667020	3239331	Mixed Oak	1728	13	330	Yes	Yes	Yes	
78	666933	3241955	Mixed Oak	1573	7	140	Yes	Yes	Yes	
79	665343	3239063	Ecotonal	1646	9	305	Yes	Yes	Yes	
80	696606	3231798	Lech-Grass-Candelilla	646	38	5	No			
81	665695	3239215	Pinyon-Juniper-Grass	1661	24	315	Yes	Yes	Yes	
82	667463	3239001	Pinyon-Juniper-Grass	1847	36	275	Yes	Yes	Yes	
83	665591	3234975	Pinyon-Juniper-Grass	2195	12	325	Yes	Yes	Yes	
84	667046	3240931	Pinyon-Juniper-Grass	1609	16	90	Yes	Yes	Yes	
85	697227	3230170	Cottonwood Grove	560	0	N/A	No			
86	665319	3239076	Pinyon-Juniper-Grass	1646	9	305	Yes	Yes	Yes	
87	697905	3231248	Lech-Grass-Candelilla	576	2	40	No			
88	686268	3235820	Lech-Grass-Candelilla	728	7	40	No			
89	682857	3239201	Lechuguilla-Grass	902	5	130	No			
90	701034	3231423	Lech-Grass-Hectia	579	18	165	No			

Table A1. – Continued.

Plumb Site #	Easting	Northing	Cover Type	Elev	Slope (%)	Aspect (deg)	Verified Site?	Loc Valid?	Cover Valid?	Note
91	702199	3232147	Lech-Grass-Hectia	594	45	255	No			
92	666922	3239045	Pinyon-Oak-Juniper	1804	38	10	Yes	Yes	Yes	
93	665431	3237093	Pinyon-Oak-Juniper	1951	47	350	Yes	Yes	Yes	
94	694745	3228994	Mesquite Thicket	560	2	90	Yes	Yes	Yes	
95	665017	3234244	Pinyon-Oak-Juniper	2198	11	70	Yes	Yes	Yes	
96	663996	3236018	Forest Meadow	2027	4	180	Yes	Yes	Yes	
97	665544	3238046	Forest Meadow	1789	3	50	Yes	Yes	Yes	
98	665189	3234581	Forest Meadow	2158	2	135	Yes	Yes	Yes	
99	694440	3229976	Lech-Grass-Hectia	588	19	270	Yes	Yes	Yes	
100	648326	3226464	Creosote-Grass	777	4	225	Yes	Yes	Yes	
101	669521	3238131	Oak-Ponderosa-Cypress	1731	27	45	Yes	Yes	Yes	
102	665587	3235825	Oak-Ponderosa-Cypress	2067	0	N/A	Yes	Yes	Yes	
103	646615	3225152	Creosote-Grass	719	2	250	Yes	Yes	Yes	
104	645697	3225235	Creosote-Grass	663	10	180	Yes	Yes	Yes	
105	645108	3224757	Creosote-Grass	685	19	125	No			
106	664541	3236155	Pinyon-Talus	2190	40	315	Yes	Yes	Yes	
107	644703	3224098	Creosote Flats	670	2	135	No			
108	643298	3224483	Desertwillow	649	1	210	No			
109	642642	3224633	Mesquite Thicket	646	0	N/A	No			
110	642203	3224932	Creosote-Grass	670	21	235	No			
111	702367	3231740	Reed Grass	549	0	N/A	No			
113	641041	3226078	Creosote-Lechuguilla	655	0	N/A	No			
114	638992	3226070	Mesquite Thicket	653	0	N/A	No			
115	635887	3228048	Creosote-Lechuguilla	682	2	210	No			
116	635228	3227110	Mesquite Thicket	658	0	N/A	No			
117	702354	3231578	Mesquite Thicket	551	0	N/A	No			
118	659625	3239889	Mixed Scrub	1158	3	300	Yes	Yes	Yes	
119	676986	3207666	Mesquite Thicket	603	0	N/A	No			
120	641700	3225506	Creosote-Grass	685	36	255	No			

Table A1. – Continued.

Plumb Site #	Easting	Northing	Cover Type	Elev	Slope (%)	Aspect (deg)	Verified Site?	Loc Valid?	Cover Valid?	Note
121	635851	3228333	Bare Ground	664	0	N/A	No			
122	636326	3228378	Creosote Flats	685	0	N/A	No			
123	638239	3230996	Ecotonal	698	4	105	No			
124	638909	3231786	Creosote Flats	713	2	235	No			
125	640225	3232404	Ecotonal	716	2	160	No			
126	639447	3231997	Creosote-Grass	692	9	270	No			
127	641523	3232108	Desertwillow	704	0	N/A	Yes	Yes	Yes	
128	642958	3233077	Desertwillow	2365	2	250	Yes	Yes	Yes	
129	657219	3244744	Ecotonal	993	3	170	Yes	Yes	Yes	
130	643312	3235369	Creosote-Grass	771	3	135	No			
131	658506	3245237	Creosote-Lechuguilla	996	5	335	Yes	Yes	Yes	
132	658778	3245926	Creosote-Lechuguilla	993	0	N/A	Yes	Yes	Yes	
133	660773	3246455	Lechuguilla-Grass	1036	5	270	Yes	Yes	Yes	
134	655059	3244630	Lech-Grass-Viguiera	1006	31	215	Yes	Yes	Yes	
135	654427	3245517	Creosote-Grass	969	49	200	Yes	Yes	Yes	
136	652442	3244914	Creosote-Tarbush	945	2	220	Yes	Yes	No	Too little tarbush
137	646115	3241090	Creosote-Grass	835	5	310	Yes	Yes	Yes	
139	670341	3245919	Lech-Grass-Viguiera	1207	5	5	Yes	Yes	No	Not much viguiera
140	623880	3233936	Lech-Grass-Candelilla	978	3	275	No			
141	625805	3232155	Lech-Grass-Hectia	1006	27	175	No			
142	650893	3216404	Water	640	0	N/A	No			
143	703415	3233845	Water	558	0	N/A	No			
144	701077	3231106	Water	567	0	N/A	No			
146	681103	3239314	Cottonwood Grove	906	5	120	Yes	Yes	Yes	
147	664481	3239865	Water	1494	0	N/A	Yes	Yes	Yes	Sewage Lagoons

Table A2. Additional Training Located for This Project

Site ID	Easting	Northing	Date Observed	Cover Type
Training Sites				
BBRTNK	674301	3275399	03-July-98	Mesquite Thicket
BBRW1	671596	3270918	03-May-99	Mixed Scrub
BBRW2	671822	3270375	03-May-99	Creosote-Grass
BBRW3	671972	3270154	03-May-99	Creosote-Grass
BBRW4	671481	3269828	03-May-99	Creosote-Grass
BBRW5	671242	3269570	03-May-99	Lechuguilla-Grass
BBRW6	671128	3269485	03-May-99	Mixed Oak
BBRW7	672172	3270255	03-May-99	Sotol-Lechuguilla-Grass
BBRWIN	671604	3271605	03-May-99	Creosote-Grass
BBRX1	669130	3272858	03-July-98	Creosote Flat
BBRX2	669013	3274179	06-May-99	Creosote Flat
BBRX3	669120	3273161	06-May-99	Bare Soil
BBSPRN	662919	3267871	03-July-98	Creosote-Tarbush
BBSVJT	658301	3232758	05-July-98	Sotol-Lechuguilla-Grass
BSTCW1	643579	3223868	17-Nov-98	Cottonwood Grove
BSTNR2	663721	3271542	06-Apr-99	Creosote-Grass
BTS01	680558	3278043	05-Apr-99	Creosote-Grass
BTS10	652244	3227272	06-Apr-99	Sotol-Lechuguilla-Grass
BTS2	662550	3246255	17-Nov-98	Mixed Oak
BTS3	650704	3226651	17-Nov-98	Bare Soil
BTSBR1	668578	3242695	17-Nov-98	Creosote Flat
BTSCW2	643946	3223827	17-Nov-98	Cottonwood Grove
BTSNR1	664111	3271323	06-Apr-99	Bare Soil
BTSNR3	663808	3271471	06-Apr-99	Creosote-Grass
BTSNR4	664051	3270951	06-Apr-99	Creosote-Grass
BTSNR5	667126	3271055	06-Apr-99	Creosote Flat
BTSNR6	667397	3270523	06-Apr-99	Mesquite Thicket
BTSNR7	667669	3272688	06-Apr-99	Creosote Flat
BTSPC1	670333	3238681	16-Nov-98	Pinyon-Juniper-Grass

Table A3. Partial List of Validation Sites Located for This Study

Note: Many other validation sites were located on USGS topographic maps and then digitized directly from the corresponding DRG.

Site ID	Easting	Northing	Date Observed	Cover Type
Validation Sites				
TBV03	680484	3276771	06-Apr-99	Creosote-Grass
TBV137	646050	3241160	04-Apr-99	Creosote Flat
TBV16	678843	3239264	09-Apr-99	Lechuguilla-Grass-Viguiera
TBV24	676530	3281999	05-Apr-99	Ecotonal
TBV28	688217	3264153	07-Apr-99	Lechuguilla-Grass-Candelilla
TBV38	652186	3227989	02-May-99	Lechuguilla-Grass
TBV40	681784	3262810	07-Apr-99	Creosote-Lechuguilla
TBV42	680687	3254480	08-Apr-99	Creosote-Grass
TBV45	686008	3263420	07-Apr-99	Lechuguilla-Grass-Viguiera
TBV49	676647	3241418	09-Apr-99	Lechuguilla-Grass-Viguiera
TBV50	670235	3247622	08-Apr-99	Lechuguilla-Grass-Viguiera
TBV5A	653355	3230946	02-May-99	Creosote-Grass
VP101	669701	3238087	16-Nov-98	Oak-Ponderosa-Cypress
VP11	677111	3243585	16-Nov-98	Sotol-Lechuguilla-Grass
VP47	676540	3243271	15-Nov-98	Creosote-Tarbush
VP61	666774	3239790	15-Nov-98	Pinyon-Juniper-Grass
VP67	664602	3239945	17-Nov-98	Mixed Scrub
VP68	665559	3239276	15-Nov-98	Mixed Scrub
VP69	670553	3238688	16-Nov-98	Sotol-Nolina-Grass
VP7	674507	3245458	16-Nov-98	Sotol-Lechuguilla-Grass
VP76	665014	3239857	17-Nov-98	Mixed Oak
VP77	667034	3239421	15-Nov-98	Mixed Oak
VP84	666720	3240273	15-Nov-98	Pinyon-Juniper-Grass
VP86	665319	3239041	15-Nov-98	Pinyon-Juniper-Grass

APPENDIX B

HISTOGRAMS OF THE TRAINING SAMPLE SIGNATURES

In the figures that follow, three histograms representing each of the three spectral bands are shown. The green band histogram is shown at the top of the page, the red band histogram is in the center, and the infrared band at the bottom. The sample size in pixels for each signature is indicated in the caption.

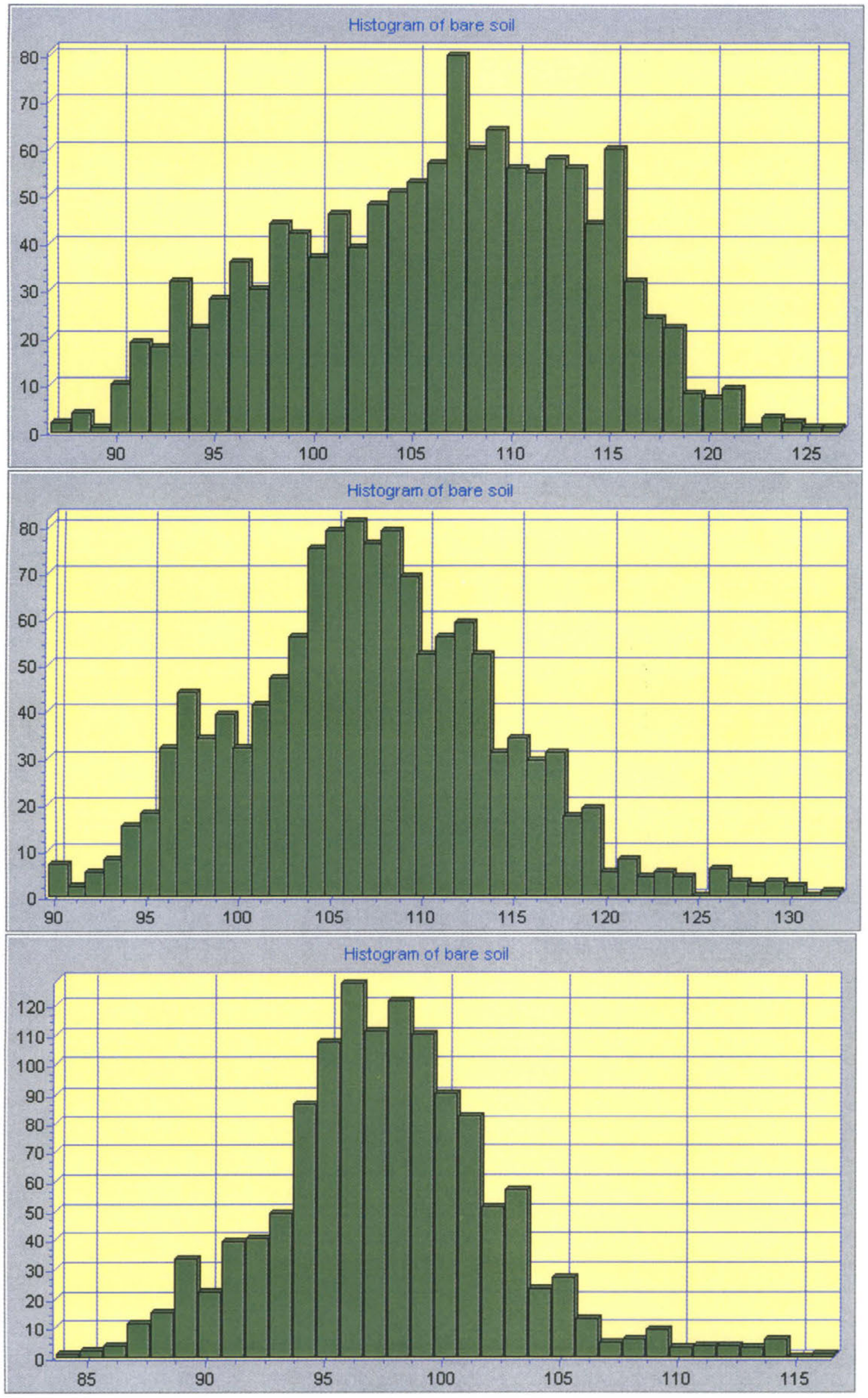

Figure 30. Histograms of Bare Soil Training Data (n=1262)

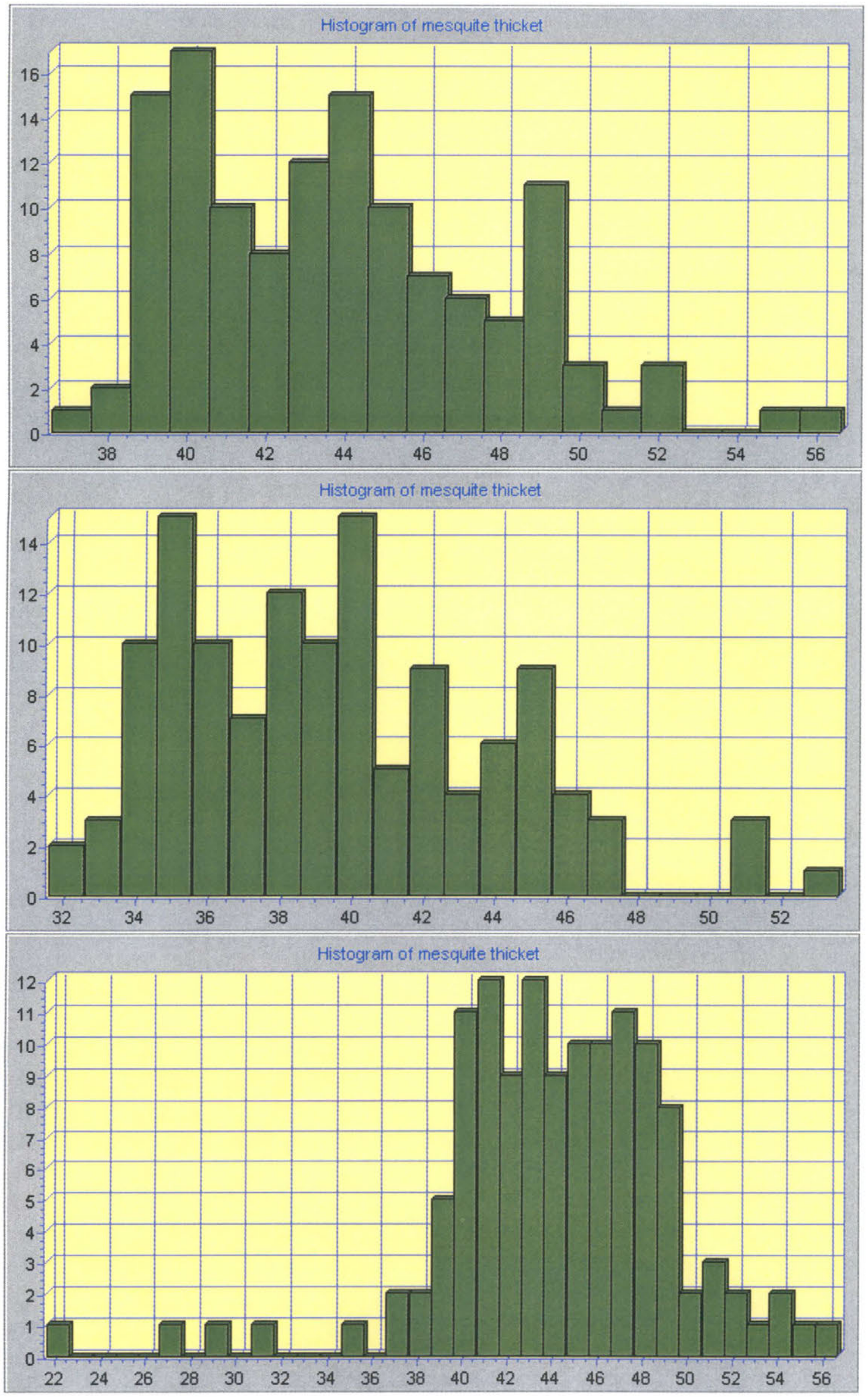

Figure 31. Histograms of Mequite Thicket (n=128)

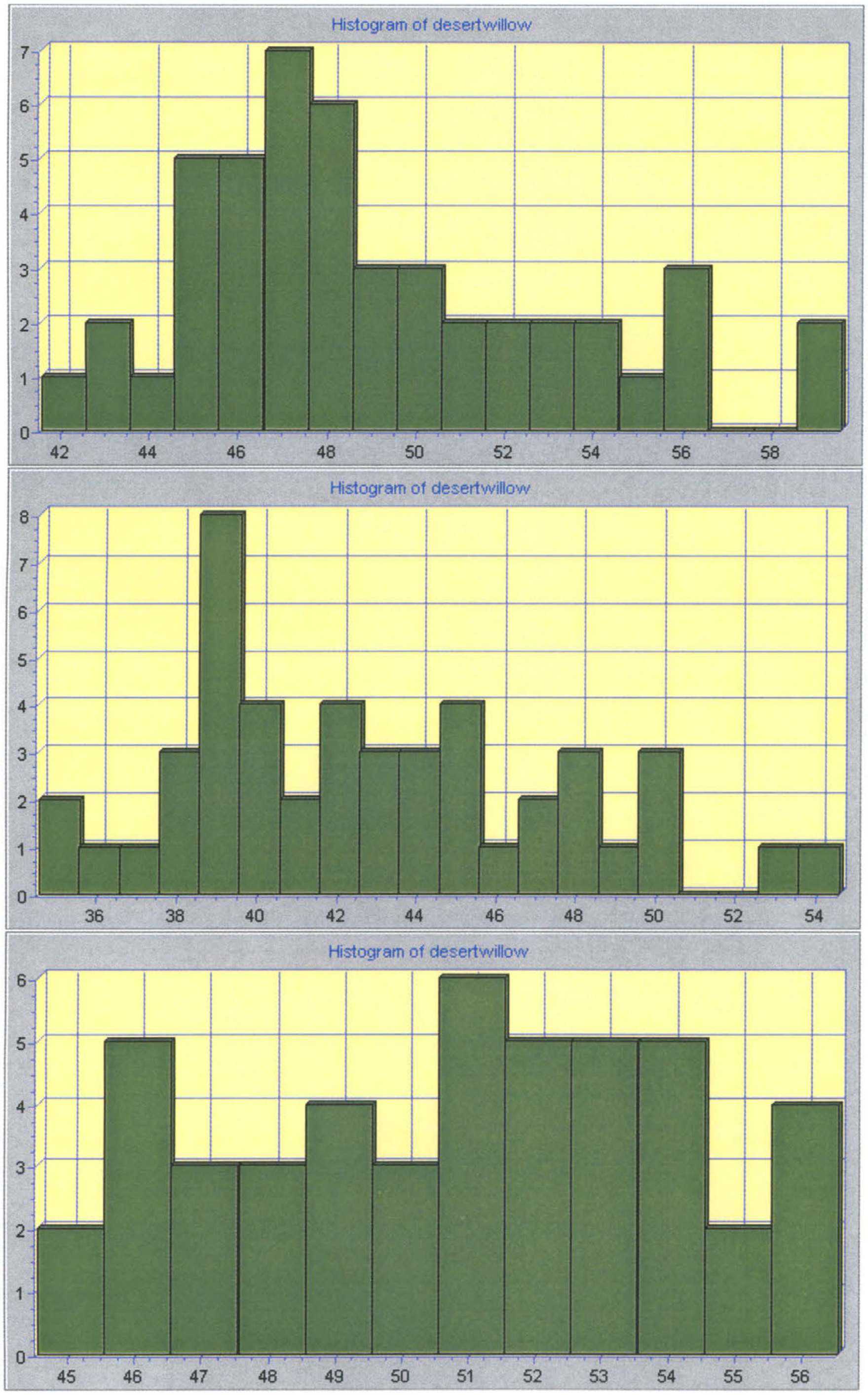

Figure 32. Histograms of Desertwillow (n=47)

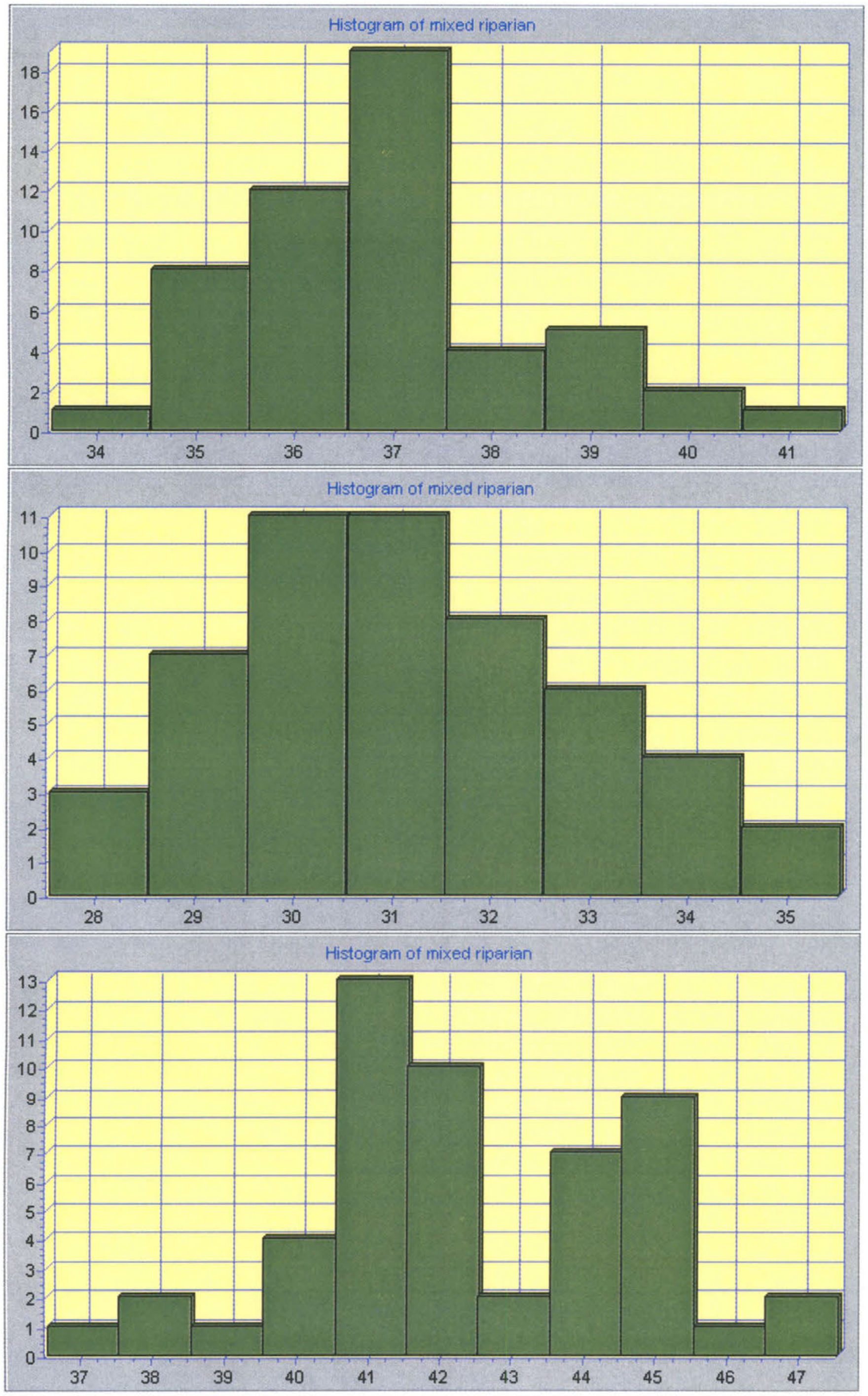

Figure 33. Histograms of Mixed Riparian (n=52)

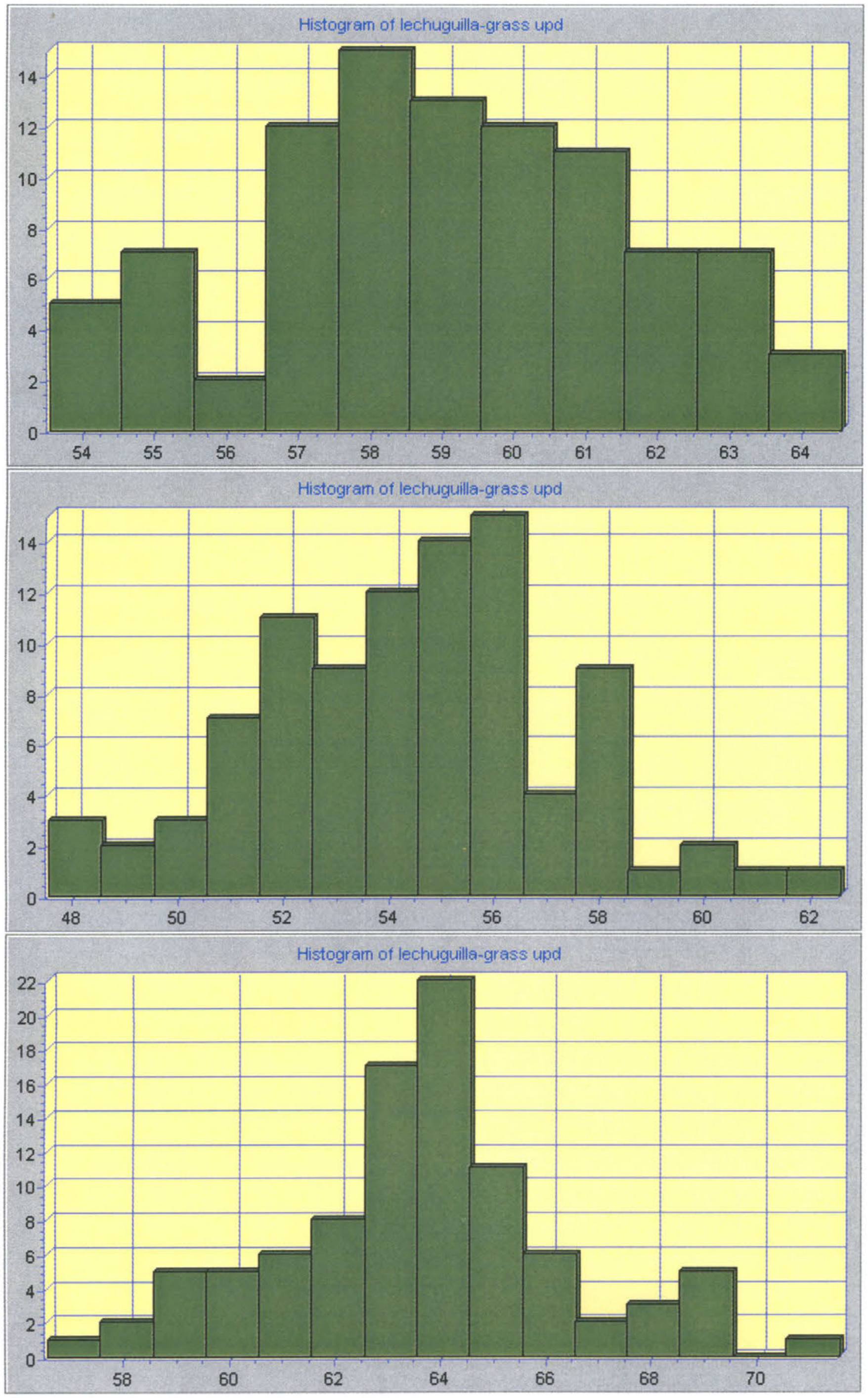

Figure 34. Histograms of Lechuguilla-Grass (n=80)

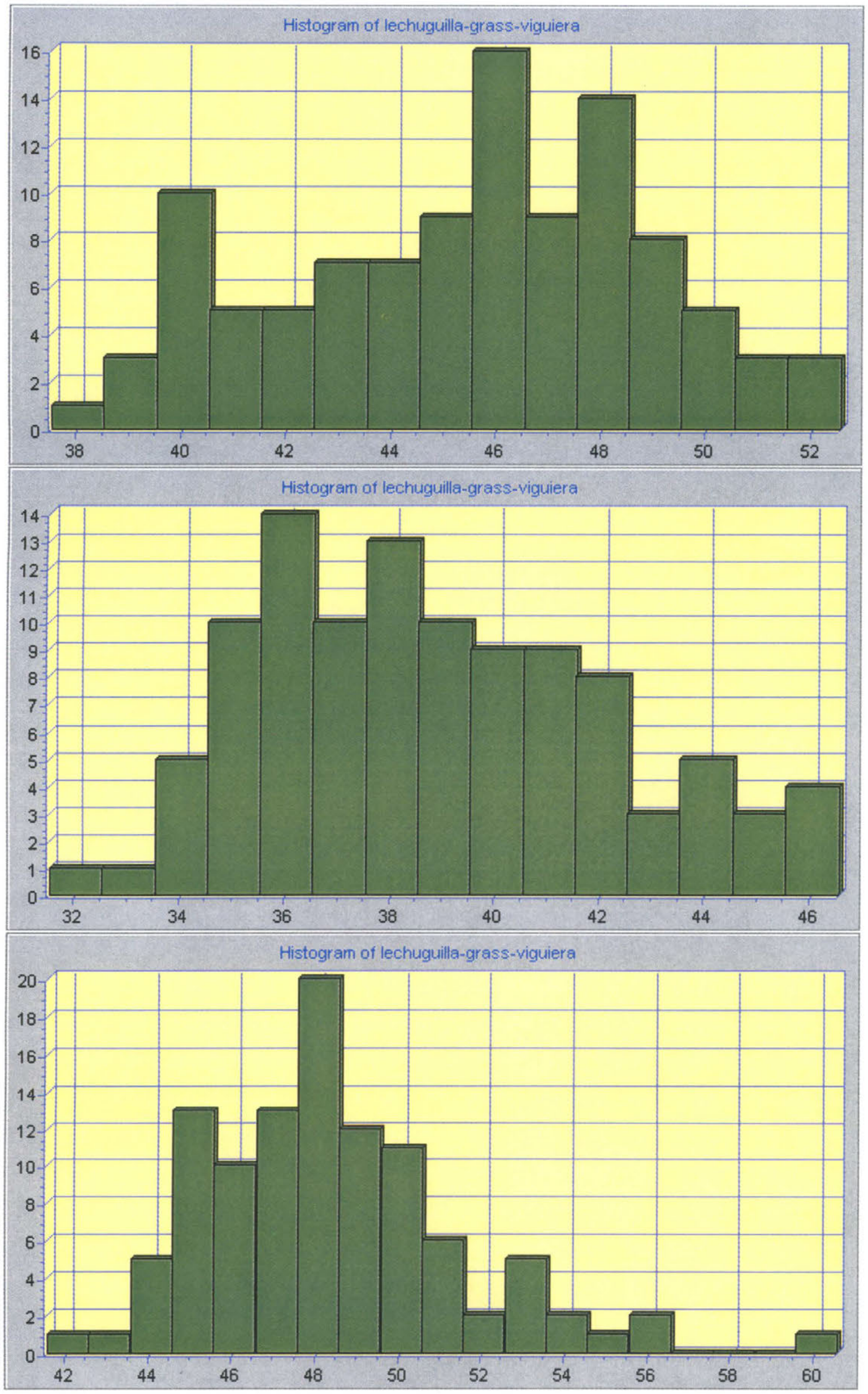

Figure 35. Histograms of Lechuguilla-Grass-Viguiera (n=294)

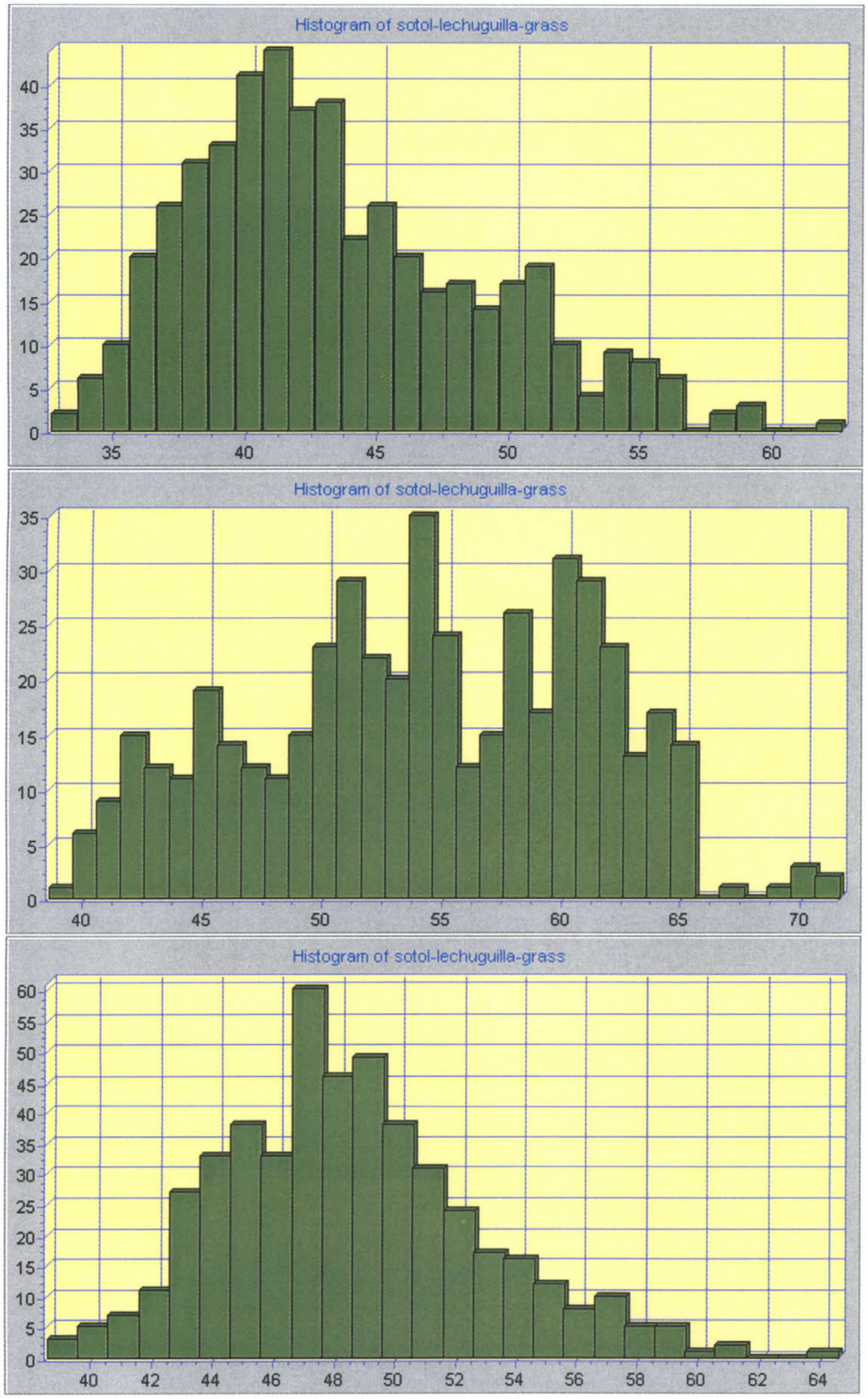

Figure 36. Histograms of Sotol-Lechuguilla-Grass (n=481)

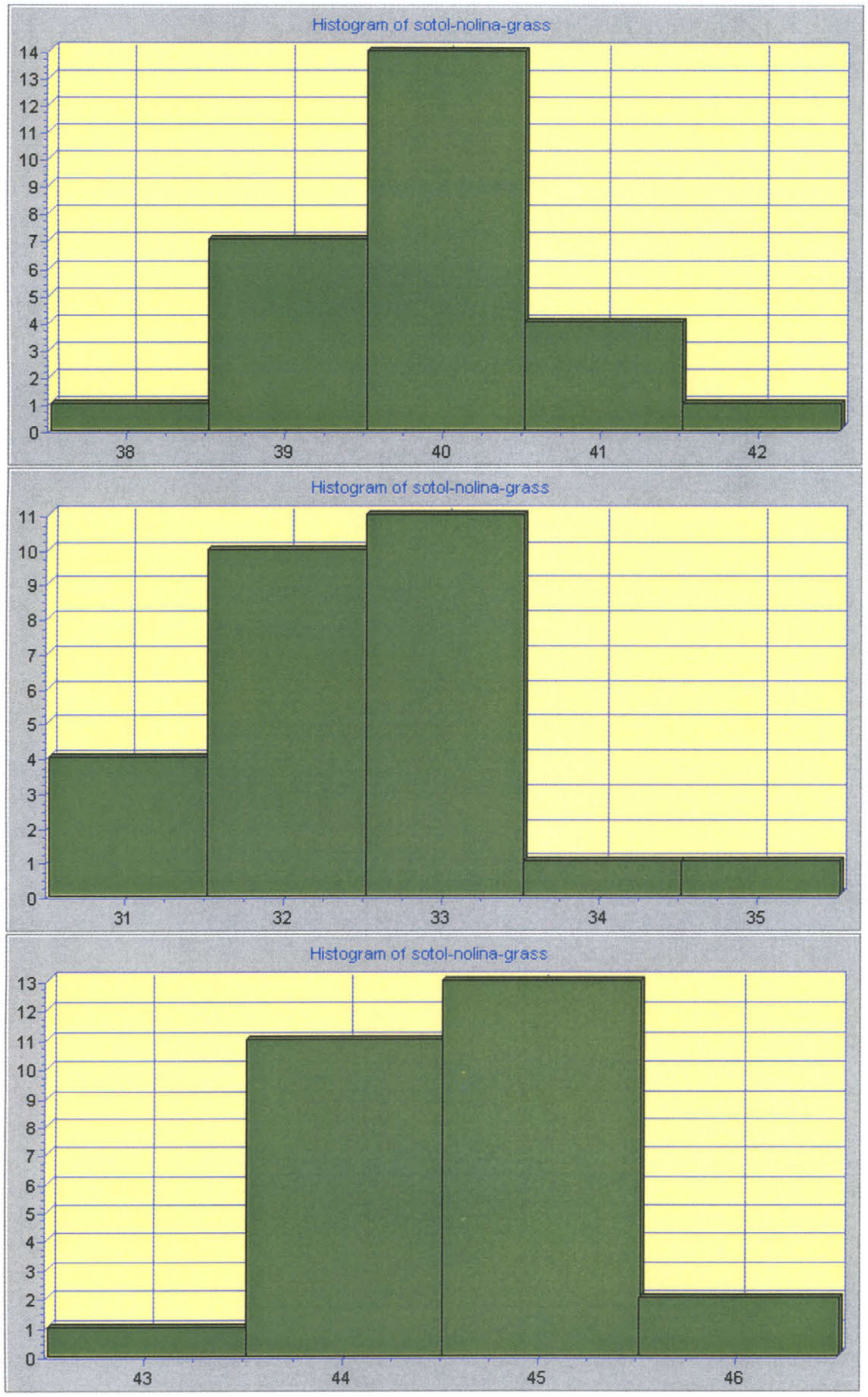

Figure 37. Histograms of Sotol-Nolina-Grass (n=27)

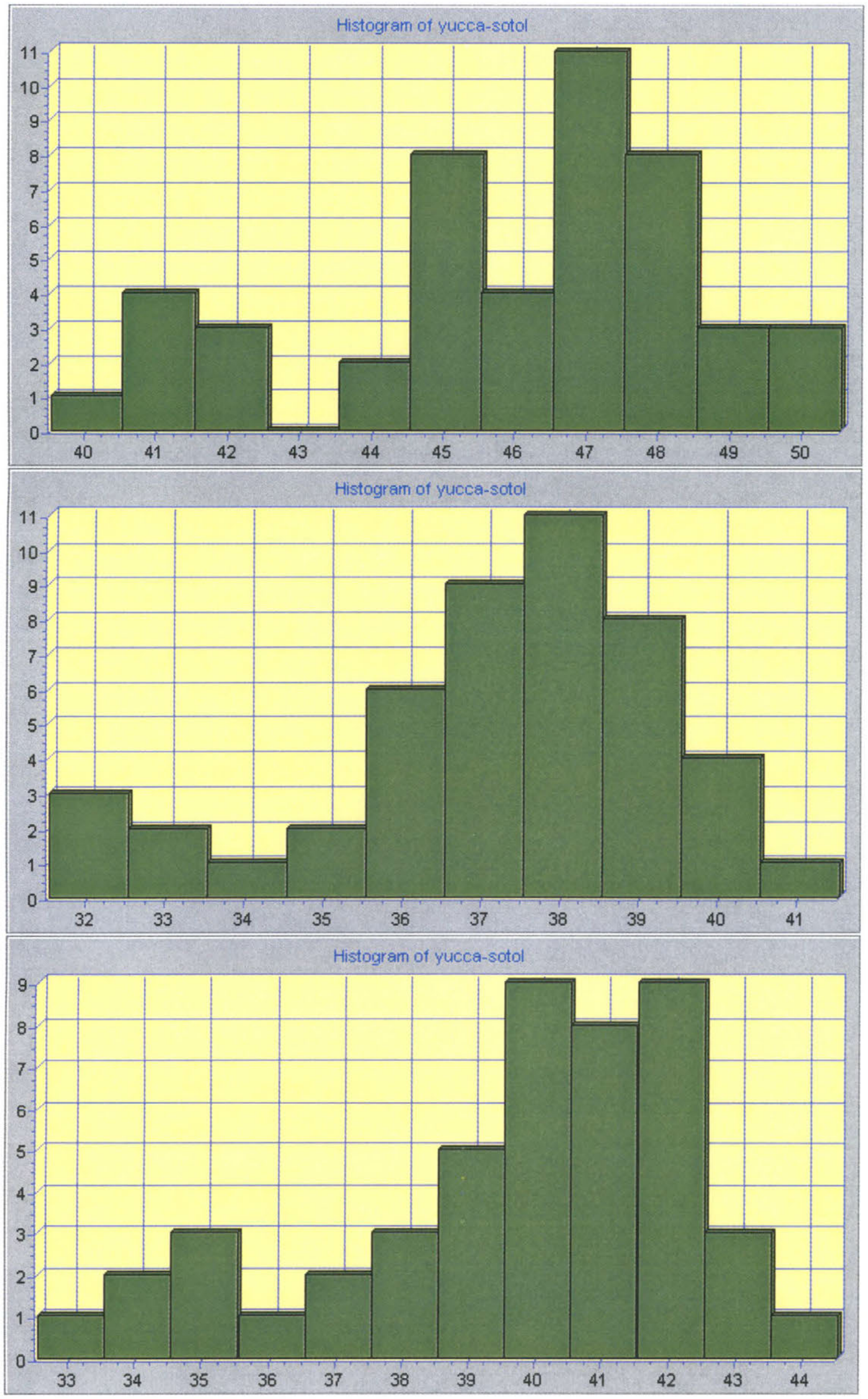

Figure 38. Histograms of Yucca-Sotol (n=52)

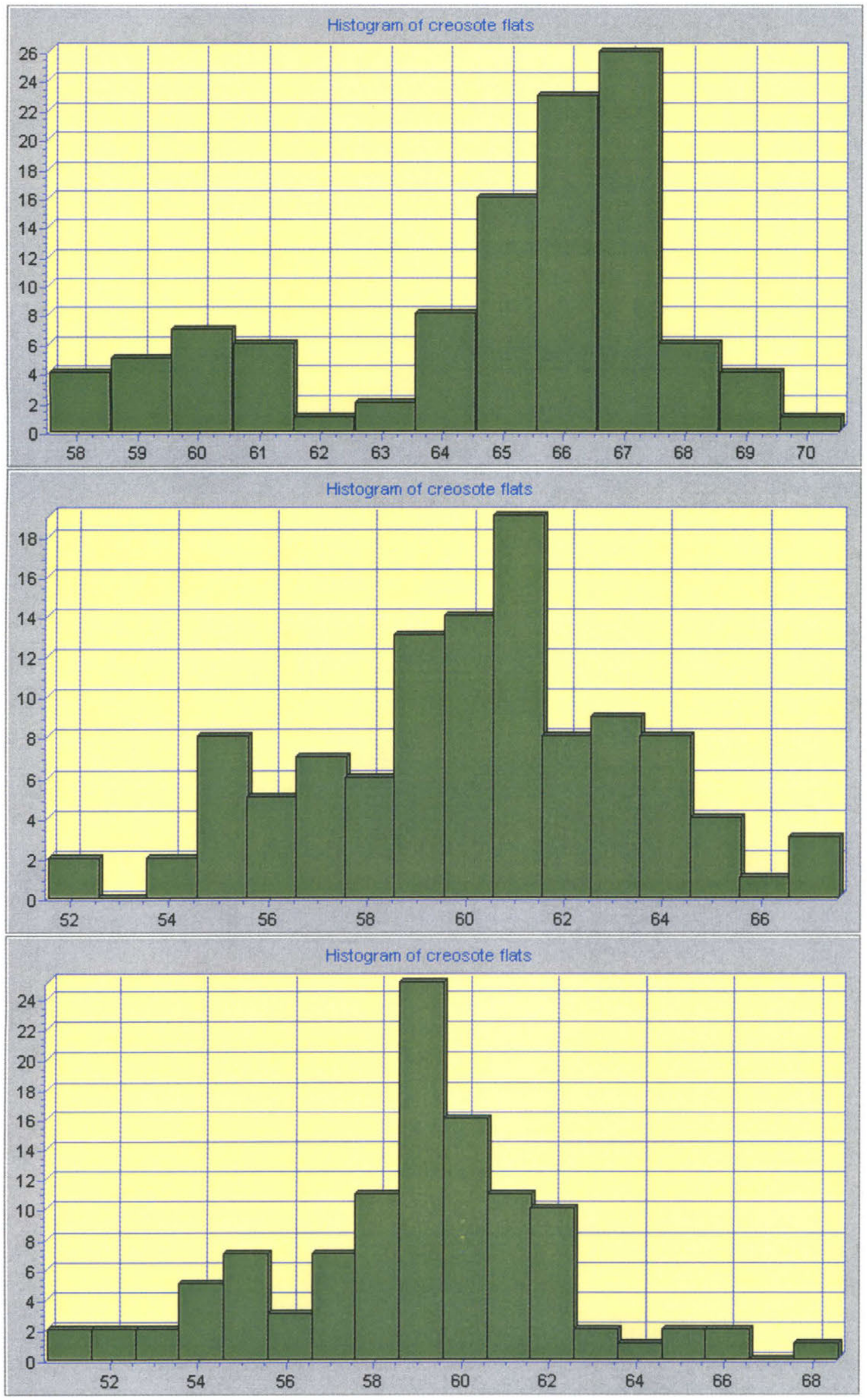

Figure 39. Histograms of Creosote Flats (n=109)

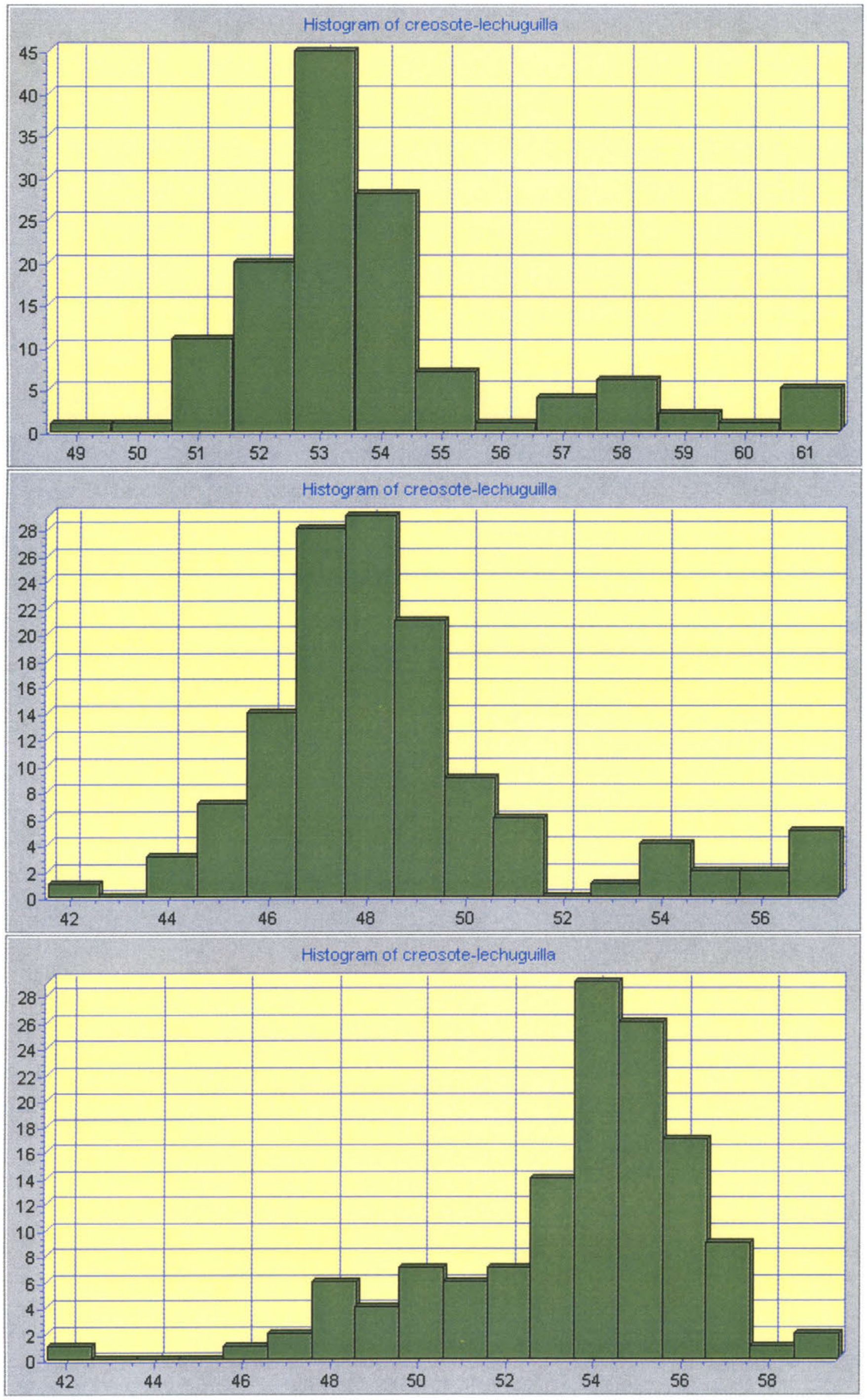

Figure 40. Histograms of Creosote-Lechuguilla (n=132)

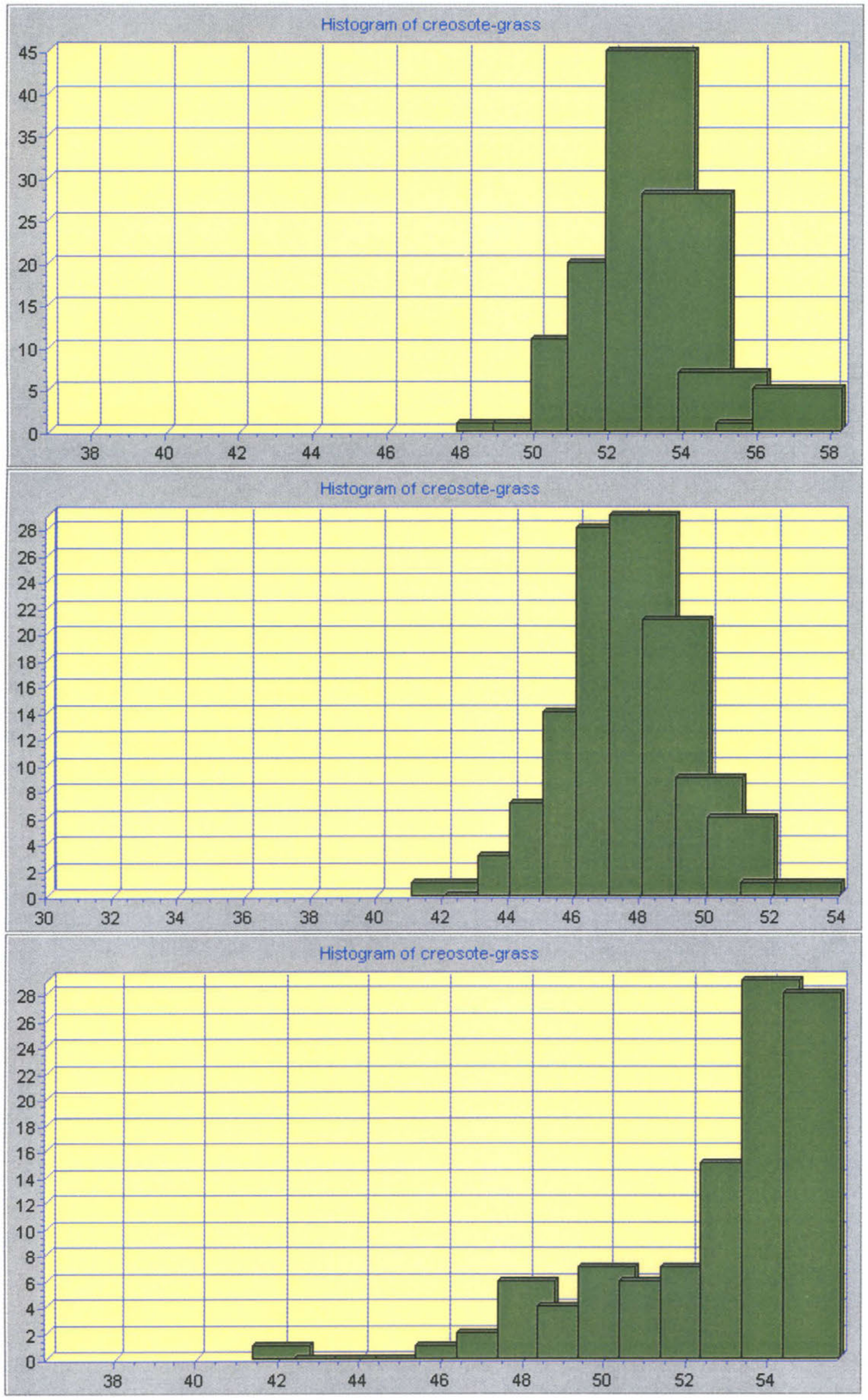

Figure 41. Histograms of Creosote Grass (n=104)

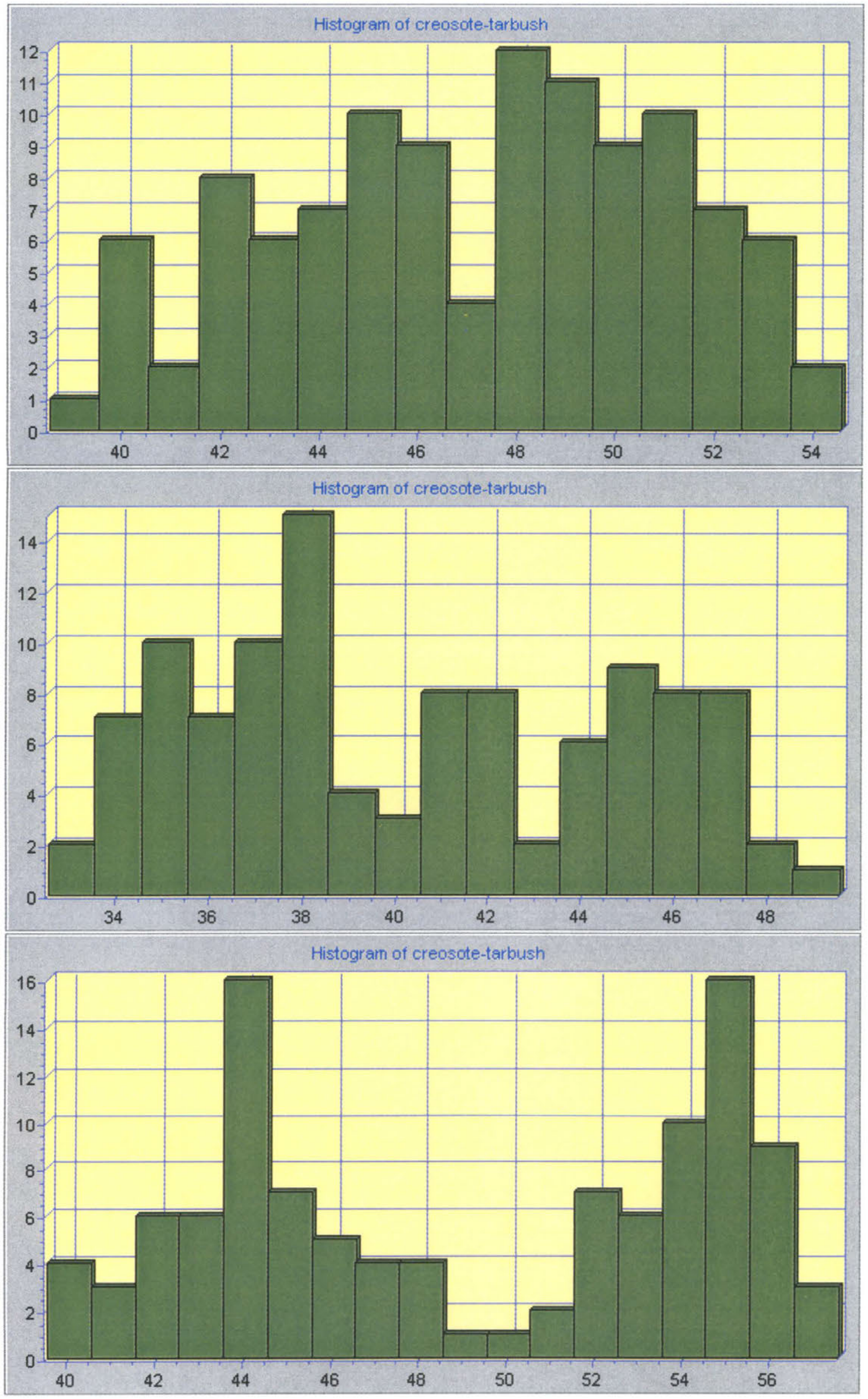

Figure 42. Histograms of Creosote-Tarbush (n=110)

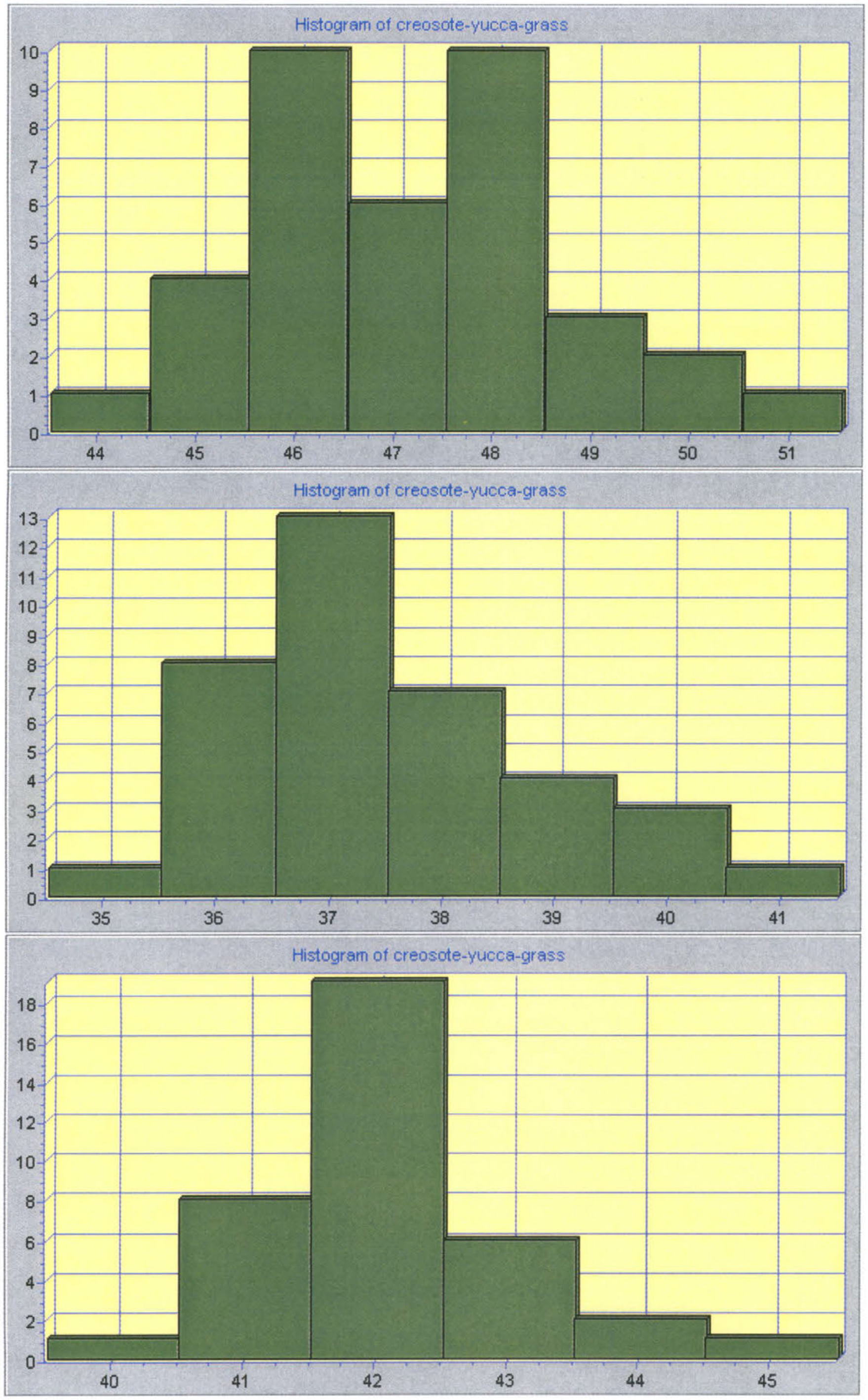

Figure 43. Histograms of Creosote-Yucca-Grass (n=37)

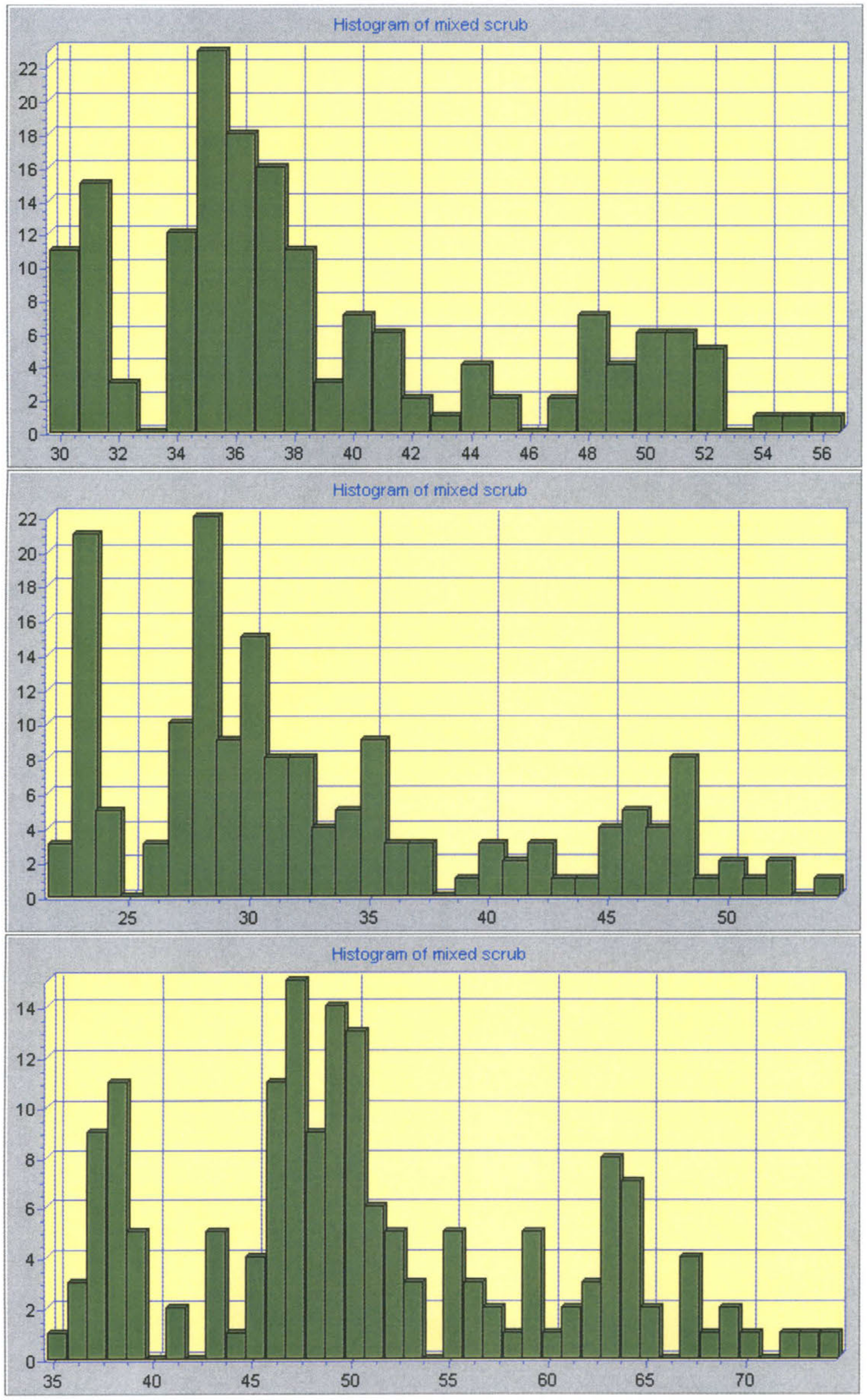

Figure 44. Histograms of Mixed Scrub (n=167)

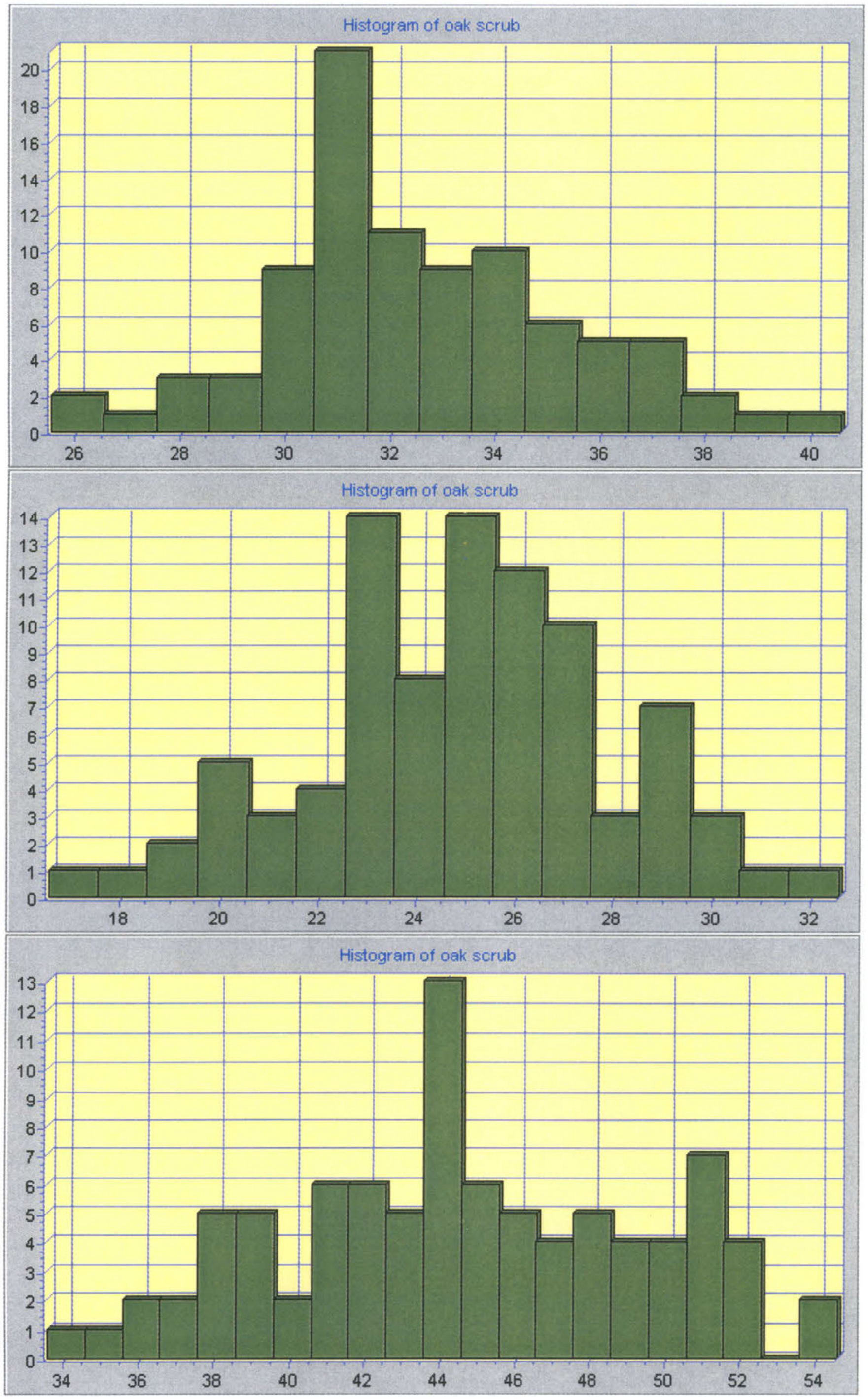

Figure 45. Histograms of Oak Scrub (n=89)

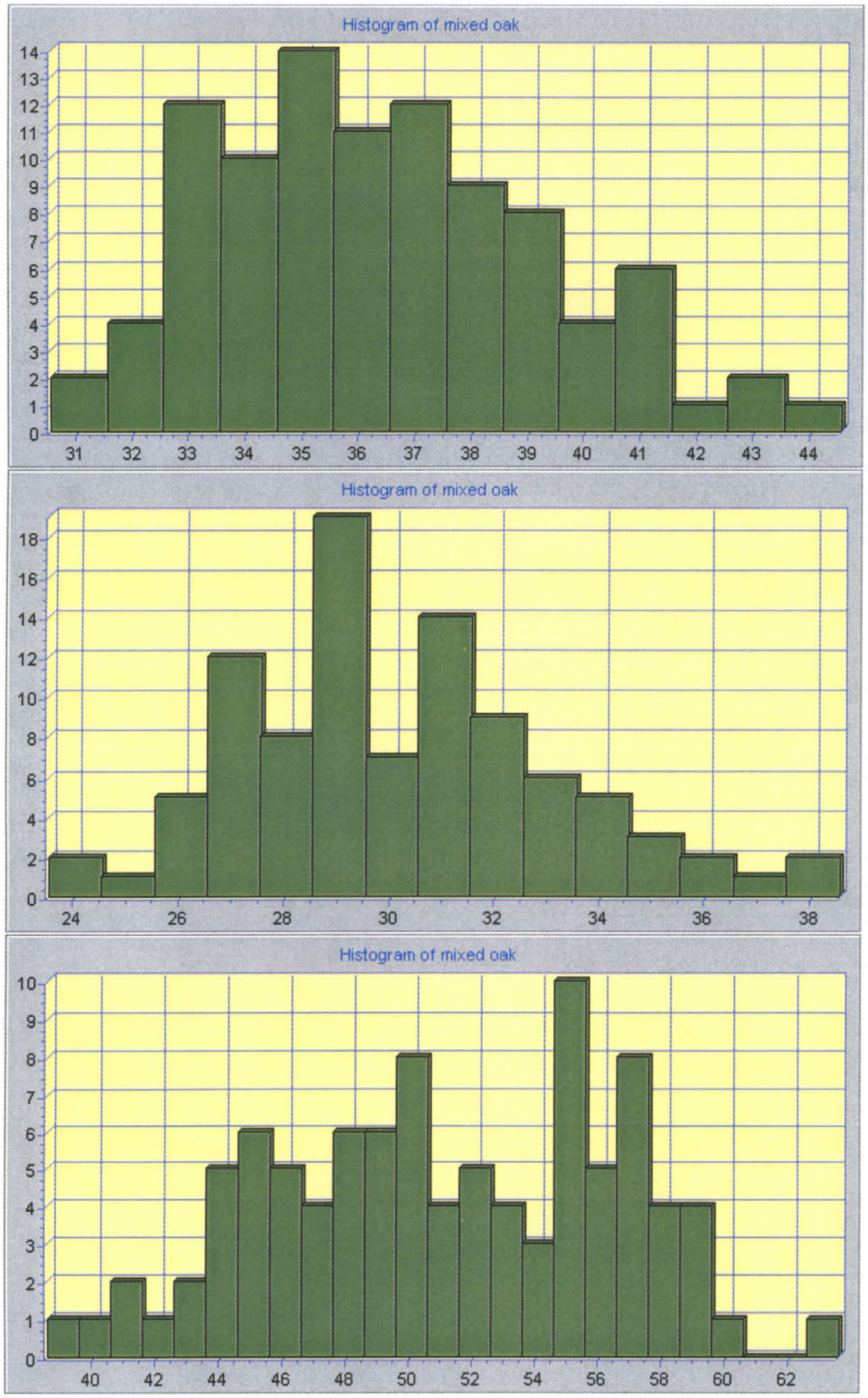

Figure 46. Histograms of Mixed Oak (n=96)

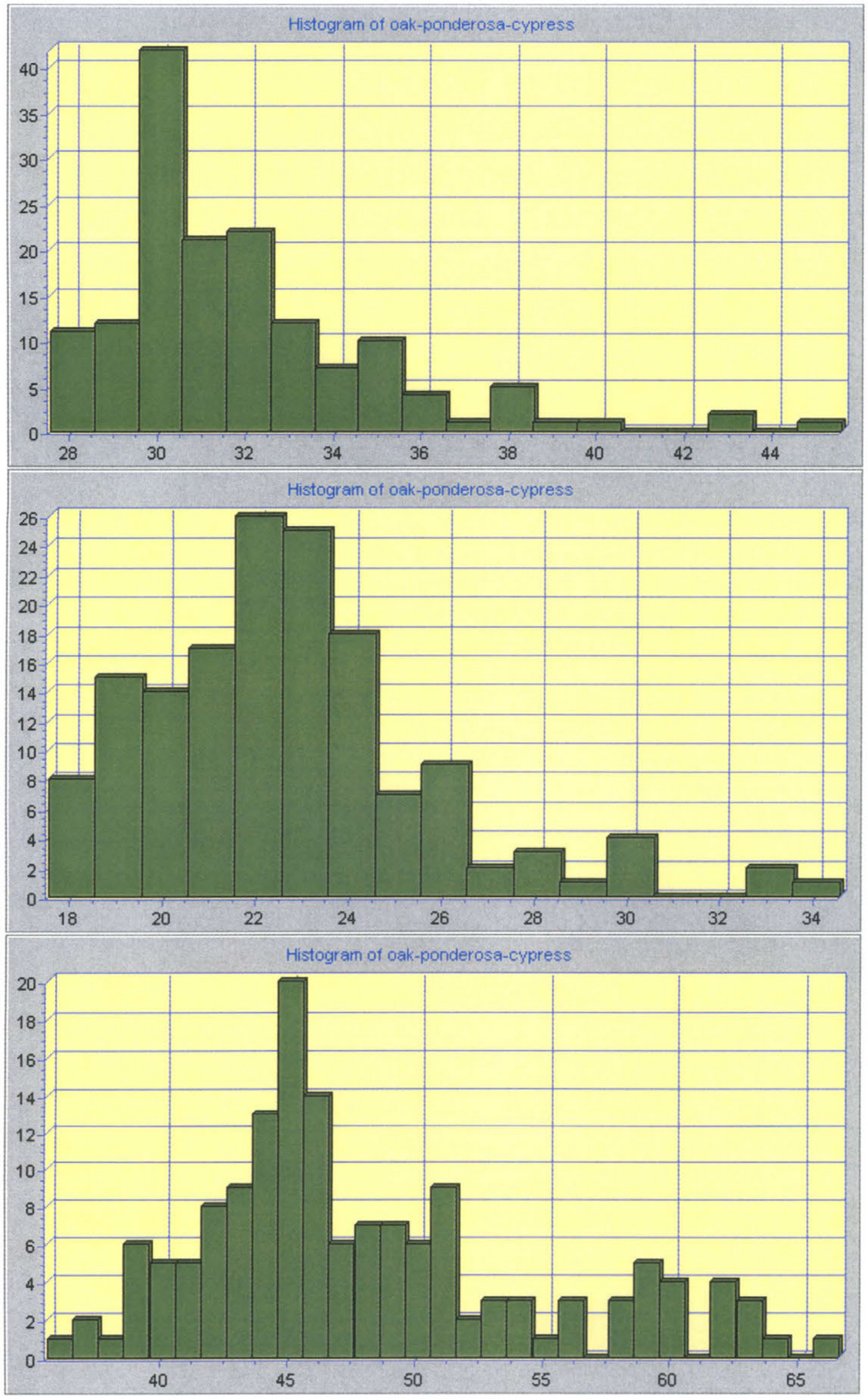

Figure 47. Histograms of Oak-Ponderosa-Cypress (n=152)

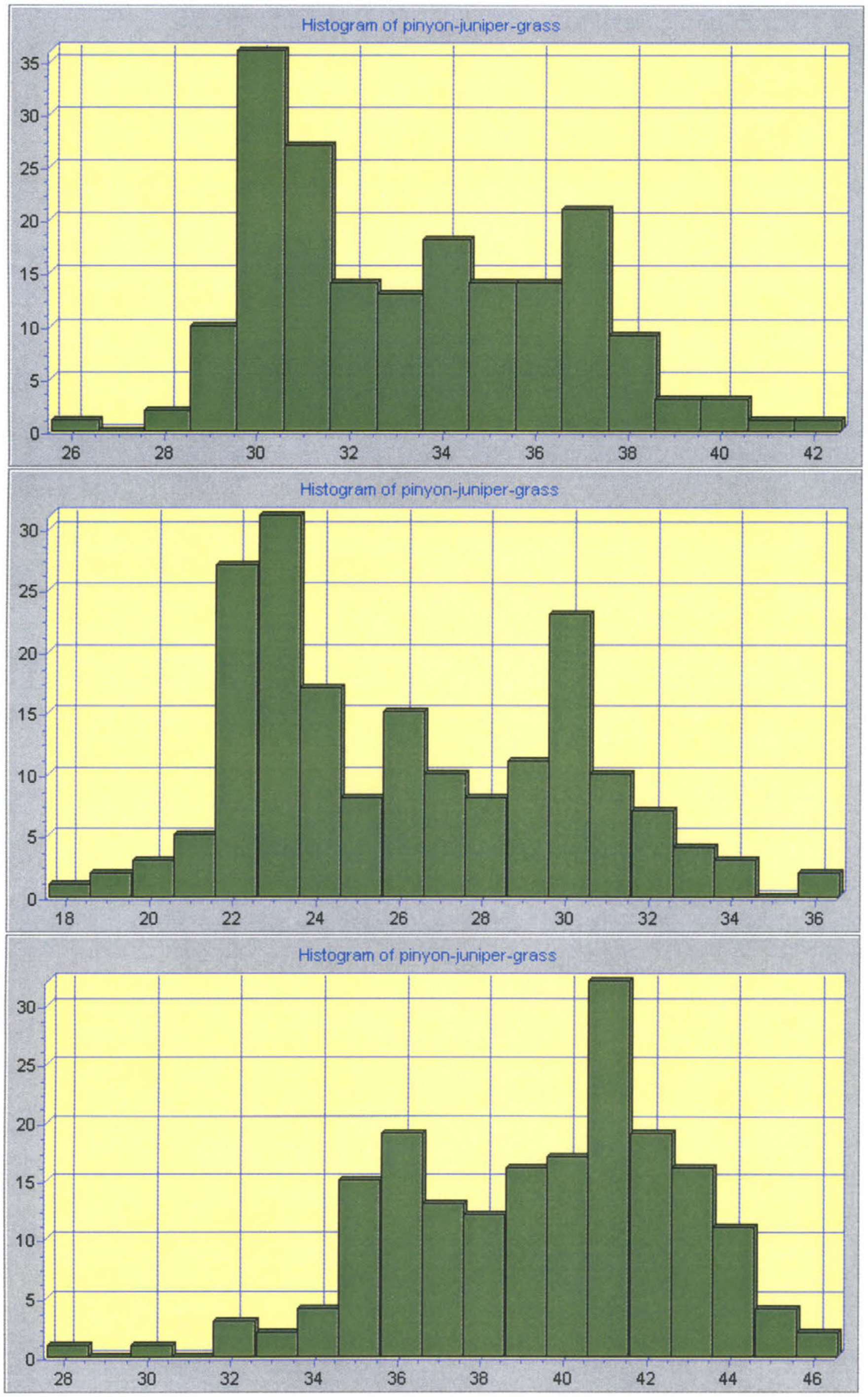

Figure 48. Histograms of Pinyon-Juniper-Grass (n=187)

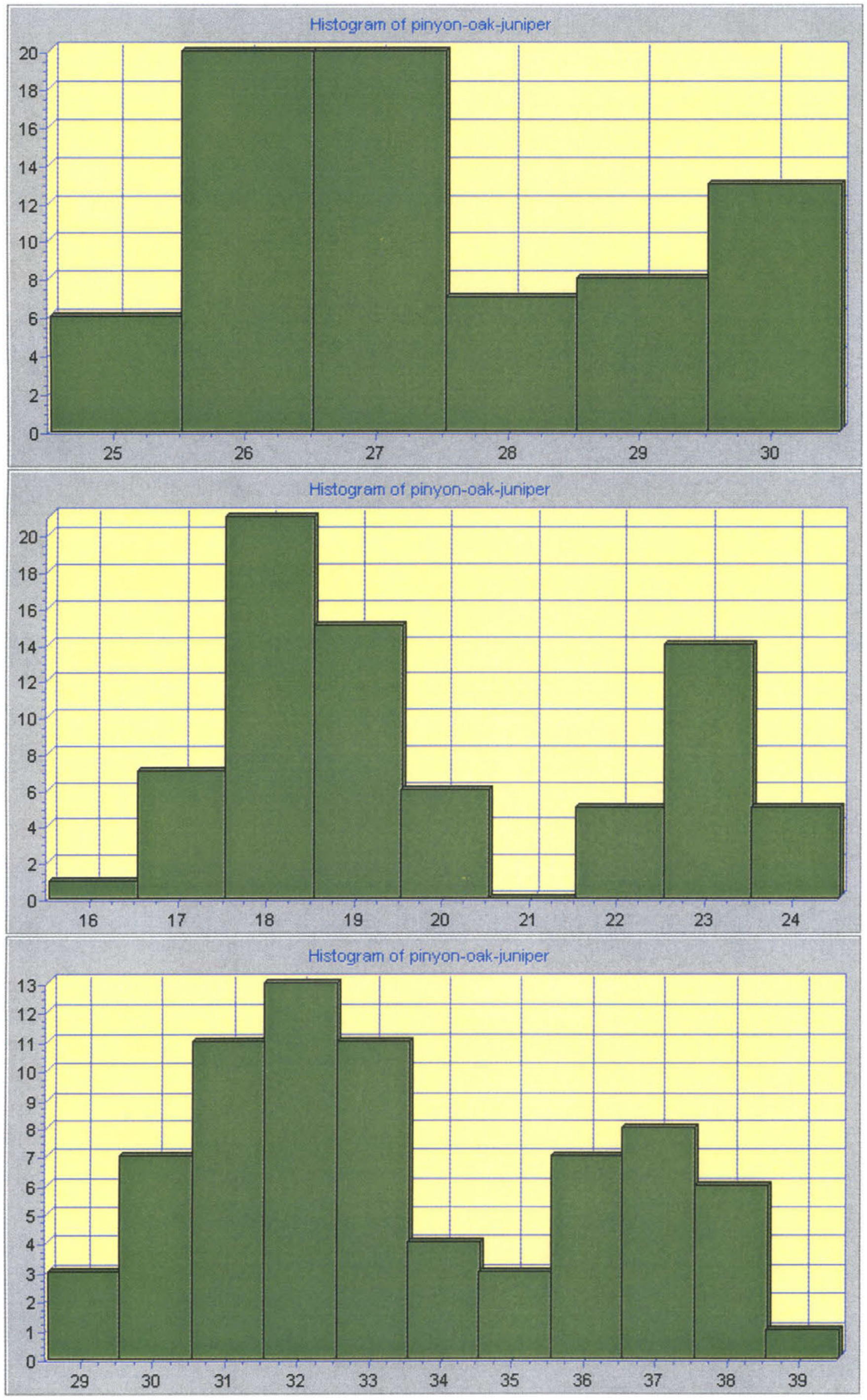

Figure 49. Histograms of Pinyon-Oak-Juniper (n=74)

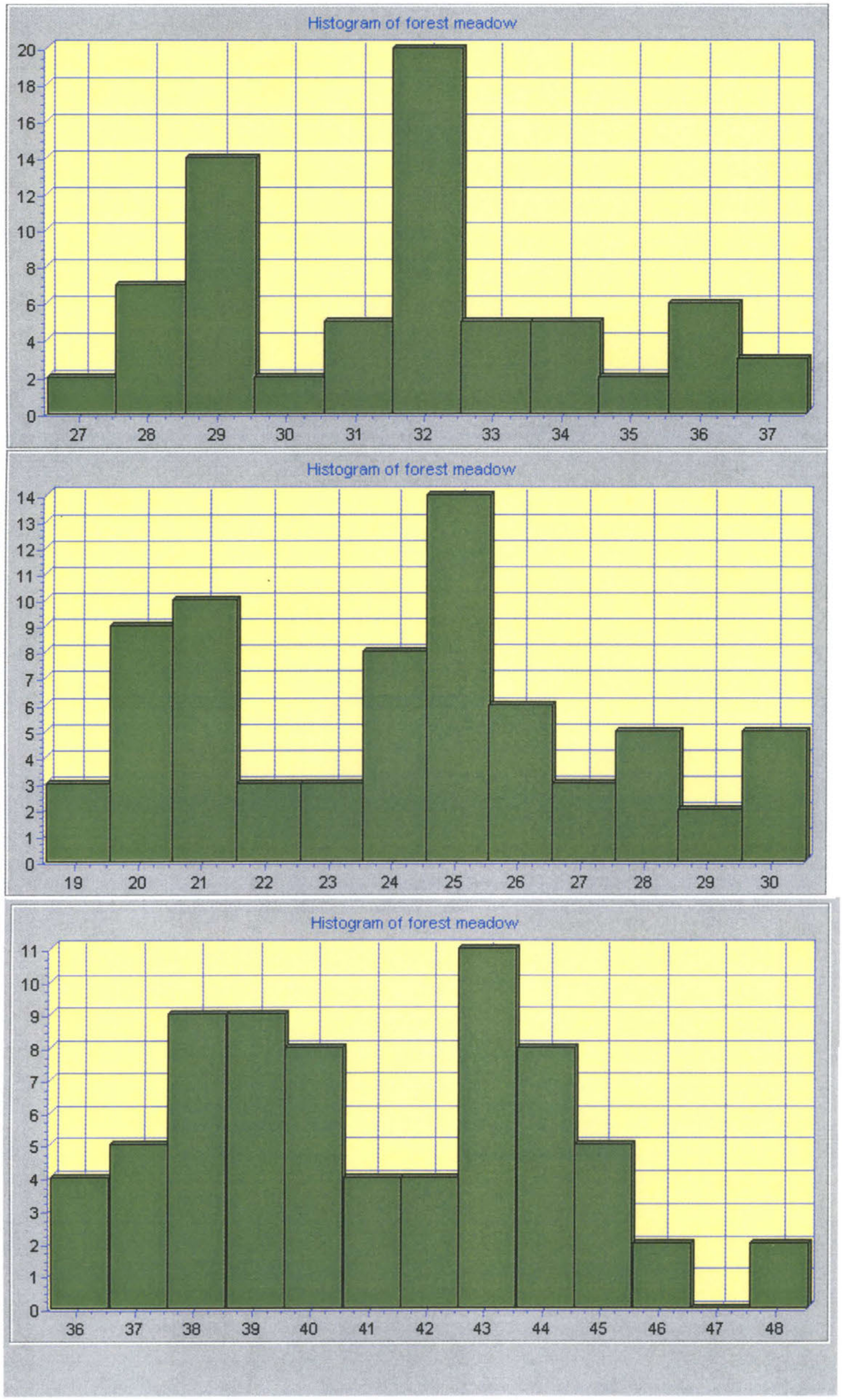

Figure 50. Histogram of Forest Meadow (n=71)

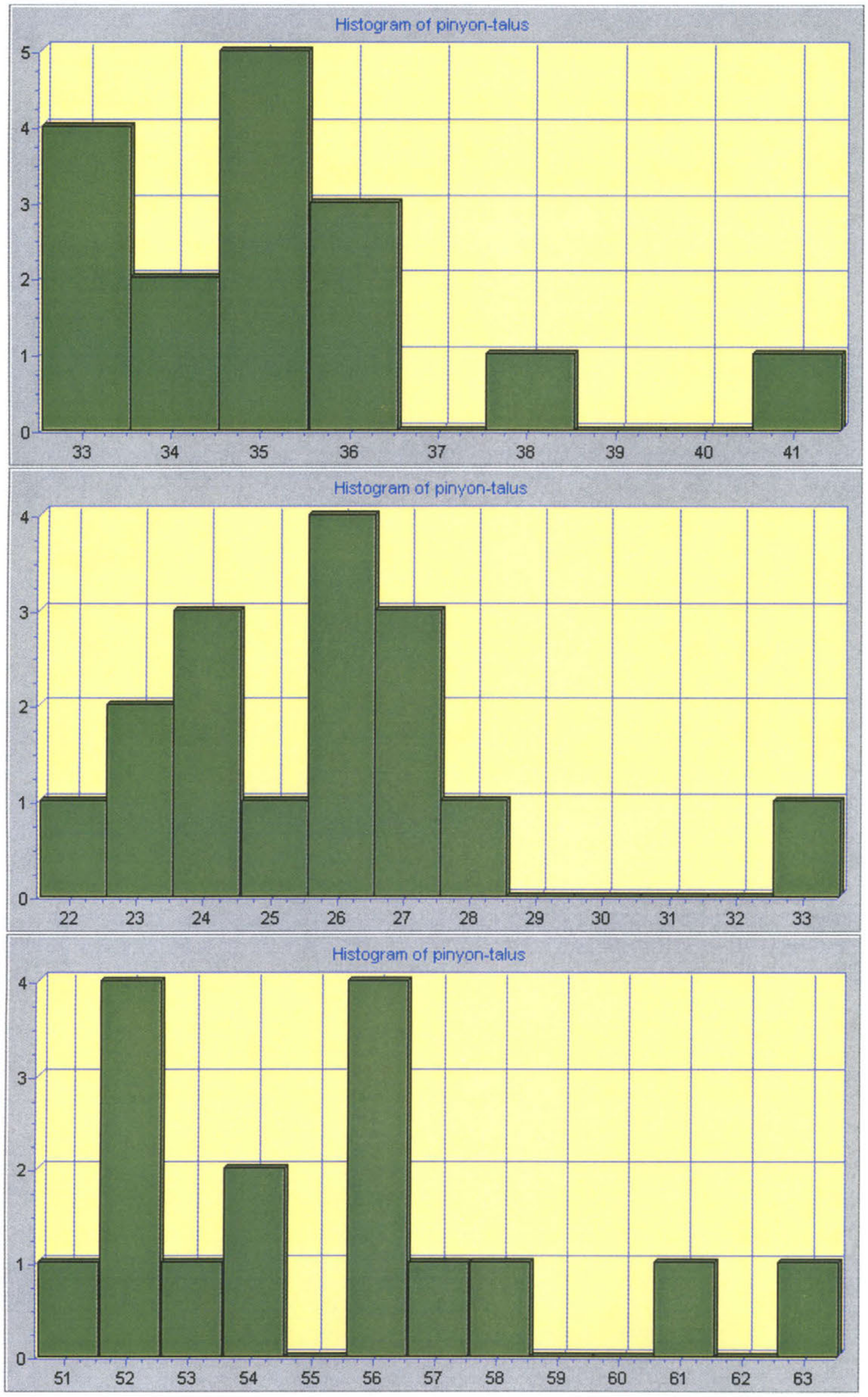

Figure 51. Histograms of Pinyon-Talus (n=16)

REFERENCES

Abeyta, Andres M. and Janet Franklin. 1998. The Accuracy of Vegetation Stand Boundaries Derived from Image Segmentation in a Desert Environment. *Photogrammatic Engineering and Remote Sensing* 64, no. 1: 59-66.

Alex, Tom. 1999. Explanation of Private Land Holdings inside Big Bend N. P. Boundary, interview by author, 7 May. Big Bend National Park.

Cochran, Rex A. and Jerry L. Rives. 1985. *Soil Survey of Big Bend National Park. Part of Brewster County, Texas*. General Soil Map Units: United States Department of Agriculture Soil Conservation Service.

Congalton, Russell G. 1991. A Review of Assessing the Accuracy of Classifciations of Remotely Sensed Data. *Remote Sensing of Environment* 46: 35-46.

Denyes, H. A. 1956. Communities of Brewster County, Texas, with Special Reference to the Distribution of Mammals. *American Midland Naturalist* 55: 289-320.

Eastman, J. Ronald. 1999a. *Guide to GIS and Image Processing Volume 2*. Worcester, MA: Clark Labs.

Eastman, J. Ronald. 1999b. *Idrisi32 Tutorial*. Worcester, MA: Clark Labs.

Etchberger, Richard C. and Paul R. Krausman. 1997. Evaluation of Five Methods for Measuring Desert Vegetation. *Wildlife Society Bulletin* 25, no. Fall '97: 604-9.

Foran, R. D. 1987. Detection of Yearly Cover Change with Landsat MSS on Pastoral Landscapes in Central Australia. *Remote Sensing of Environment* 23, no. 333-350.

Forman, Richard T. T. 1995. *Land Mosaics - The Ecology of Landscapes and Regions*. New York: Cambridge University Press.

Gould, Frank W. 1975. *The Grasses of Texas*. College Station, TX: Texas A&M University Press.

Gould, Frank W. 1978. *Common Texas Grasses*. College Station, TX: Texas A&M University Press.

Henrickson, James and Marshall C. Johnston. 1983. Vegetation and Community Types of the Chihuahuan Desert. In *Second Symposium on Resources of the Chihuahuan*

Desert Region, ed. Jon C. Barlow, A. Michael Powell, and Barbara N. Timmermann:20-39. Alpine, TX: Chihuahuan Desert Research Institute

Huete, A. R. and R. D. Jackson. 1987. Suitability of Spectral Indices for Evaluating Vegetation Characteristics on Arid Rangelands. *Remote Sensing of Environment* 23: 213-232.

Jensen, John R. 1996. *Introductory Digital Image Processing: A Remote Sensing Perspective*. Edited by Keith C Clark. Prentice Hall Series in Geographic Information Sciences. Upper Saddle River, NJ: Prentice Hall.

Kreyszig, Erwin. 1968. *Advanced Engineering Mathematics*. New York: John Wiley and Sons, Inc.

Kuchler, August Wilhelm and Isaak Samuel Zonneveld. 1988. *Vegetation Mapping*. Dordrecht, The Netherlands: Kluwer Academic Publishers.

Langford, J. O. 1952. *Big Bend: A Homsteader's Story*. Austin: University of Texas Press.

Leopold, Luna B., M. Gordon Wolman, and John P. Miller. 1964. *Fluvial Processes in Geomorphology*: San Francisco: W. H. Freeman and Company.

Maxwell, Ross A. 1968. *The Big Bend of the Rio Grande: A Guide to the Rocks, Landscape, Geologic History, and Settlers of the Area of Big Bend National Park*. Austin: Bureau of Economic Geology, The University of Texas at Austin.

Maxwell, Ross A, John T Lonsdale, Roy T Hazzard, and John A Wilson. 1967. *Geology of Big Bend National Park, Brewster County, Texas*. Austin: Bureau of Economic Geology, University of Texas at Austin.

McAuliffe, Joseph R. 1994. Landscape Evolution, Soil Formation and Ecological Patterns and Processes in Sonoran Desert Bajadas. *Ecological Monographs* 64: 111-48.

Montaña, Carlos. 1992. The Colonization of Bare Areas in Two-phase Mosaics of an Arid Ecosystem. *The Journal of Ecology* 80: 315-327.

Montaña, Carlos, J. Lopez-Portillo, and A. Mauchamp. 1990. The Response of Two Woody Species to the Conditions Created by a Shifting Ecotone in an Arid Ecosystem. *The Journal of Ecology* 78: 789-98.

National Park Service. 1999a. The National Park System Caring for the American Legacy, http://www.nps.gov/legacy/mission.html.

National Park Service. 1999b. National Park Service Summary of Acreage by Area Type 31-Dec-1998, http://www2.nature.nps.gov/stats/acreage3.pdf.

National Park Service Division of Science and Resource Management Big Bend National Park, Texas. 1995. The Vascular Flora of Big Bend National Park, Texas.

National Park Service Division of Science and Resource Management Big Bend National Park, Texas. 1998. History of Land Ownership and Periods of Construction.

Plumb, Gregory A. 1988. *An Algorithmic Approach to Automated Vegetation Mapping of Big Bend National Park, Texas*. Geography. Lawrence, KS: University of Kansas.

Plumb, Gregory A. 1992. Vegetation Classifications of Big Bend National Park, Texas. *Texas Journal of Science* 44, no. 4: 375-387.

Powell, A. Michael. 1998. *Trees and Shrubs of the Trans-Pecos and Adjacent Areas*. Austin: University of Texas Press.

Schmidt, Robert H. 1983. Chihuahuan Climate. In *Second Symposium on Resources of the Chihuahuan Desert Region*, ed. Jon C. Barlow, A. Michael Powell, and Barbara N. Timmermann:40-63. Alpine, Texas: Chihuahuan Desert Research Institute.

Silvertown, Jonathan and J. Bastow Wilson. 1994. Community Structure in a Desert Perennial Community. *Ecology* 75: 409-17.

Simpson, Brad, Donnie Frels, Tim Lawyer, Todd Merendino, Ellen Meyers, Chip Ruthven, Sylvestre Sorola, and Matt Wagner. 1996. Baseline Inventory and Monitoring Procedures on Texas Parks and Wildlife Department Lands. Austin, TX: Texas Parks and Wildlife Department.

Steele, Brain M., J. Chris Winne, and Roland L. Redmond. 1998. Estimation and Mapping of Misclassification Probabilities for Thematic Land Cover Maps. *Remote Sensing of Environment* 66: 192-202.

Todd, Stella W. and Roger M. Hoffer. 1998. Responses of Spectral Indices to Variations in Vegetation Cover and Soil Background. *Photogrammetric Engineering and Remote Sensing* 64, no. 9: 915-921.

Treitz, Paul M., Philip J. Howarth, Paul Smith, and Roger C. Suffling. 1992. Application of Detailed Ground Information to Vegetation Mapping with High Spatial Resolution Digital Imagery. *Remote Sensing of Environment* 42: 65-82.

Tueller, Paul T. 1987. Remote Sensing Science Applications in Arid Environments. *Remote Sensing of Environment* 23: 143-154.

Turner, Raymond M. 1990. Long-term Vegetation Change at a Fully Protected Sonoran Desert Site. *Ecology* 71, April: 464-77.

Tyler, Ronnie C. 1975. *The Big Bend: A History of the Last Texas Frontier*. Washington, D. C.: National Park Service.

Walsh, Stephen J. 1985. Geographic Information Systems for Natural Resource Management. *Journal of Soil and Water Conservation* 40: 202-205.

Warnock, Barton H. 1970. *Wildflowers of the Big Bend Country Texas*. Alpine, TX: Sul Ross State University.

Warnock, Barton H. 1977. *Wildflowers of the Davis Mountains and the Marathon Basin, Texas*: Alpine, TX: Barton H. Warnock.

Wauer, Roland H. 1971. Ecological Distribution of Birds in the Chisos Mountains, Texas. *Southwestern Naturalist*, no. 16: 1-29.

Wauer, Roland H. 1973a. *Birds of Big Bend National Park and Vicinity*. Austin, TX: University of Texas Press.

Wauer, Roland H. 1973b. *Naturalist's Big Bend*. College Station, TX: Texas A&M University Press.

Whitson, P. D. 1970. Dynamics of the Shrub Desert Formation-Succulent Desert Formation Transition in Big Bend National Park, Texas. Unpublished Dissertation, University of Oklahoma.

Wulfkuhle, Virginia A. 1986. The Buttrill Ranch Complex Brewster County, Texas: Evidence of Early Ranching in the Big Bend. Austin: Texas Historical Commission.

VITA

Terence Patton Booth was born in Lamar, Colorado on October 31, 1948, the son of Jane Nordgren Booth and Jean Donald Booth. After graduating from Clinton Senior High School in Clinton, Missouri, he entered the University of Missouri-Rolla. Mr. Booth graduated with high honors with a Bachelor of Science degree in mathematics in July 1970. That same month Mr. Booth began a career as a programmer with International Business Machines (IBM) in Raleigh, North Carolina. Mr. Booth attained the position of Senior Systems Engineer-Manager and retired early from IBM in 1992. While working at IBM, Mr. Booth pursued continuing education in geology and later land surveying at Austin Community College. In 1993 Mr. Booth began working as a land surveyor. That same year he married Dawn Smith. In August 1994, he entered the Graduate School at Southwest Texas State University to pursue the Master of Applied Geography degree. Mr. Booth is currently employed as a Senior Contract Manager, Management Information Systems, at the Texas Department of Human Services.

Permanent address: 3863 Williamsburg Circle
Austin, Texas 78731

This thesis was typed by Terence P. Booth.